

**Differential expression of pro- and anti-inflammatory  
mediators in pulmonary macrophages upon Toll-like  
receptor activation**

Dissertation  
zur Erlangung des Grades  
des Doktors der Naturwissenschaften  
der Naturwissenschaftlich-Technischen Fakultät III  
Chemie, Pharmazie, Bio- und Werkstoffwissenschaften  
der Universität des Saarlandes

von  
Jessica Hoppstädter

Saarbrücken  
2010

Tag des Kolloquiums: 20.12.2010  
Dekan: Prof. Dr.-Ing. Stefan Diebels  
Berichterstatter: Prof. Dr. Alexandra K. Kiemer  
Prof. Dr. Ludwig Gortner  
Prof. Dr. Bernhard Brüne  
Vorsitz: Prof. Dr. Petra Bauer  
Akad. Mitarbeiter: Dr. Britta Diesel

# Contents

<b>Abbreviations</b>	<b>1</b>
<b>Abstract / Zusammenfassung</b>	<b>5</b>
<b>1. Background</b>	<b>7</b>
<b>1.1 Inflammatory lung diseases</b>	<b>9</b>
1.1.1 Tuberculosis	9
1.1.2 Asthma and allergic diseases	10
1.1.3 Chronic obstructive pulmonary disease (COPD)	11
<b>1.2 Macrophages as mediators of pulmonary inflammation</b>	<b>12</b>
1.2.1 Overview of macrophage functions	12
1.2.2 Macrophages in inflammatory lung disease	14
1.2.3 Macrophage populations within the respiratory tract	15
<b>1.3 Toll-like receptors (TLRs)</b>	<b>17</b>
1.3.1 Ligands	17
1.3.2 Signalling	19
1.3.3 TLR expression within the lung	20
1.3.4 TLRs and pulmonary inflammation	20
<b>1.4 Glucocorticoid-induced leucine zipper (GILZ)</b>	<b>22</b>
1.4.1 Structure	22
1.4.2 The diverse functions of GILZ	23
1.4.3 GILZ in pulmonary inflammation	25
<b>1.5 Aim of the present work</b>	<b>26</b>
<b>2. Chapter I</b>	<b>29</b>
<b><i>Attenuated activation of macrophage TLR9 by DNA from mycobacteria</i></b>	
<b>2.1 Introduction</b>	<b>31</b>
<b>2.2 Results</b>	<b>33</b>
2.2.1 Human macrophages are responsive to mycobacterial DNA	33
2.2.2 Different potency of mycobacterial DNA to activate human macrophages	39
<b>2.3 Discussion</b>	<b>41</b>
2.3.1 Responsiveness of human macrophages towards mycobacterial DNA	41
2.3.2 Differential activatory potential of mycobacterial DNA	42
2.3.3 What distinguishes DNA from virulent and attenuated mycobacteria	43

---

**3. Chapter II 45**

***Differential cell reaction upon Toll-like receptor activation in human alveolar and lung interstitial macrophages***

<b>3.1</b>	<b>Introduction</b>	<b>47</b>
<b>3.2</b>	<b>Results</b>	<b>49</b>
	3.2.1 Cell number and appearance	49
	3.2.2 Expression of intracellular and surface markers	51
	3.2.3 Phagocytosis	52
	3.2.4 TLR expression	54
	3.2.5 Cell reaction upon TLR4 and TLR9 stimulation	54
	3.2.6 Response to MyD88-dependent and –independent TLR activation	59
<b>3.3</b>	<b>Discussion</b>	<b>61</b>
	3.3.1 Isolation procedure	61
	3.3.2 Morphology	61
	3.3.3 CD14 and HLA-DR expression	61
	3.3.4 Comparison to dendritic cells	62
	3.3.5 Phagocytic activity	62
	3.3.6 TLR expression	62
	3.3.7 Baseline cytokine expression and response to LPS	63
	3.3.8 Differential response to TLR1/2, TLR3 and TLR4 activation	65
	3.3.9 Cell reaction upon TLR9 activation	66

---

**4. Chapter III 69**

***Downregulation of the glucocorticoid-induced leucine zipper upon Toll-like receptor activation in human alveolar macrophages***

<b>4.1</b>	<b>Introduction</b>	<b>71</b>
<b>4.2</b>	<b>Results</b>	<b>73</b>
	4.2.1 Constitutive and dexamethasone –induced GILZ expression in AM	73
	4.2.2 TLR9 activation attenuates GILZ expression	74
	4.2.3 GILZ downregulation in response to TLR4 activation	75
	4.2.4 Enhanced expression of pro-inflammatory cytokines due to reduced GILZ levels	77
	4.2.5 GILZ downregulation upon MyD88-dependent and –independent TLR activation	79
	4.2.6 MyD88-dependent GILZ mRNA downregulation	82
	4.2.7 Decrease of GILZ mRNA half-life in response to LPS	83
	4.2.8 Involvement of TTP in GILZ mRNA destabilization	84
	4.2.9 Proteasome-dependent GILZ downregulation	88
	4.2.10 TNF- $\alpha$ -mediated GILZ downregulation	89
	4.2.11 GILZ mRNA expression in endotoxin tolerance	90
<b>4.3</b>	<b>Discussion</b>	<b>92</b>
	4.3.1 Constitutive and dexamethasone-induced GILZ expression in pulmonary macrophages	92

4.3.2 TLR-mediated GILZ downregulation	93
4.3.3 MyD88- and TTP-dependent GILZ mRNA downregulation	94
4.3.4 Proteasome-dependent GILZ downregulation	96
4.3.5 TNF- $\alpha$ -mediated GILZ downregulation	98
4.3.6 GILZ in endotoxin tolerance	98
<b>5. Experimental procedures</b>	<b>101</b>
<b>5.1 Materials</b>	<b>103</b>
<b>5.2 Mice</b>	<b>104</b>
<b>5.3 Cell culture</b>	<b>104</b>
5.3.1 Alveolar macrophages (AM)	104
5.3.2 Lung interstitial macrophages (IM)	105
5.3.3 Monocyte-derived macrophages	105
5.3.4 Monocyte-derived immature and mature dendritic cells (iDC, mDC)	106
5.3.5 Cell lines	106
5.3.6 Determination of cell viability	107
<b>5.4 Bacterial culture</b>	<b>108</b>
5.4.1 <i>Escherichia coli</i> ( <i>E. coli</i> ) strains	108
5.4.2 Culture of mycobacteria	109
<b>5.5 Plasmid generation</b>	<b>109</b>
5.5.1 Vectors for mammalian cell transfections	109
5.5.2 Real-Time RT-PCR standard plasmids	110
<b>5.6 Isolation of bacterial DNA</b>	<b>110</b>
5.6.1 Plasmid purification	110
5.6.2 Isolation, digestion and methylation of mycobacterial DNA	110
5.6.3 Determination of DNA concentrations	111
<b>5.7 Agarose gel electrophoresis</b>	<b>112</b>
5.7.1 Detection of DNA	112
5.7.2 Detection of RNA	112
<b>5.8 RNA isolation and reverse transcription</b>	<b>112</b>
5.8.1 RNA isolation	112
5.8.2 Measurement of RNA concentrations	112
5.8.3 Alu PCR	113
5.8.4 Reverse transcription	113
<b>5.9 Real time RT-PCR</b>	<b>114</b>
5.9.1 Primer and probe sequences	114
5.9.2 Standard dilution series	115
5.9.3 Experimental procedure	116
<b>5.10 Western Blot analysis</b>	<b>118</b>
5.10.1 Preparation of protein samples	118
5.10.2 SDS-polyacrylamide gel electrophoresis (SDS-PAGE)	118
5.10.3 Blotting	119
5.10.4 Immunodetection	119

<b>5.11</b>	<b>Transfection of THP-1 cells</b>	<b>120</b>
	5.11.1 Plasmid transfection	120
	5.11.2 siRNA transfection	120
<b>5.12</b>	<b>Determination of mRNA stability</b>	<b>120</b>
<b>5.13</b>	<b>Flow cytometry</b>	<b>121</b>
	5.13.1 Antibodies	121
	5.13.2 Cell staining and analysis	121
<b>5.14</b>	<b>Phagocytosis Assay</b>	<b>122</b>
	5.14.1 Sample preparation	122
	5.14.2 Flow cytometry assessment of fluorosphere uptake	122
	5.14.3 Confocal laser scanning microscopy	122
<b>5.15</b>	<b>Pappenheim staining</b>	<b>123</b>
<b>5.16</b>	<b>Cytokine measurement</b>	<b>123</b>
<b>5.17</b>	<b>Atomic force microscopy</b>	<b>124</b>
<b>5.18</b>	<b>Statistics</b>	<b>124</b>
<b>6. Summary</b>		<b>126</b>
<b>7. References</b>		<b>130</b>
<b>Publications</b>		<b>159</b>
<b>Acknowledgements / Danksagungen</b>		<b>161</b>

## Abbreviations

A	Ampere
amp	ampicillin
AM	alveolar macrophage
AP-1	activator protein 1
APS	ammonium persulfate
atto	$10^{-18}$
BHQ1	black hole quencher 1
BAL	bronchoalveolar lavage
BCG	<i>M. bovis</i> Bacille Calmette-Guerin
bp	base pairs
BSA	bovine serum albumin
CD	cluster of differentiation
cDNA	complementary DNA
COPD	Chronic obstructive pulmonary disease
CpG	undermethylated 5'-CG-3' sequences
DAMP	danger-associated molecular pattern
dATP	2'-deoxyadenosine-5'-triphosphate
DC	dendritic cell
dCTP	2'-deoxycytidine 5'-triphosphate
DEPC	diethyl dicarbonate
dGTP	2'-deoxyguanosine 5'-triphosphate
DMEM	Dulbecco's modified eagle medium
DMSO	dimethyl sulfoxide
DNA	deoxyribonucleic acid
DNase	deoxyribonuclease
dNTP	dATP, dCTP, dGTP or dTTP
dTTP	2'-deoxythymidine 5'-triphosphate
<i>E. coli</i>	<i>Escherichia coli</i>
EDTA	ethylenediaminetetraacetic acid
EtBr	ethidium bromide
FACS	fluorescence activated cell sorter
Fc	fragment crystalline
FCS	fetal calf serum
FITC	fluorescein isothiocyanate
FSC	forward scatter
x g	x-fold gravitational force

g	gram
G	guanine
GILZ	glucocorticoid-induced leucine zipper
h	fluorescein isothiocyanate
H37Ra	<i>M. tuberculosis</i> , attenuated strain H37Ra
H37Rv	<i>M. tuberculosis</i> , virulent strain H37Rv
HLA-DR	human leukocyte antigen-DR
HMGB1	high-mobility group box 1 protein
HuR	human antigen R
iDC	immature dendritic cell
IFN	interferon
I $\kappa$ B	inhibitory protein $\kappa$ B
IL	Interleukin
IL1ra	IL1 receptor antagonist
IM	Interstitial macrophage
IP10	IFN $\gamma$ inducible protein 10
IRF	IFN regulating factor
ISS	immunostimulatory sequences
kb	kilo bases
kDa	kilo Dalton
l	litre
LB	Luria Bertani
LPS	lipopolysaccharide
m	milli ( $10^{-3}$ )
M	molar
MAPK	mitogen-activated protein kinase
<i>M. bovis</i>	<i>Mycobacterium bovis</i>
MCP-1	macrophage chemoattractant protein-1
mDC	mature dendritic cell
MHC	major histocompatibility complex
$\mu$	micro ( $10^{-6}$ )
min	minute
MIP	macrophage inflammatory protein
MOPS	3-(N-morpholino)propanesulfonic acid
mRNA	messenger RNA
<i>M. tuberculosis</i>	<i>Mycobacterium tuberculosis</i>
MyD88	myeloid differentiation factor 88
n	nano ( $10^{-9}$ )
N	normal

NF-κB	nuclear factor-κb
ODN	oligodeoxynucleotide
p	pico ( $10^{-12}$ )
PAMP	pathogen-associated molecular pattern
PBS	phosphate buffered saline
PCR	polymerase chain reaction
Poly(I:C)	polyinosinic:polycytidylic acid
PRR	pattern recognition receptor
RNA	ribonucleic acid
RNase	ribonuclease
RNI	reactive nitrogen intermediates
ROS	reactive oxygen species
rpm	rounds per minute
RPMI	Roswell Park Memorial Institute
RT	reverse transcription
SAGM	small airway epithelial cell growth medium
SEM	standard error of the mean
SSC	sideward scatter
STAT	signal transducer and activator of transcription
TBE	tris borate EDTA buffer
TE	tris EDTA buffer
TGF	transforming growth factor
TIR	Toll/IL-1 receptor
Th	T helper
TLR	toll-like Receptor
TNF-α	tumor necrosis factor-α
TRIF	TIR domain-containing adapter inducing IFN-β
Tris	α,α,α-tris-(hydroxymethyl)-methylamine
TTP	tristetraprolin
U	unit
UV	ultra violet
[v/v]	volume per volume
V	volt
[w/v]	weight per volume
zeo	zeocin



## **Abstract**

Toll-like receptor (TLR) activation plays a crucial role in both infectious as well as non-infectious lung disease. TLRs are capable of sensing different microbial and viral molecular patterns, and TLR engagement is a prerequisite for the initiation of macrophage responses to infections. Thus, aim of this work was to elucidate different aspects of TLR activation in human pulmonary macrophages.

Interestingly, the activation profiles of the two macrophage populations examined, i.e. alveolar and interstitial macrophages, differed largely, indicating that alveolar macrophages are more effective as a non-specific first line of defence against inhaled pathogens, whereas interstitial show a more pronounced regulatory function.

The glucocorticoid-induced leucine zipper (GILZ) is highly expressed in human alveolar macrophages and critically attenuates inflammatory signalling pathways. The mechanisms of GILZ regulation in inflammation, however, have as yet been completely unknown. Our investigations on the expression of GILZ in human alveolar macrophages upon TLR activation reveal that GILZ is downregulated by different post-transcriptional mechanisms. Both the TLR signalling pathways and GILZ have emerged as potential therapeutic targets for the treatment of inflammatory lung diseases. Our results support this concept and contribute to a better understanding of their role in pulmonary immune homeostasis.

## **Zusammenfassung**

Die Aktivierung von Toll-like Rezeptoren (TLRs) ist von großer Bedeutung für den Verlauf infektiöser sowie nicht infektiöser Erkrankungen der Lunge. TLRs ermöglichen die Erkennung verschiedenster mikrobieller und viraler Muster, und die Aktivierung von TLRs stellt eine Voraussetzung für die Einleitung von Abwehrmechanismen in Lungenmakrophagen dar.

Im Rahmen dieser Arbeit wurde die Expression von pro- und anti-inflammatorischen Mediatoren nach TLR-Aktivierung in humanen Lungenmakrophagen untersucht. Dabei ließen sich große Unterschiede zwischen Alveolarmakrophagen und interstitiellen Makrophagen feststellen. Unsere Ergebnisse legen nahe, dass Alveolarmakrophagen eine

effektive erste Abwehr von Pathogenen vermitteln, während interstitielle Makrophagen eher in regulatorische Prozesse involviert sind.

Der anti-inflammatorische Faktor GILZ (*glucocorticoid-induced leucine zipper*) wird von Lungenmakrophagen stark exprimiert. Die Regulationsmechanismen, denen GILZ im Rahmen einer Entzündungsreaktion unterliegt, waren bisher jedoch unbekannt. Unsere Untersuchungen zur Expression von GILZ in Alveolarmakrophagen zeigen erstmals, dass GILZ nach TLR-Aktivierung herabreguliert wird und liefern Einblicke in die zugrunde liegenden Mechanismen.

Die Aufklärung der Mechanismen, die in die Regulation von GILZ und TLR-Signalwegen involviert sind, kann zu einem besseren pathophysiologischen Verständnis und somit zu einer besseren Therapierbarkeit von entzündlichen Lungenerkrankungen beitragen.

# 1. Background



## 1.1. Inflammatory lung diseases

Inflammatory processes in the lung play an important role in pulmonary diseases, such as bacterial and viral infections. The pharyngeal mucosa is colonized by microorganisms, which do not necessarily cause inflammatory reactions (Wissinger et al., 2009; Tlaskalová-Hogenová et al., 2004). In contrast, the lower respiratory tract is considered to be sterile, and invasion of pathogenic microbes into the lower respiratory tract leads to immediate immune responses (Harris et al., 2007). The World Health Organization (WHO) estimates 429 million cases of acute lower respiratory tract infections in 2004 worldwide, making it the third leading cause of death in the world (WHO, 2010a). Besides infectious diseases like tuberculosis, also non-infectious diseases, such as asthma and chronic obstructive pulmonary disease (COPD), are characterized by chronic inflammatory processes and have gained major clinical relevance (Caramori and Adcock, 2003; Peden and Reed, 2010).

### 1.1.1 Tuberculosis

Tuberculosis is the one of the most important examples of pulmonary infections: one third of the world population is infected with its causative agent, *Mycobacterium tuberculosis*, and an estimated 1.3 million people died from TB in 2008 (WHO, 2010b). Those infected with *Mycobacterium tuberculosis* usually display an asymptomatic, latent infection progression, with only a 10% lifetime chance that a latent infection will progress to active tuberculosis (WHO, 2010b). If untreated, however, the mortality in active cases of tuberculosis was reported to be greater than 50% (Onyebujoh and Rook, 2004).

When mycobacteria reach the pulmonary alveoli, they invade and replicate within the endosomes of alveolar macrophages (Houben et al., 2006). Bacteria are also engulfed by dendritic cells, leading to the transport of mycobacteria to local lymph nodes. In this manner, bacteria are enabled to further spread through the bloodstream. As a result, secondary tuberculosis lesions can develop in other parts of the lung, but also in peripheral lymph nodes, kidneys, brain, and bone (Herrmann and Lagrange, 2005). Tuberculosis is characterized by the formation of granulomas, in which different cell types, such as macrophages, T cells, B cells, and fibroblasts are involved, with lymphocytes surrounding the infected macrophages. The granuloma not only prevents spreading of the mycobacteria, but also provides an environment for a rather efficient immune response.

However, bacteria are not always eliminated within the granuloma, which results in a latent infection (Houben et al., 2006; Onyebujoh and Rook, 2004).

Antibiotic therapy of tuberculosis is difficult due to the structure of the mycobacterial cell wall (Onyebujoh and Rook, 2004; Brennan and Nikaido, 1995). The two antibiotics commonly used are rifampicin and isoniazid, which have to be applied up to 24 months to entirely eliminate mycobacteria from the body. Increasing numbers of extensively drug-resistant tuberculosis infections complicate efficient tuberculosis treatment (WHO, 2010b). Attempts to prevent tuberculosis involve the *Bacillus Calmette-Guérin* (BCG) vaccine, which originates from an attenuated mycobacterial strain, *Mycobacterium bovis*. Although BCG provides protection against serious forms of tuberculosis in children, it has been shown to be ineffective against adult pulmonary tuberculosis (Onyebujoh and Rook, 2004).

### **1.1.2 Asthma and allergic diseases**

The prevalence of allergic respiratory diseases such as rhinosinusitis and bronchial asthma has risen in industrialized countries over the last 30 years (D'Amato et al., 2010), possibly as a result of the decreasing number of childhood infections (Cookson and Moffatt, 1997; Rook and Stanford, 1998).

In 2009, 300 million people worldwide were affected by asthma, leading to 250,000 deaths per year. Bronchial asthma is characterized by airway inflammation, hyperresponsiveness and chronic airflow obstruction. Bronchoconstriction not only occurs in response to allergens to which an individual is sensitized, but also to a range of nonspecific stimuli, such as cold air and air pollutants (D'Amato et al., 2010). Acute symptoms are usually treated with bronchodilators like salbutamol, whereas symptom prevention can be achieved by long-term usage of inhaled glucocorticoids or leukotriene modifiers (Yawn, 2008).

Apart from environmental parameters including allergen exposure, the development of an asthma or atopy phenotype is also influenced by genetic factors (Cookson and Moffatt, 2000; von Mutius et al., 1992). Sequence variants in hundreds of genes have been found to be related to asthma (Halapi and Bjornsdottir, 2009). Many of these genes are coding for factors associated with immune response, e.g. the interleukin (IL) 4 receptor or Major Histocompatibility Complex (MHC) II molecules. In fact, various cell types of innate and adaptive immunity, such as macrophages, mast cells and T helper 2 (Th2) cells, were found to be critically involved in dysregulation of lung homeostasis in asthma, resulting in

airway inflammation and tissue damage (Ichinose, 2009; Schröder, 2009). However, mechanisms underlying this chronic inflammatory state are poorly understood.

### **1.1.3 Chronic obstructive pulmonary disease (COPD)**

COPD is a chronic inflammatory disease characterized by chronic bronchitis, fibrosis, irreversible narrowing of small airways, and emphysema. The WHO estimates that more than 3 million people died of COPD in 2005, which is equal to 5% of all deaths globally that year, and total deaths from COPD are projected to increase by more than 30% in the next 10 years (WHO, 2010c). In contrast to asthma, airway obstruction associated with COPD is poorly reversible and usually progresses over time. Cigarette smoking represents the primary risk factor for COPD, as inhalation of noxious components of tobacco smoke leads to a dysregulation of the inflammatory response in the lung (Rabe et al., 2007; Hogg et al., 2004; Barnes, 2004). Inflammation of the larger airways results in chronic bronchitis, whereas in the alveoli, the inflammatory response causes destruction of the lung parenchyma, thus leading to emphysema. In addition, respiratory infections might also play a role in the development and progression of the disease and are the major cause of acute exacerbations (Sethi and Murphy, 2008; Barnes, 2008; Sabroe et al., 2007).

There is a specific pattern of inflammation in COPD, characterized by increased numbers of macrophages, neutrophils, and cytotoxic (CD8+) T-lymphocytes (Barnes et al., 2003). This pattern of inflammation is also seen in cigarette smokers with normal lung function, but the intensity of the inflammation is increased in COPD with increased numbers of inflammatory cells and mediators. The chronic inflammation in COPD is associated with increased expression of multiple inflammatory genes, involving cytokines, chemokines, and adhesion molecules. Many of these inflammatory genes are regulated by the transcription factor nuclear factor (NF)- $\kappa$ B, which has been shown to be constitutively activated in inflammatory cells of COPD patients, particularly in alveolar macrophages (Di Stefano et al., 2002). COPD is not curable, but treatment can slow the progress of the disease. Besides the avoidance of risk factors such as smoking, bronchodilator medications are central to the symptomatic management of COPD.

Additional treatment with inhaled glucocorticosteroids is considered to be appropriate for patients with severe forms of COPD and repeated exacerbations (Rabe et al., 2007). Interestingly, in COPD and asthma patients who smoke, glucocorticoids fail to suppress inflammation, which is considered to be due to a loss of histone deacetylase (HDAC2) activity and expression as a result of oxidative and nitrative stress (Barnes et al., 2004).

## 1.2. Macrophages as mediators of pulmonary inflammation

### 1.2.1 Overview of macrophage functions

Macrophages are a major component of the mononuclear phagocyte system that consists of cells of bone marrow origin, including blood monocytes, and tissue macrophages (Hume, 2006). They are capable of many functional activities that contribute to the initiation of a cell-mediated immune response and also act as effectors of inflammation. During the course of their activation, macrophages can display both inflammatory and anti-inflammatory activities (Mosser and Edwards, 2008; Fujiwara and Kobayashi, 2005; figure 1).

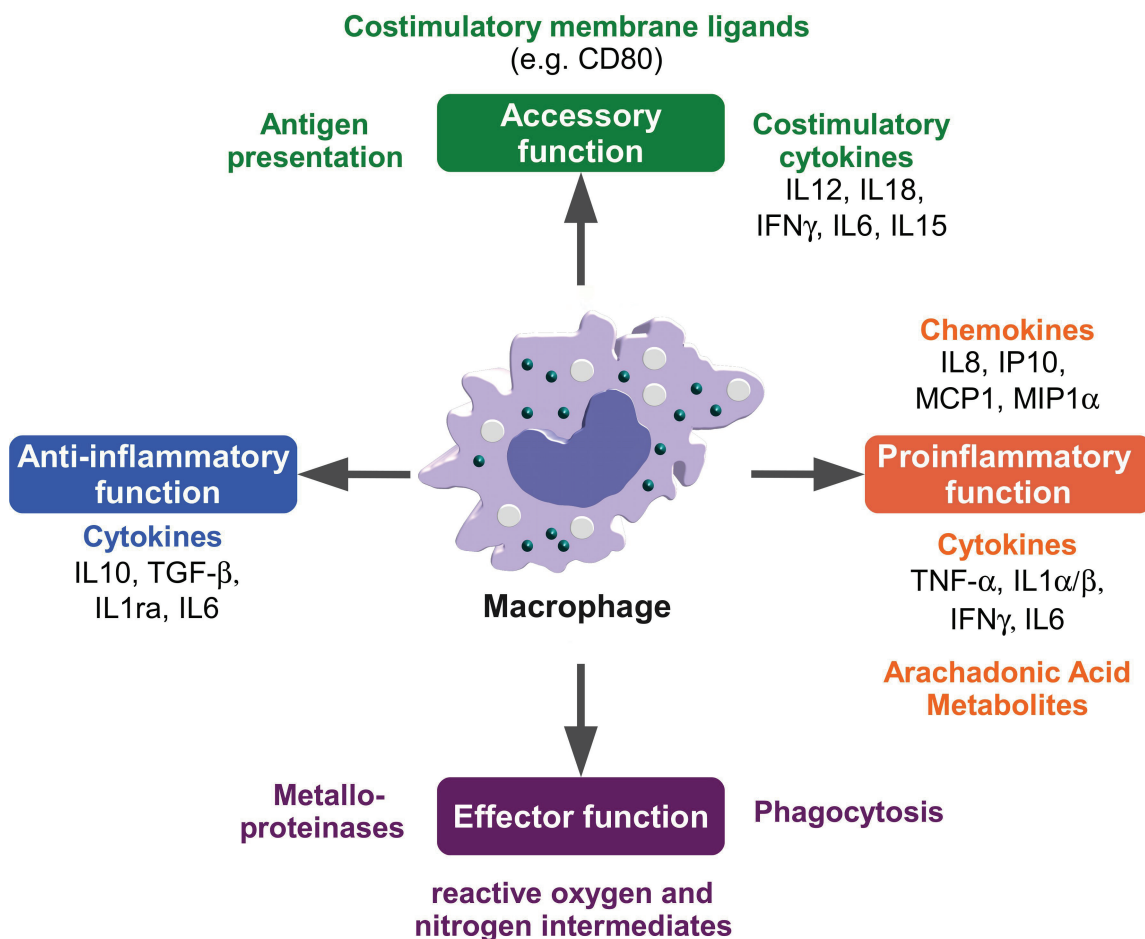


**Figure 1: The diverse functions of macrophages.** Modified after Stout and Suttles (1997). IL: interleukin, IFN: interferon, IP10: IFN inducible protein 10, MCP1: macrophage chemoattractant protein 1, MIP1 $\alpha$ : macrophage inflammatory protein 1 $\alpha$ , TNF- $\alpha$ : tumor necrosis factor- $\alpha$ , TGF- $\beta$ : transforming growth factor- $\beta$ , IL1ra: IL1 receptor antagonist.

Macrophages differentiate from circulating peripheral blood mononuclear cells, which migrate into tissue in the steady state or in response to inflammation (Gordon and Taylor, 2005). Mononuclear cells develop from a common myeloid progenitor cell in the bone marrow, which represents the precursor of many different cell types, including neutrophils, eosinophils, basophils, macrophages, dendritic cells, and mast cells. Myeloid progenitor cells sequentially develop to monoblasts, pro-monocytes, and finally monocytes, which are released from the bone marrow into the bloodstream (Gordon and Taylor, 2005). Monocytes then migrate from the blood into tissue to differentiate into long-lived tissue specific macrophages of the alveoli, liver (Kupffer cells), central nervous system (microglia), skin (Langerhans cells), bone (osteoclasts), connective tissue, gastrointestinal tract, spleen and peritoneum (Gordon and Taylor, 2005).

Macrophages are highly phagocytic cells. One of their major functions is to clear extraneous cellular material, such as erythrocytes, apoptotic cells or cellular debris generated during tissue remodelling. Interestingly, the removal of apoptotic cells seems to result in little or no production of inflammatory mediators by unstimulated macrophages (Kono and Rock, 2008). The receptors that mediate phagocytosis in these clearance processes include scavenger receptors, phosphatidyl serine receptors, integrins and complement receptors (Erwig and Henson, 2007). Generally, activation of these receptors either fails to induce transcription of proinflammatory mediators or actively induces inhibitory signals and cytokines. Thus, most processes involving phagocytosis by macrophages are independent of other immune cells (Mosser and Edwards, 2008).

In contrast, uptake of cellular debris resulting from necrosis due to trauma or stress markedly alters the physiology of macrophages. The released endogenous molecules are then called danger-associated molecular patterns (DAMPs) and include heat-shock proteins, nuclear proteins, such as high-mobility group box 1 protein (HMGB1), histones, DNA and other nucleotides, and components of the extracellular matrix (Zhang and Mosser, 2008). The DAMP recognition by macrophages leads to inflammatory responses upon sterile tissue damage by production of cytokines and pro-inflammatory mediators (Kono and Rock, 2008).

During infections, macrophages recognize components of bacterial or viral origin (pathogen associated molecular patterns, PAMPs) *via* pathogen recognition receptors (PRRs). These include the well-characterized Toll-like receptors (TLRs), as well as the recently described cytosolic NOD-like receptors, RIG-I-like receptors, and DNA sensors (Opitz et al., 2010). Additionally, many PRRs are also activated by DAMPs. Once a

pathogen is recognized and engulfed, macrophages produce a wide range of biologically active molecules, including proinflammatory cytokines, chemokines, growth factors, and immunomodulatory mediators (figure 1). Cytokines released by macrophages, such as interferons, TNF- $\alpha$ , and IL1 $\alpha/\beta$ , stimulate activity of both the innate and adaptive immune response. Moreover, macrophages represent professional antigen presenting cells, as they are able to present antigens to T cells, thus generating a highly specific T-cell response (Fujiwara and Kobayahi, 2005).

Activated macrophages are deactivated in response to various mediators, including IL10, prostaglandins, G-protein coupled receptor ligands or glucocorticoids (Mosser and Edwards, 2008). IL10 and other anti-inflammatory factors, such as C-C chemokine ligand 1 (CCL1), are also produced by macrophages themselves, and failure to induce these mediators might lead to nonresolving inflammation (Fujiwara and Kobayashi, 2005; Mosser and Edwards, 2008; Nathan and Ding, 2010). Macrophages not only contribute to resolution of inflammation by suppression of inflammation, but also by driving tissue repair. Macrophages associated with wound healing arise in response to IL4 secreted by granulocytes during an innate immune response as well as Th2 cells during an adaptive immune response and contribute to tissue repair by producing components of the extracellular matrix (Mosser and Edwards, 2008).

### **1.2.2 Macrophages in inflammatory lung disease**

During infections, the first line of defense in the respiratory tract is provided by the barrier function of epithelia, the mucociliary system that carries inhaled particles away from the lower respiratory tract, and constitutively expressed antimicrobial peptides, lysozyme, and surfactant proteins (Bals et al., 2004; Mizgert, 2008). In addition, the pharyngeal microflora also contributes to host defense by out-competing some pathogenic species, but can also become harmful when aspirated into the lower respiratory tract (Wissinger et al., 2009). The important second- and third-line defenses are provided by the innate and the adaptive immune responses, both of which, directly or indirectly, depend on macrophage action. In addition, DAMP recognition by macrophages leads to inflammatory responses upon sterile tissue damage and appears to be critically involved in noninfectious inflammations associated with lung injury (Rock and Kono, 2008; Jiang et al., 2005; Imai et al., 2008). Stimulation of macrophages by PAMPs, DAMPs or tobacco smoke is involved in remodeling and destruction of lung parenchyma, potentially leading to emphysema or interstitial fibrosis (Dostert et al., 2008; Barnes, 2008; Doz et al., 2008). There is also

evidence for macrophages being critically involved in pathogenesis of allergic and granulomatous diseases like asthma and sarcoidosis (Ichinose, 2009; Bedoret et al., 2009; Gerke and Hunninghake, 2008). Excessive macrophage activation is also considered to play a key role in the pathogenesis of COPD (Barnes, 2004).

### 1.2.3. Macrophage populations within the respiratory tract

At least three different types of mononuclear cells were reported to reside within distinct compartments of the lung: the alveolar macrophage (AM) the interstitial macrophage (IM), and the dendritic cell (DC) (figure 2; Lohmann-Matthes et al., 1994; Laskin et al., 2001; Bedoret et al., 2009). AM and IM represent the two largest macrophage populations of the lung, with the number of AM being equal to or slightly exceeding the number of IM, whereas lung DC account for less than 4% of all pulmonary mononuclear cells (Demedts et al., 2004; Lohmann-Matthes et al., 1994).

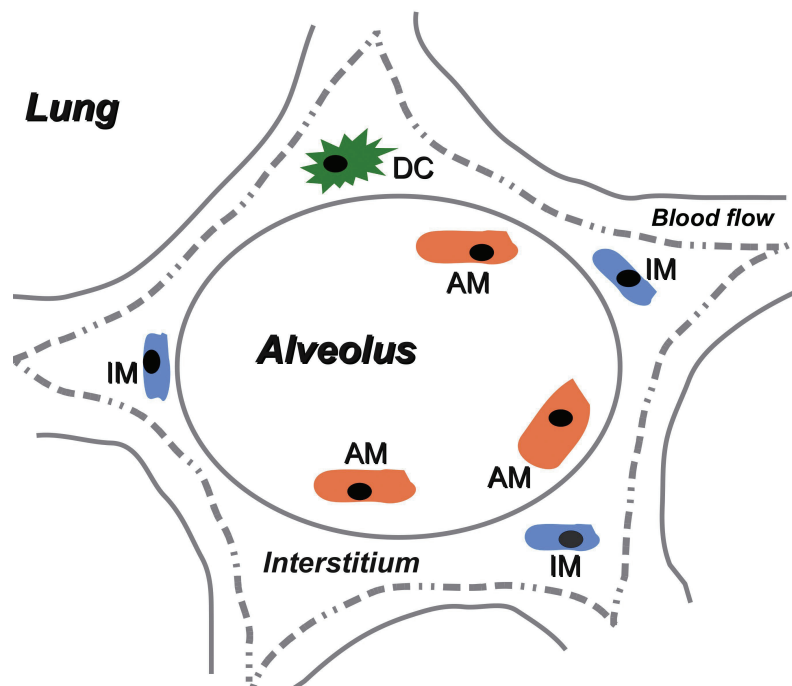


**Figure 2: Localization of AM, IM and lung DC.** Modified after Laskin et al. (2001).

AM are located within the alveoli, thus taking a unique position with direct contact to both air- and bloodborne materials. They represent the primary defence against inhaled microorganisms, particles, and environmental toxins that enter the lower respiratory tract. AM constitute the best characterized lung macrophage population, as they are easily accessible by bronchoalveolar lavage. The less extensively characterized IM reside within

the connective tissue surrounding the alveoli. They have been described as small compared to alveolar macrophages, and in general more closely resemble monocytes. This lead to the conclusion that IM might be a precursor of AM, with the interstitium providing the environment for maturation of freshly arrived monocytes (Laskin et al., 2001). However, there is some evidence in the literature indicating that AM and IM are distinct cell populations with their own functional properties. Several studies using primary rat or mouse macrophages suggest that AM are more effective than IM in producing cytokines involved in an antimicrobial defence whereas IM express higher levels of MHCII molecules and have a more pronounced accessory function (Lohmann-Matthes et al., 1994; Franke-Ullmann et al., 1996; Laskin et al., 2001; Bedoret et al., 2009).

Lung DC, which may or may not belong to the macrophage lineage (Hume, 2008), can be morphologically distinguished by their typical cytoplasmatic extensions (“dendrites”). Lung DCs are localized within airway epithelium and in the connective tissue surrounding pulmonary vessels and alveoli. They exhibit a high expression of major histocompatibility complex (MHC) II molecules, as their major function is to process antigens and to present them on their surface. Once activated, they migrate to the local lymph nodes to interact with B and T cells, thereby initiating an adaptive immune response. In general, lung DC possess an immature phenotype with an enhanced endocytotic capacity, but, unlike other immature DC populations, they are powerful stimulators of T cell response (Demedts et al., 2004; Cochand et al., 1999; Lohmann-Matthes et al., 1994).

Most interestingly, a recently published study indicated that IM can be distinguished from AM by their ability to suppress lung DC maturation and migration upon LPS stimulation (Bedoret et al., 2009). In this manner, IM are considered to prevent LPS-triggered responses to harmless inhaled antigens, which would otherwise provoke the development of allergic diseases or asthma.

### 1.3. Toll-like receptors (TLRs)

TLRs represent the most prominent family of PRRs. TLRs enable cells, especially those of the innate immune system, to recognize a broad spectrum of PAMPs associated with bacterial and viral infections. Moreover, many TLRs are involved in DAMP recognition and thereby also play a crucial role in sterile inflammation.

TLRs owe their name to their homology to the Toll-protein, which was originally identified in *Drosophila melanogaster* (Anderson and Nüsslein-Vollhardt, 1984). Ten human and thirteen murine TLRs have as yet been identified. The members of the TLR family consist of a cytoplasmic Toll/IL-1 receptor homology (TIR) domain mediating downstream signalling, and of an extracellular leucine-rich repeat (LRR) domain, that is most likely responsible for ligand binding. All TLRs function as homodimers, except TLR2 which also forms heterodimeric complexes with TLR1 and TLR6. TLRs are either located at the cell surface (TLR1/2 and TLR2/6 heterodimers, TLR2 homodimers, TLR4, TLR5, TLR10) or in endosomal membranes (TLR3, TLR7–9; figure 3) (Lundberg and Hansson, 2010, Opitz et al., 2010, Kawai and Akira, 2006).

#### 1.3.1 Ligands

Different microbial as well as endogenous ligands have been identified for most human TLRs except TLR10, whose function presently remains elusive (Lundberg and Hansson, 2010; Opitz et al., 2010; figure 3).

TLR2, together with TLR1, recognizes bacterial triacetylated lipopeptides from Gram negative bacteria or mycobacteria as well as the synthetic compound Pam<sub>3</sub>CSK<sub>4</sub>. In cooperation with TLR6, TLR2 detects diacylated lipopeptides from mycoplasma or Gram positive bacteria, bacterial lipoteichoic acids, and zymosan from yeast (Lundberg and Hansson, 2010; Opitz et al., 2010; Kawai and Akira, 2006). Recognition of lipoteichoic acids by TLR2 homodimers has also been described (Beutler, 2004). Moreover, TLR2 appears to be involved in the recognition of endogenous hyaluronan and high-mobility group box 1 (HMGB1) (Jiang et al., 2005; Park et al., 2006).

TLR3 detects double-stranded (ds)RNA, which represents an intermediate in viral replication, as well as its synthetic analogon Poly(I:C) (Alexopoulou et al., 2001; Blasius and Beutler, 2010). TLR3 has also been reported to respond to endogenous mRNA released from necrotic cells (Cavassani et al., 2008; Kariko et al., 2004).

TLR4 recognizes LPS of Gram negative bacteria, but also other bacterial structures or toxins. Binding of LPS to TLR4 is considered to require a number of accessory proteins, namely CD14, Ligand Binding Protein (LBP), and MD2. Additionally, TLR4 also detects endogenous compounds, such as HMGB1, hyaluronan, and oxidized lipoproteins and phospholipids (Kawai and Akira, 2006; Opitz et al., 2010)

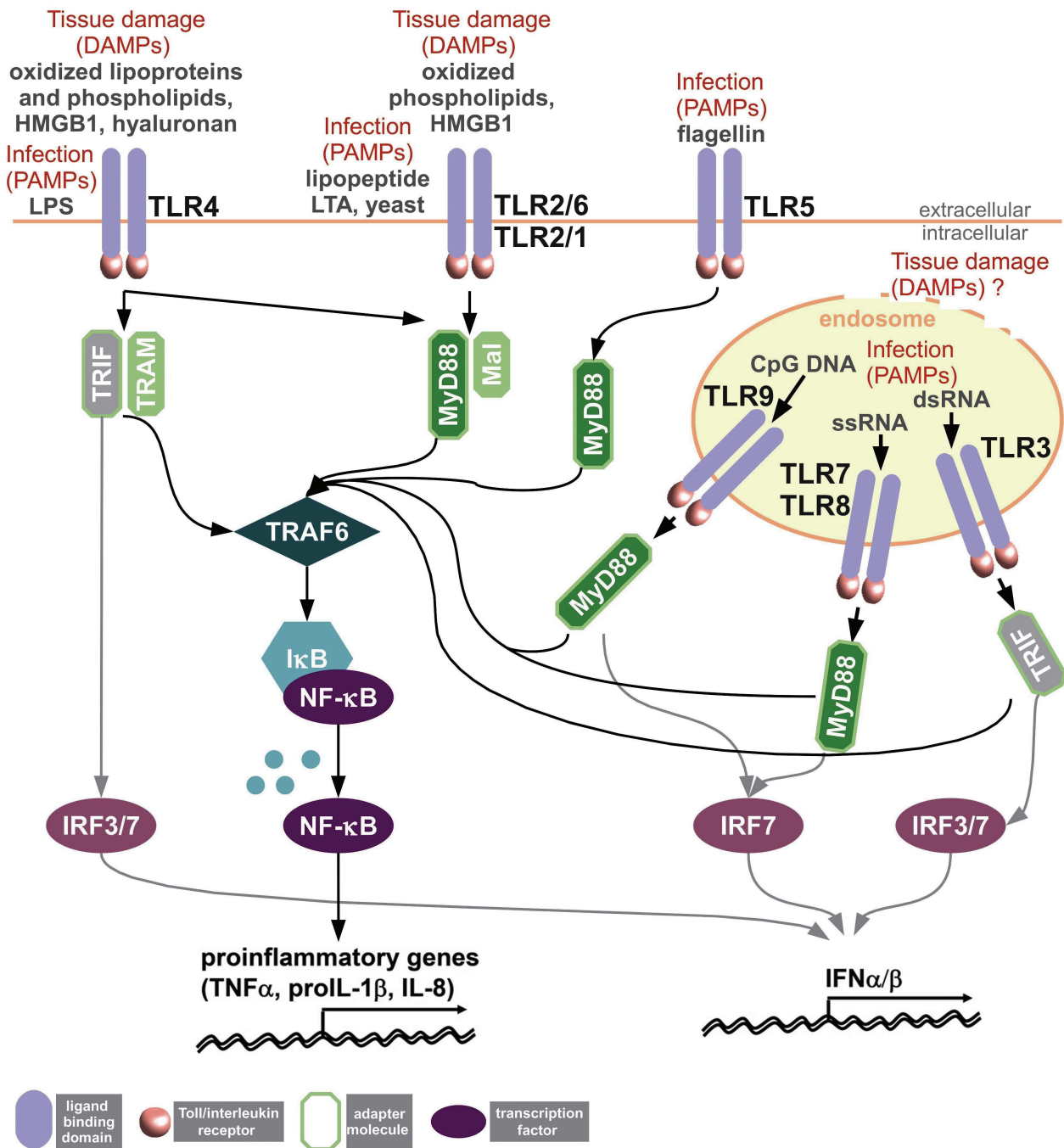


**Figure 3: TLR activation and signalling.** See text for details. Modified after Opitz et al. (2010).

In contrast to the TLRs described above, TLRs 5, 7, 8 and 9 seem to be specific for only one type of pathogen associated structure, each. TLR5 recognizes extracellular bacterial flagellin, TLR7 and TLR8 are both intracellular receptors for microbial single-stranded (ss)RNA. Bacterial DNA is recognized by TLR9 *via* its unmethylated CpG motifs, thereby distinguishing mammalian from bacterial DNA (Lundberg and Hansson, 2010; Opitz et al., 2010; Kawai and Akira, 2006).

### 1.3.2 Signalling

The binding of TLR ligands initiates the activation of transcription factors, such as NF- $\kappa$ B and IRFs (IFN regulating factors), finally resulting in a proinflammatory response. TLRs display a differential ability to activate transcription factors due to varying involvement of the four TIR domain-containing adapter molecules MyD88 (myeloid differentiation primary response gene 88), Mal (MyD88-adapter-like, also known as TIRAP, Toll/IL1 domain containing adapter protein), TRIF (TIR domain-containing adapter inducing IFN- $\beta$ ), and TRAM (TRIF-related adapter molecule) in their signalling pathways (Lundberg and Hansson, 2010, Opitz et al., 2010; figure 3).

#### *MyD88 dependent signalling*

All TLRs with the exception of TLR3 are able to initiate MyD88-dependent signalling. Whereas TLRs 5, 7, 8 and 9 directly interact with MyD88, TLR2 and 4 signalling additionally requires Mal for MyD88 association. Binding of MyD88 subsequently recruits protein kinases of the IL1 receptor associated kinase family (IRAK), thus leading to IRAK1 phosphorylation by IRAK4. IRAK1 then binds to tumor necrosis factor receptor associated factor (TRAF) 6, which activates the inhibitor  $\kappa$ B kinase (IKK) complex in return. As a result, the NF- $\kappa$ B inhibitor I $\kappa$ B is sequentially phosphorylated, ubiquitinated and degraded, thereby allowing NF- $\kappa$ B to translocate into the nucleus. NF- $\kappa$ B induces the transcription of proinflammatory genes, such as TNF- $\alpha$ , IL-8, and other cytokines, which subsequently regulate the inflammatory response and contribute to leukocyte recruitment (Jenkins and Mansell, 2010). Additionally, TRAF6 is capable to induce the mitogen activated protein kinase (MAPK) signalling cascade *via* activation of transforming growth factor (TGF)- $\beta$  activated kinase 1 (TAK1). Phosphorylation of c-Jun NH2-terminal kinase (JNK) and the p38 MAPK *via* TAK1 finally results in the activation of transcription factor activator protein 1 (AP-1) and thereby in proinflammatory gene expression.

Apart from NF- $\kappa$ B and MAPK activation, TLRs 7 and 8 are able to activate IRF transcription factors. Thereby, they mediate type I IFN responses, which play a key role in the antiviral defense (Jenkins and Mansell, 2010; Opitz et al., 2010).

#### *MyD88 independent signalling*

MyD88 independent signalling *via* TLR3 or TLR4 utilizes the TIR domain containing adapter inducing IFN- $\beta$  (TRIF) for signal transduction. In contrast to TLR3, TLR4 signalling additionally requires the TRIF-related adapter protein (TRAM). Upon activation, TRIF interacts with TRAF6 and/or TRIF/receptor-interacting protein 1 (RIP1), resulting in NF- $\kappa$ B activation due to I $\kappa$ B degradation. In addition, TRIF can also activate the TRAF family member-associated NF- $\kappa$ B activator (TANK)-binding kinase 1 (TBK1), which phosphorylates the transcription factors IRF3 and 7, which subsequently leads to the expression of type I IFNs (Jenkins and Mansell, 2010; Opitz et al., 2010).

### **1.3.3 TLR expression within the lung**

Most cell types residing in the lung, including macrophages, DCs, epithelial and endothelial cells, express TLRs. Human AM were recently shown to express all ten TLRs (Kiemer et al., 2009), although previous studies suggested that TLR3, TLR5 and TLR9 were absent in this cell type (Maris et al., 2006). Similarly, murine AM were reported to lack TLR9 (Suzuki et al., 2005). IM were reported to respond to LPS, indicating that they express TLR4 (Lohmann-Matthes et al., 1994; Bedoret et al., 2009). Both TLR9 and TLR7 were highly expressed in plasmacytoid DCs of the human lung, whereas TLRs 1-4 were detected in human myeloid lung DCs (Holt et al., 2008). Tracheal, bronchial, and alveolar epithelial cells express most TLRs, including TLR1-6 as well as TLR9 (Mayer et al., 2007; Greene and McElvaney, 2005). Lung endothelial cells are equipped with TLR2, TLR4, TLR8 and possibly additional TLRs (Li et al., 2004; Fan et al., 2003). Furthermore, lung fibroblasts have been shown to express TLRs 2, 3, 4, and 9 (He et al., 2009; Meneghin et al., 2008; Sugiura et al., 2009), and airway smooth muscle cells were shown to respond to ligands of TLRs 2, 3, and 4 (Sukkar et al., 2006).

### **1.3.4 TLRs and pulmonary inflammation**

TLRs play a key role in infections of the lung, but also in noninfectious diseases such as COPD and asthma. Specifically, the cell surface TLRs (e.g. TLR2, 4, and 5) are key players in immune responses to extracellular bacteria, whereas the endosomal TLRs

(TLR7–9) are particularly important in viral infections, but also contribute to host defence against bacterial infections. Mice deficient in the TLR adapter molecule MyD88 are highly susceptible to *Streptococcus pneumoniae* or *Klebsiella pneumoniae* infections due to an impaired immune response. Similar findings were reported for TLR4 or TLR9 knockout mice (Opitz et al., 2010). Furthermore, *Mycobacterium tuberculosis* bears agonists for several TLRs, such as TLR1/2 or TLR9. Accordingly, MyD88<sup>-/-</sup> mice fail to control the replication of *M. tuberculosis* H37Rv, resulting in reduced cytokine production, acute necrotic pneumonia and increased mortality (Scanga et al., 2004; Fremont et al., 2004).

Interestingly, studies in mice and human macrophages suggested that exposure to tobacco smoke activates TLR4, either directly by smoke components or release of DAMPs upon cell injury. As a result, TLR4 activation might trigger chronic inflammation in COPD (Doz et al., 2008; Karimi et al., 2006). COPD patients also exhibit an increased susceptibility to pulmonary infections, e.g. with *S. pneumoniae* or *Haemophilus influenzae*. Infections with these and other pathogens are considered to contribute to chronic inflammation as well as acute exacerbations. The increased pulmonary colonization with pathogens appears to be related to an impaired innate immune response in addition to a dysfunctional mucociliary clearance (Opitz et al., 2010). In line with those findings, AM isolated from bronchoalveolar lavage fluids from smokers and COPD patients were shown to express decreased levels of TLR2 and to produce less TNF- $\alpha$  in response to TLR3 and 4 ligands (Droemann et al., 2005; Gaschler et al., 2008), suggesting that TLRs are critically involved in the pathogenesis of COPD.

The influence of TLRs on the pathogenesis of asthma presently remains elusive. A common mouse model for asthma is based on the combined inhalation of ovalbumin as an antigen and low dose LPS or dsRNA for sensitization and challenge. Exposure to ovalbumin alone does not result in sensitization, suggesting a critical role for TLRs (Eisenbarth et al., 2002; Bedoret et al., 2009; Schröder, 2009). However, epidemiologic studies focusing on TLR polymorphisms yielded conflicting results. For example, the Asp299Gly polymorphism of TLR4, which is found at a frequency of approximately 10% among whites and impairs cytokine induction by LPS, was either positively correlated to the prevalence of asthma in children, positively associated with milder forms of asthma, or not found to be related to the pathogenesis of asthma at all (Schröder, 2009).

## 1.4. Glucocorticoid-induced leucine zipper (GILZ)

### 1.4.1 Structure

The glucocorticoid-induced leucine zipper (GILZ) was originally identified as an anti-inflammatory protein inducible by glucocorticoids in murine T-lymphocytes (D'Adamio et al., 1997). Later on, GILZ was found to mediate numerous glucocorticoid actions, mainly *via* direct interaction and subsequent inhibition of the transcription factors NF- $\kappa$ B and AP-1 (Ayroldi and Riccardi, 2009).

The human GILZ gene, located on chromosome X, encodes a 135 amino acid (aa) protein. The similarity of the nucleotide sequence of human GILZ to murine GILZ is 89% in the entire mRNA and 97% in the coding region, and the human GILZ protein has been reported to be highly homologous to murine GILZ (Cannarile et al., 2001). Murine GILZ is a 137 aa protein with a molecular mass of 17 kDa, characterized by a leucine zipper (LZ) domain (76–97 aa) containing a heptad repeat of leucine residues, an N-terminal domain (1–75 aa) that, contrary to other leucine zipper family members, does not display an obvious DNA-binding sequence, and a C-terminal (98–137 aa), proline (P) and glutamic acid (E) rich (PER) region. GILZ homodimerization, by which GILZ becomes functionally active, occurs through the LZ domain *via* the formation of short parallel coiled-coil  $\alpha$ -helices (figure 4). Both GILZ homodimerization and the PER region have been reported to be necessary for GILZ interaction with the p65 subunit of NF- $\kappa$ B (DiMarco et al., 2007).

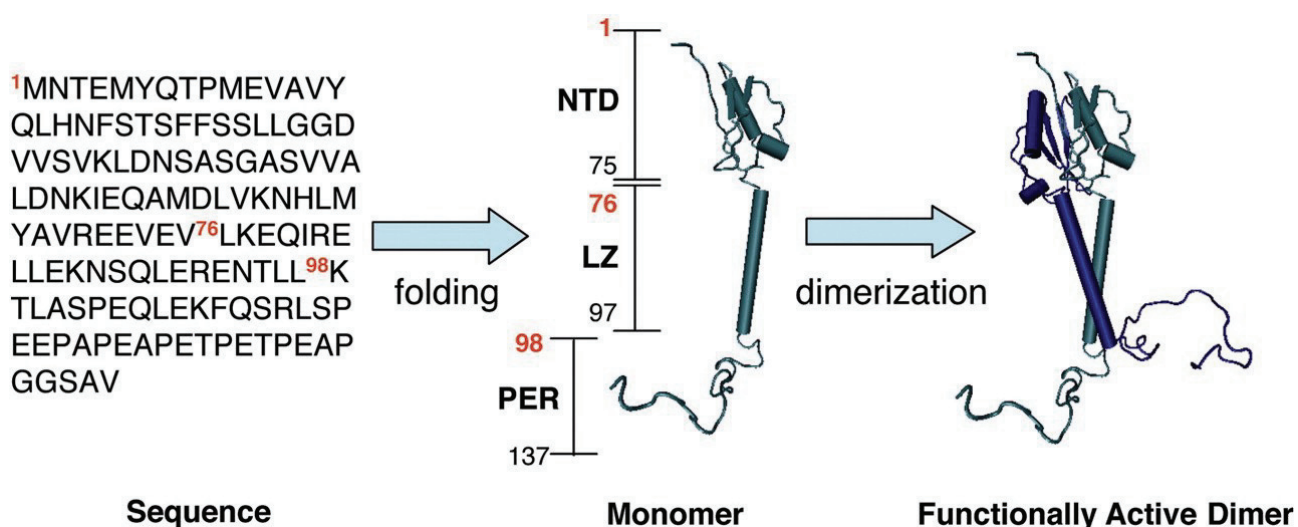


**Figure 4: Correlation of GILZ protein sequence and homodimerization.** Adapted from DiMarco et al. (2007). NTD: N-terminal domain, LZ: leucine zipper, PER: proline and glutamic acid rich region.

Other GILZ isoforms were found in mice, but have not been described for human GILZ yet (Soundajaran et al., 2007; Bruscoli et al., 2010).

The promoter region of human GILZ includes six glucocorticoid responsive elements (GREs), putative binding sites for signal transducer and activator of transcription 6 (STAT6), nuclear factor of activated T cell (NFAT), Oct-1, *c-myc*, cyclic AMP response element-binding protein (CREB), Forkhead responsive elements (FHREs) and estrogen-responsive sequences. GILZ induction by glucocorticoids involves interaction of the activated glucocorticoid receptor with the GRE sequences and might require additional activation of the transcription factor Forkhead box class O3 (FoxO3) (Ayroldi and Riccardi, 2009).

#### **1.4.2 The diverse functions of GILZ**

GILZ plays a role in distinct cell functions, such as the inflammatory response, cell proliferation, and renal sodium transport (figure 5). It is constitutively expressed in many murine and human tissues and has been shown to be upregulated by glucocorticoids in numerous cell types, e.g. macrophages, monocytes, dendritic cells, B cells, T cells, and epithelial cells (Ayroldi and Riccardi, 2009). In addition, GILZ was reported to be induced by IL10 in macrophages (Berrebi et al., 2003) and by aldosterone in murine kidney cells (Ayroldi and Riccardi, 2009).

Both glucocorticoids and IL10 attenuate inflammation and favour immune tolerance by deactivating macrophages and antigen-presenting cells. These actions are considered to be mediated to a significant extent *via* induction of GILZ (Berrebi et al., 2003; Eddleston et al., 2007; Ayroldi and Riccardi, 2009). GILZ impairs the inflammatory process mainly *via* inhibition of the nuclear translocation of NF- $\kappa$ B by direct binding to the NF- $\kappa$ B subunit p65 (Berrebi et al., 2003; Ayroldi and Riccardi, 2009). GILZ was reported to inhibit AP-1 activation in a similar fashion by interaction with its subunits c-fos and c-jun (Ayroldi and Riccardi, 2009). In this manner, GILZ decreases the expression of proinflammatory mediators, such as MIP1 $\alpha$ , TNF- $\alpha$  or IFN $\gamma$ , and inhibits TLR2 expression (Berrebi et al., 2003; Gomez et al., 2010; Hirschfelder et al., 2010). Moreover, GILZ regulates T cell activation and development and redirects the maturation of dendritic cells, thereby preventing an antigen-specific T-cell response (Cohen et al., 2006; Ayroldi and Riccardi, 2009). Interestingly, GILZ was reported to be downregulated in macrophages from inflammatory lesions of delayed-type hypersensitivity reactions, activated lymphocytes and

cytokine challenged epithelial cells (Ayroldi and Riccardi, 2009; Eddleston et al., 2007; Berrebi et al., 2003).

The antiproliferative effects of GILZ, mainly described for T cells, are associated with its interaction with the small GTPase Ras and the kinase Raf. GILZ binds Ras and Raf in dimeric or trimeric complexes and diminishes the activation of Ras / Raf downstream targets, including extracellular-signal regulated kinase (ERK) 1/2 and Akt / protein kinase B (PKB), which results in inhibition of Ras and Raf dependent cell proliferation (Ayroldi and Riccardi, 2009). Accordingly, GILZ was reported to mediate the antiproliferative effects of glucocorticoids in multiple myeloma (Grugan et al., 2008).

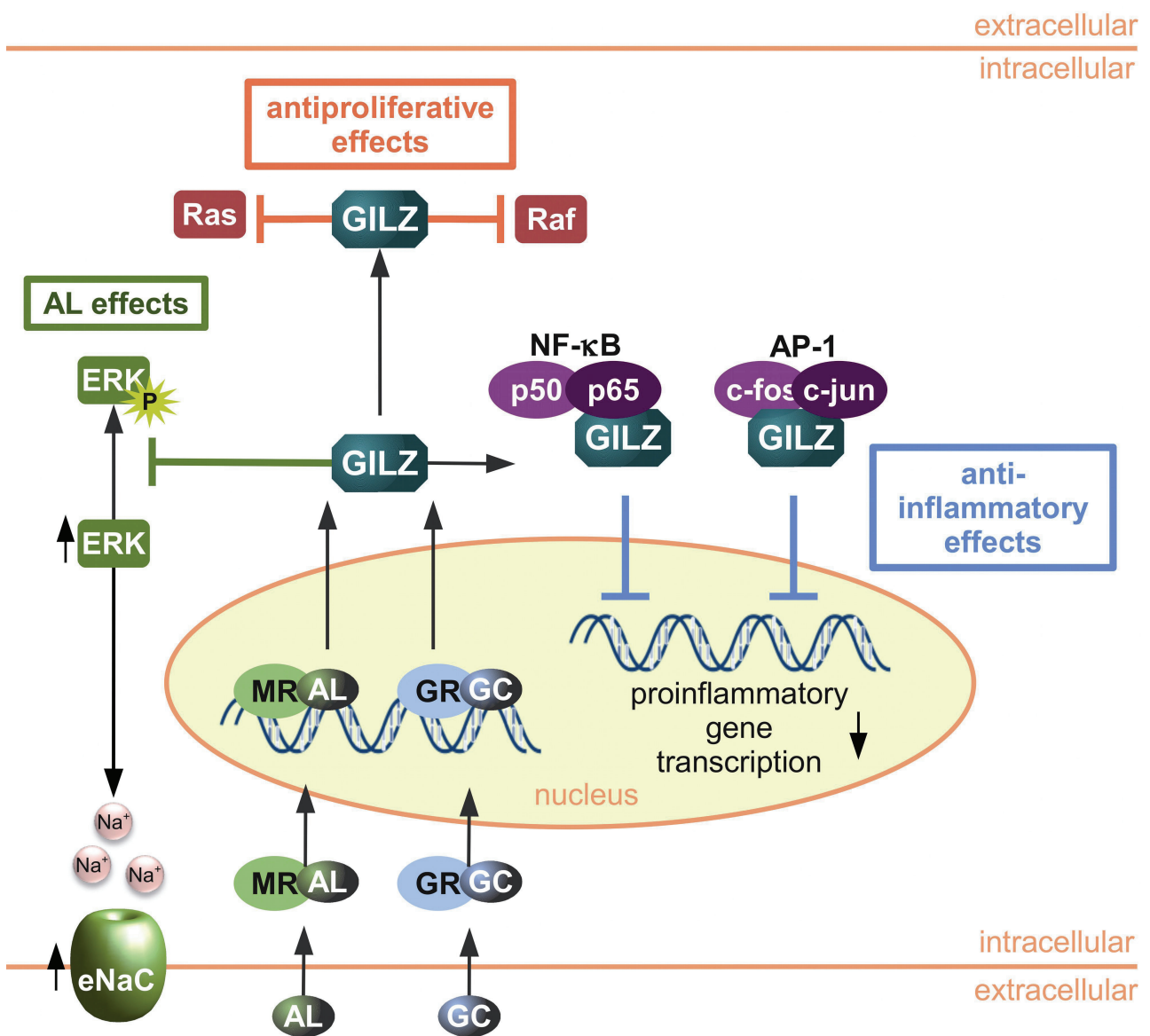


**Figure 5: The diverse functions of GILZ expression.** Modified after Ayroldi and Riccardi (2009). See text for details. AL: aldosterone; GC: glucocorticoid; MR: mineral corticoid receptor; GR: glucocorticoid receptor; eNaC: epithelial sodium channel.

The role of GILZ in oncogenesis, however, is poorly understood. In contrast to the reports mentioned above, GILZ expression was shown to promote proliferation in epithelial ovarian cancer (Redjimi et al., 2009). Moreover, tumor infiltrating macrophages in Burkitt lymphomas were reported to express high levels of GILZ. Thus, GILZ expression in tumor associated macrophages might contribute to immune tolerance, thereby helping the tumor to avoid detection by the immune system (Berrebi et al., 2003).

Besides its influence on inflammation and cell proliferation, GILZ also modulates epithelial sodium transport in the kidney. GILZ, induced by aldosterone, inhibits ERK phosphorylation, leading to increased expression of the epithelial sodium channel (eNaC) and thus stimulates eNaC mediated sodium transport (Ayroldi and Riccardi, 2009; figure 5).

### **1.4.3 GILZ in pulmonary inflammation**

The highest GILZ expression throughout the human body is found within the lung, indicating that GILZ plays an important role in respiratory immune homeostasis (Berrebi et al., 2003; Cannarile et al., 2001). The fact that GILZ is able to trigger pathways central to inflammation, such as TLR signalling, underlines that thesis. However, only few studies described the effects of GILZ expression within the respiratory tract.

GILZ was recently shown to be constitutively expressed in airway epithelial cells and to mediate NF- $\kappa$ b dependent glucocorticoid actions in this cell type. Moreover, GILZ is downregulated by cytokines involved in airway inflammation (Eddleston et al., 2007). Alcohol abuse and smoking are both considered to predispose individuals to infections by bacteria, fungi and viruses (van der Haart et al., 2004; Nelson and Kolls, 2002), although the mechanisms underlying this phenomenon are not entirely clear. Interestingly, cigarette smoke was reported to induce GILZ expression while attenuating TLR3 signalling in airway epithelial cells (Lee et al., 2009). In rats, chronic ethanol ingestion was shown to diminish inflammatory cytokine production of AM (D'Souza et al., 1996). Accordingly, exposure of airway epithelial cells to ethanol leads to a reduced responsiveness to inflammatory stimuli, whereas GILZ was upregulated, and overexpression of GILZ partially mimicked the anti-inflammatory actions of ethanol in these cells (Gomez et al., 2010). These findings suggest that GILZ upregulation might contribute to pulmonary immune suppression due to smoking and chronic alcohol abuse.

## 1.5. Aim of the present work

Inflammatory processes in the lung caused by infections or tissue damage are often associated with TLR-mediated activation of lung macrophages. The primary function of macrophages in the innate immune response is to contain and kill invading microbial pathogens, which is achieved by a series of rapid and coordinated responses. Macrophages have a potent antimicrobial arsenal that includes reactive oxygen and nitrogen species, proteolytic enzymes and cationic microbicidal proteins. Under pathological circumstances, however, unregulated release of microbicidal compounds into the extracellular space can damage host tissues. In contrast, an impaired immune response leads to persistence of the infection and prevents recovery. Thus, macrophage actions can both be beneficial or detrimental to the host. Aim of the present work was to elucidate macrophage actions upon TLR activation, as an understanding of the mechanisms involved might help to develop strategies for the therapy of diseases resulting from unbalanced macrophage activation. The three sections of this thesis focus on distinct aspects of TLR activation in macrophages.

### I.

In tuberculosis, AM are the first line of host defence against mycobacteria. However, an insufficient host response allows survival of bacteria within macrophages. Thus, the first part of this work focuses on the role of TLR9 activation in macrophage defence against mycobacteria.

### II.

Investigations on pulmonary macrophages mostly focus on AM as a well-defined cell population, whereas characteristics of IM are rather ill-defined. In the second part of the present study, we therefore aimed to examine differences between AM and IM obtained from human lung tissue.

### III.

Induction of glucocorticoid-induced leucine zipper (GILZ) by glucocorticoids is critical for their anti-inflammatory action, whereas GILZ expression is reduced under inflammatory conditions. The mechanism regulating GILZ expression during inflammation, however, has not yet been fully characterized. Therefore, we aimed to examine GILZ expression in

primary human alveolar macrophages under inflammatory conditions, i.e. following Toll-like receptor activation. The results of our investigations are presented in the third and final part of this work.



## **2. Chapter I**

Attenuated activation of macrophage TLR9  
by DNA from virulent mycobacteria



## 2.1 Introduction

*Mycobacterium tuberculosis* is an intracellular pathogen that can persist and propagate within human macrophages. Control and resolution of mycobacterial infections has been shown to depend on a coordinated innate and adaptive immune response, primarily involving macrophages and CD4<sup>+</sup> T cells, respectively (Doffinger et al., 2006). Over the last several years, TLRs have emerged as important transducers of the innate immune response (Kawai and Akira, 2006; Opitz et al., 2010). Although DNA isolated from mycobacteria was the first DNA to be shown to induce immunostimulatory action in mammalian cells more than 25 years ago (Shimada et al., 1985; Tokunaga et al., 1984), the relevance of TLR activation by mycobacterial DNA during tuberculosis infection has only recently been a matter of interest (Bafica et al., 2005; Juarez et al., 2010).

Bacterial DNA is now recognized as the natural ligand for toll-like receptor 9 (TLR9) (Hemmi et al., 2000; Schneberger et al., 2010). What distinguishes bacterial from mammalian DNA is its highly increased content of undermethylated 5'-CG-3' sequences, usually referred to as CpG. The frequency of the base sequence CG is suppressed in mammals.

In addition to these differences in the frequency of CpG sequences between bacterial and mammalian DNA, there are also differences in the methylation state of the DNA. Whereas most CpG sequences in mammalian DNA are methylated, practically all bacterial CpG sequences are non-methylated. Non-methylated CpG sequences within defined motifs have been shown to bind to and signal *via* intracellular TLR9 (Leifer et al., 2004; Latz et al., 2004).

Whether human monocytes or human macrophages express functional TLR9 and therefore can be activated by bacterial DNA or synthetic CpG oligonucleotides has been controversial (Miettinen et al. 2001; Hornung et al., 2002; Doyle et al., 2004; Takeshita et al., 2004). Evidence that these mononuclear phagocytes do not express TLR9 was supported by a study showing lack of responsiveness of primary monocyte-derived macrophages and THP-1 cells towards CpG oligonucleotides (Remer et al., 2006). While activation of human monocytes by CpG had been described (Hartmann and Krieg, 1999), this activation was suggested to depend on a contamination of the primary monocyte preparation with plasmacytoid dendritic cells (Hornung et al., 2005). Other data, however, argue in favour of the presence of TLR9 in cells of the human monocytic lineage (Sawamura et al., 2005; Fenhalls et al., 2003; Hoene et al., 2006; Mao et al., 2005; Juarez

et al., 2010) and reveal that bacterial DNA might represent a much better stimulus for TLR9 activation in macrophages than CpG oligonucleotides (Roberts et al., 2005a). Moreover, low but readily detectable levels of TLR9 mRNA in THP-1 macrophages, monocyte-derived macrophages, and AM were previously found by our group. TLR9 protein was also clearly detectable in THP-1 macrophages, human monocyte-derived macrophages, and human AM.

Thus, TLR9 activation by mycobacterial DNA could influence the innate response of macrophages to infection. Therefore, we sought to clarify the impact of mycobacterial DNA on macrophage function.

## 2.2 Results

### 2.2.1 Human macrophages are responsive to bacterial DNA

We first tested whether TLR9 in human macrophages was functional by determining whether macrophages were responsive to stimulation with TLR9 ligands. Monocyte-derived human macrophages were treated with different concentrations of a CpG-containing oligonucleotide (phosphorothioate-modified immunostimulatory sequence ISS 1018, 5'-TGA CTG TGA ACG TTC GAG ATG A-3'), then induction of cytokine mRNA was measured by real-time RT-PCR. While we observed a dose-dependent increase in TNF- $\alpha$  mRNA (figure 6 A), the extent of cytokine induction observed was relatively weak compared to the increase of cytokine induction in other TLR9 ligand-responsive cells (Krug et al., 2001).

Employment of a different ISS (ODN 2006, sequence: 5'-TCG TCG TTT TGT CGT TTT GTC GTT-3') also resulted in a low but significant induction of TNF- $\alpha$  at a concentration of 10  $\mu$ g/ml, whereas the respective GC-control (sequence: 5'- TGC TGC TTT TGC TTT TGT GCT T -3') did not induce TNF- $\alpha$  in the highest concentration tested (figure 6 C). This suggests that the activatory potential of ISS is not due to an unspecific effect of phosphorothioate groups.

Since bacterial DNA has previously been reported to be a much stronger inducer of TLR9-dependent responses in macrophages compared to CpG-containing oligonucleotides (Roberts et al., 2005a), we assessed the impact of genomic DNA (isolated from the attenuated *M. bovis* BCG strain) as an alternative activator of TLR9 (Tokunaga et al., 1984). Interestingly, we saw a markedly higher TNF- $\alpha$  response in human macrophages treated with BCG DNA compared to treatment with ISS (figure 6A). We also confirmed that stimulation of macrophages with BCG DNA caused a marked induction of other cytokine mRNAs, such as IP10 as well as IL12 and IL10 (figure 6 B, Kiemer et al., 2009).

Indeed, the fold-induction of IP10 mRNA by BCG DNA was even greater than that observed for TNF- $\alpha$  (figure 6 B).

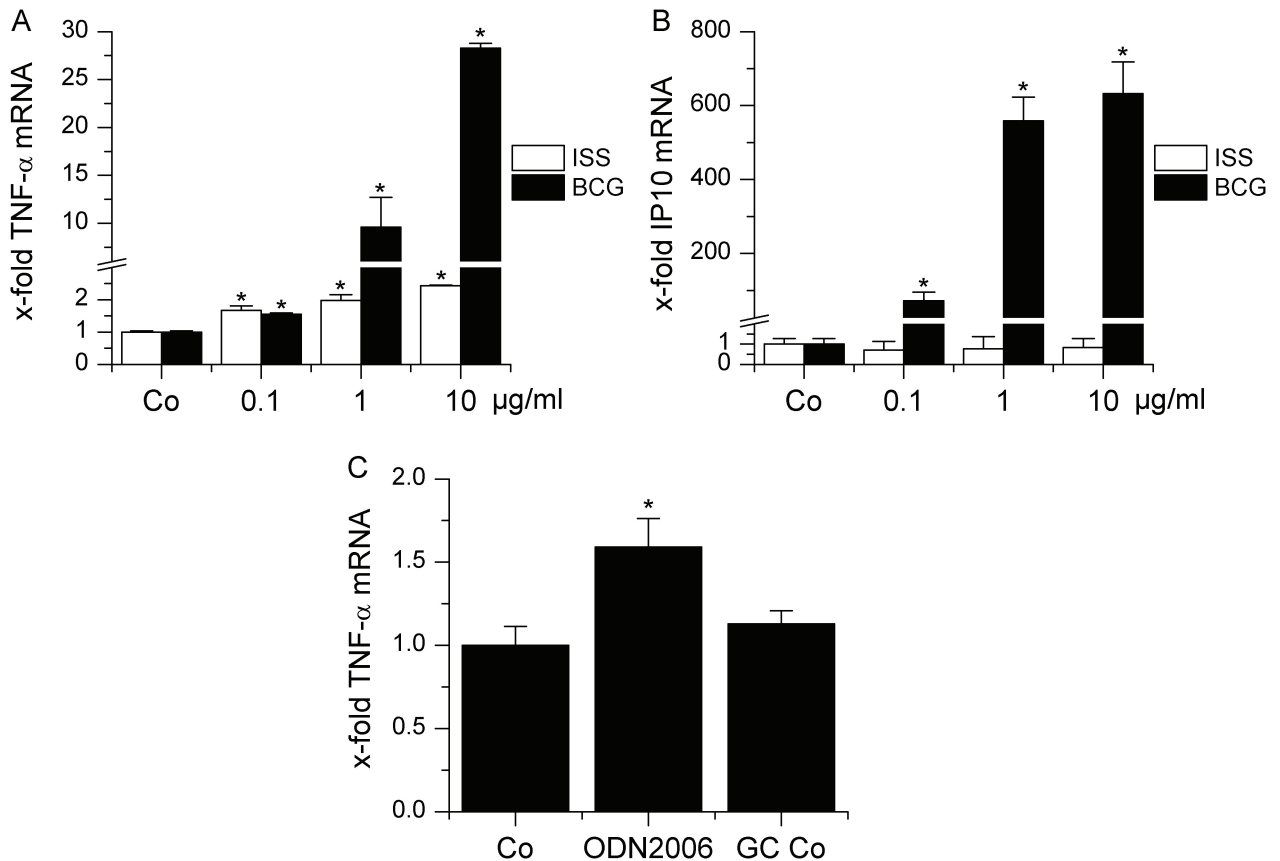


**Figure 6 : Activation of human monocyte-derived macrophages by immunostimulatory oligonucleotides and mycobacterial DNA** – A, B: Primary monocyte-derived macrophages were left untreated (Co) or treated with immunostimulatory sequences (ISS 1018) or with genomic DNA from *M. bovis* BCG for 3 h in the indicated concentrations (0.1-10 µg/ml). C: Cells were treated for 3 h with ODN2006 (10 µg/ml), the respective GC-control (10 µg/ml) or left untreated (Co). Treatment was followed by real-time RT-PCR analysis for TNF-α (A, C) or IP10 (B). Values were normalized to the housekeeping gene β-actin. Data are expressed as x-fold induction with expression levels of untreated cells set as 1. Data show means ± SEM from two experiments with cells from different donors performed in triplicate. \*  $P < 0.05$  compared to Co.

The differences in the extent of activation seen between BCG DNA and ISS DNA were not due to differences in the kinetics of the cytokine mRNA induction since induction time patterns were comparable for ISS and BCG DNA (figure 7).

Although we did observe an inter-experiment variability in the extent of macrophage activation depending on the blood donor, the intra-experiment variability was low. Thus, we always stimulated macrophages with ISS and mycobacterial DNA on the same day using the same macrophage preparation in order to allow direct comparison. All experiments show means from two or three cell preparations performed in triplicate, each.

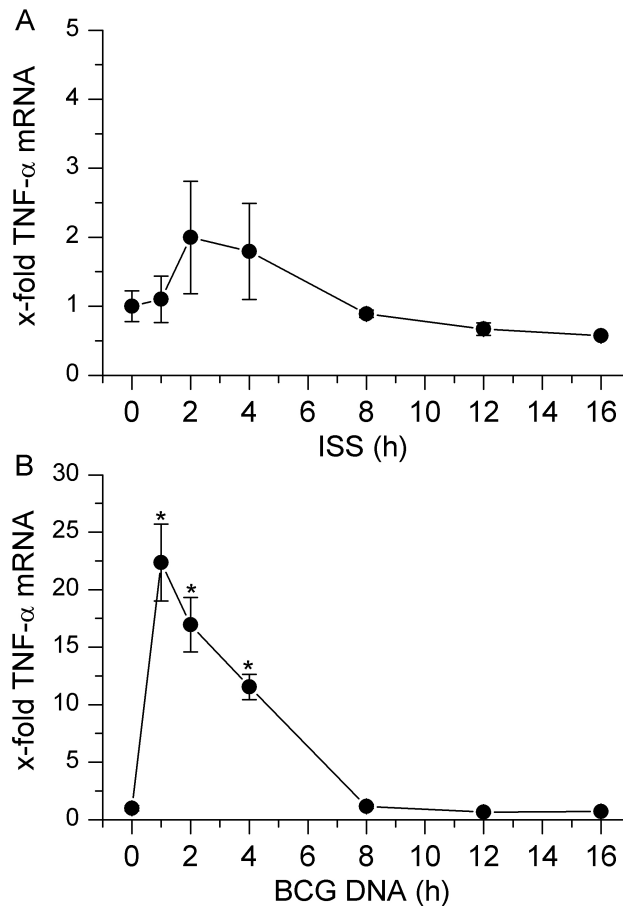


**Figure 7: Time patterns for ISS and BCG DNA induced activation** – Primary monocyte-derived macrophages were left untreated (Co) or treated with either ISS1018 (10  $\mu$ g/ml, A) or genomic DNA from *M. bovis* BCG (5  $\mu$ g/ml, B) for the indicated times (1-16 h). Treatment was followed by real-time RT-PCR for TNF- $\alpha$ . Data were normalized to b-actin and are expressed as x-fold induction with Co values set as 1. Data show means  $\pm$  SEM from two experiments performed in triplicate. \*  $P < 0.05$  compared to Co.

We then performed several experiments to demonstrate that the activation of human macrophages by BCG DNA was due to DNA and not evoked by contaminants. Potential contamination of the DNA preparations with endotoxin was assessed using a commercially available endotoxin assay (Limulus Amoebocyte Lysate, LAL) with a detection sensitivity of 0.03 EU/ml. None of our DNA preparations showed any reactivity using this sensitive assay. Additional controls were performed in order to exclude effects from other potential contaminants, most likely TLR2 agonists as mycobacterial cell wall components. First, we co-treated cells with the TLR9 inhibitor chloroquine, which does not interfere with TLR2 activation (Rutz et al., 2004; Sanjuan et al., 2006), together with BCG DNA. Chloroquine completely abrogated TNF- $\alpha$  induction by BCG DNA treatment whereas it had no effect when given to the cells alone (figure 8 A).

The effects of chloroquine were not due to impaired macrophage viability, as assessed by MTT assay (figure 8 B). As a complementary control, we methylated cytosine residues (C5) on BCG DNA with SssI methylase. As expected, methylation of the cytosine residues largely abrogated TNF- $\alpha$  mRNA induction by our DNA preparation (figure 8 C). Taken together, these experiments strongly support the interpretation that it is the DNA itself that mediates the profound effect of mycobacterial DNA preparations on macrophage activation, and that this effect is transduced through its interaction with TLR9.

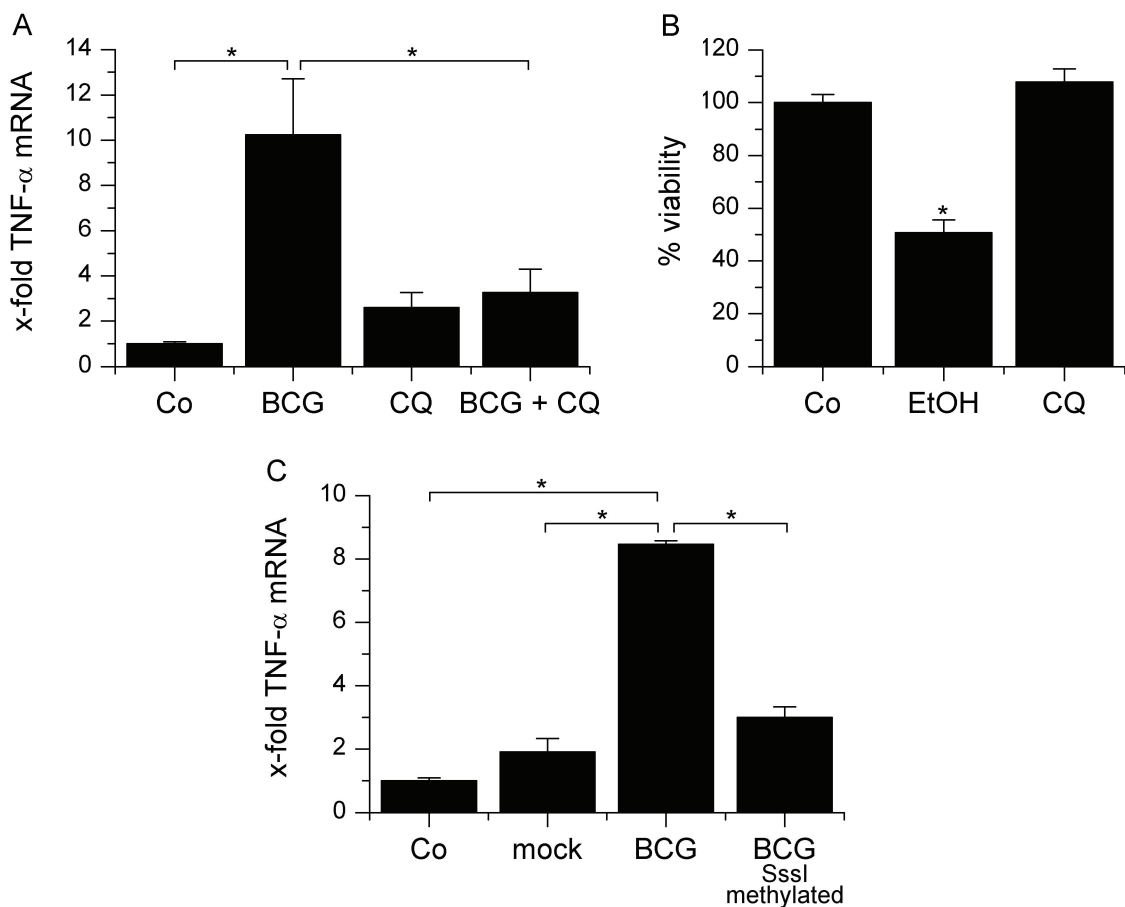


**Figure 8: Activation by DNA preparations is specific for non-methylated DNA** – A, C: DNA from *M. bovis* BCG mycobacteria was added to primary monocyte-derived macrophages for 3 h, followed by real-time RT-PCR for TNF- $\alpha$ . Expression levels for TNF- $\alpha$  were normalized to  $\beta$ -actin and data are expressed as x-fold TNF- $\alpha$  induction. Data show means  $\pm$  SEM of two or three experiments performed in triplicates, each. A: Cells were either left untreated (Co), or treated with chloroquine (CQ, 10  $\mu$ M), BCG DNA (5  $\mu$ g/ml) or a combination of both whereby CQ was added to the cells 1 h before BCG DNA. B: Monocyte-derived macrophages were either treated with CQ (10  $\mu$ M) or left untreated (Co) for 20 h and an MTT assay was performed. In addition, cells were treated with 10% [v/v] ethanol (EtOH) to confirm the functionality of our assay. Viability is expressed as percentage of absorbance of untreated cells. Data show means  $\pm$  SEM of n = 10. C: DNA from BCG mycobacteria was methylated with SssI methylase. *In vitro* differentiated macrophages were either left untreated (Co), mock treated (inactivated methylase and respective buffers only), or treated with methylated or respectively mock-treated (w/o methylase) DNA. \*  $P < 0.05$ .

Next, we wondered how the differences in activation by ISS and BCG DNA preparations can be explained, since the chemical nature of the stimulants is comparable. As the sole distinction is the difference in molecule lengths, we hypothesized that the difference in activation might be related to different uptake mechanisms. Since macrophages represent a cell type well equipped with phagocytic and endocytic capacity, we speculated that macromolecular DNA might spontaneously form nanoparticulate structures (Kerkmann et al., 2005), which can be taken up into the cells by a mechanism involving the actin cytoskeleton. We therefore aimed to test whether genomic DNA containing macromolecular DNA molecules formed nanoparticulate structures leading to an increased activatory profile. Atomic force microscope measurements of the two DNA preparations were performed in collaboration with Prof. Karin Jacobs (Saarland University, Department of Physics) according to a previously described method (Kerkmann et al., 2005). The experiments revealed that the large genomic DNA molecules in fact spontaneously formed nanoparticles, whereas oligonucleotides did not (figure 9 A - C).

Inhibition of actin polymerization by cytochalasin D attenuated BCG DNA-induced TNF- $\alpha$  expression (figure 9 D), suggesting that the cytoskeleton is involved in the activation mechanism induced by BCG DNA particles, most likely by mediating their uptake.

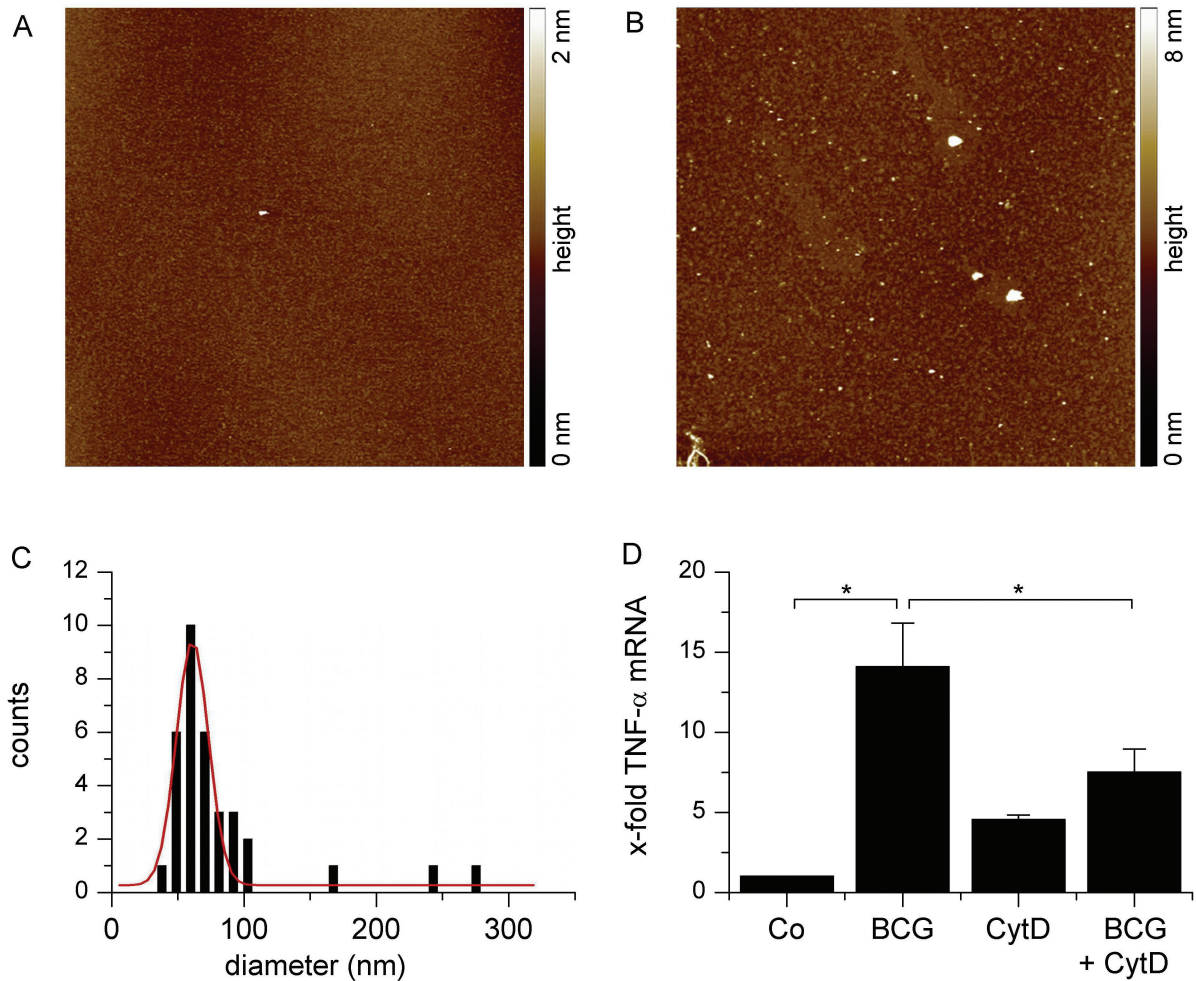


**Figure 9: Activation of macrophages by nanoparticulate BCG DNA requires actin polymerization – A-C:** Macromolecular DNA spontaneously forms nanoparticles. A - B: AFM analysis of DNA dried from a solution of 6 mg/ml in PBS on  $\text{MgCl}_2$  pretreated mica. Measurement was performed in dynamic mode ( $5 \times 5 \mu\text{m}$ ). A: oligonucleotide DNA (ISS1018) B: genomic macromolecular BCG DNA. White dots represent nanoparticulate DNA aggregates (detected by height). C: Number of particles of macromolecular BCG DNA on an area of  $5 \times 5 \mu\text{m}$  vs. diameter. D: AM were left untreated (Co) or treated with BCG DNA for 2 h with or without pretreatment with the actin polymerization inhibitor cytochalasin D (CytD,  $10 \mu\text{M}$ , 30 min) followed by real-time RT-PCR quantification of  $\text{TNF-}\alpha$ . Values were normalized to the housekeeping gene  $\beta$ -actin. Data are expressed as x-fold induction with expression levels of untreated cells set as 1. Data show means  $\pm$  SEM from two experiments. \*  $P < 0.05$  compared to Co. AFM imaging was performed by Ralf Jungmann (Saarland University, Department of Physics).

### 2.2.2 Different potency of mycobacterial DNA to activate human macrophages

Data obtained within a collaboration of our group with the group of Lee W. Riley (UC Berkeley) had shown that intracellular replication of attenuated mycobacteria (H37Ra) was higher in TLR9-deficient mouse macrophages than in wild-type macrophages, whereas virulent mycobacteria (H37Rv) showed equal survival in wild-type or mutant cells. Increased bacterial survival was accompanied by altered cytokine production. *In vivo* infection experiments also showed differential cytokine production in TLR9-deficient mice compared to wild-type animals (Kiemer et al., 2009)

We reasoned that there could be several mechanisms explaining the differences in macrophage activation in response to acute infection with H37Rv *versus* H37Ra mycobacteria as well as the diminished activation of macrophages in TLR9 deficient macrophages *versus* wild-type macrophages following infection with H37Ra mycobacteria. One possibility is that virulent mycobacteria fail to activate TLR9 because less efficient intracellular bacterial killing of the virulent organisms results in less free genomic DNA able to interact with intracellular TLR9.

Alternatively, DNA from virulent bacteria could have less potency to activate human macrophages than DNA from attenuated bacteria. To discriminate between these possible mechanisms, we isolated DNA from virulent and attenuated mycobacteria, and then treated human AM with equal concentrations of the different DNA preparations. Remarkably, DNA from attenuated mycobacteria (H37Ra and *M. bovis* BCG) consistently stimulated a more vigorous macrophage TNF- $\alpha$  response than did DNA from virulent mycobacteria (H37Rv, figure 10 A). This observation was also confirmed in human monocyte derived macrophages (Kiemer et al., 2009). In order to check whether the action of H37Ra DNA preparations results in fact from its DNA content and not from any contaminants, H37Ra DNA was digested with DNase. The effect of this preparation was compared to the stimulatory potency of non-digested DNA. We saw that digestion in fact abrogated the ability to stimulate TNF- $\alpha$  mRNA when added to human macrophages (figure 10 B). Taken together, our data suggest that virulent mycobacteria have evolved a mechanism of attenuated TLR9 activation by their genomic DNA.

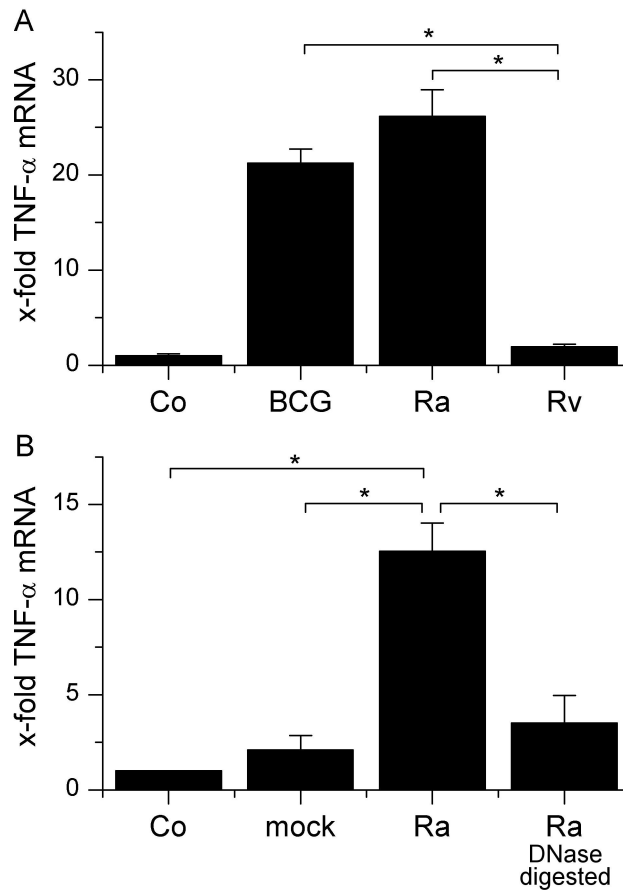


**Figure 10: Activation of human macrophages by DNA from virulent and attenuated mycobacteria –** AM were treated with DNA from the virulent *M. tuberculosis* (H37Rv) strain or from the attenuated H37Ra and *M. bovis* BCG strains for 2 h. Subsequently, real-time RT-PCR analysis for TNF- $\alpha$  was performed. Data are expressed as TNF- $\alpha$  induction after normalization to  $\beta$ -actin expression. Data show means  $\pm$  SEM of four experiments with cells obtained from 2 donors. B: DNA was isolated from H37Ra mycobacteria and digested with DNase. Primary monocyte-derived macrophages were either left untreated (Co), mock treated (inactivated DNase and respective buffers only) or treated with digested or respectively mock-treated (w/o DNase) DNA followed by RNA isolation and real-time RT-PCR analysis for TNF- $\alpha$ . Data are expressed as x-fold TNF- $\alpha$  induction after normalization to  $\beta$ -actin values. Data show means  $\pm$  SEM of four experiments (A) or two experiments performed in triplicate (B). \*  $P < 0.05$ .

## 2.3 Discussion

Control of infection by *Mycobacterium tuberculosis* requires an effective combined innate plus adaptive immune response by the host. The innate response mounted by infected macrophages and the adaptive CD4 T-cell response are key contributors to an effective host defence (Doffinger et al., 2006). Studies using MyD88 null mice have demonstrated that TLR signalling plays a critical role in the success of the innate host response (Scanga et al., 2004; Fremont et al., 2004). The specific role of individual TLRs, however, remains elusive. The results presented within this chapter and in Kiemer et al. (2009) suggest that TLR9, the sensor for bacterial CpG DNA, plays an important role in shaping the innate macrophage response to mycobacterial infection.

### 2.3.1 Responsiveness of human macrophages towards mycobacterial DNA

Several reports had suggested that human monocytic cells contained functional TLR9 receptors. Sawamura et al. (2005) showed that monocytes were primarily responsible for the inflammatory reaction induced by injection of plasmid DNA into human skin. Mao et al. (2005) reported that human monocytes showed marked responsiveness to CpG stimulation, and two groups reported THP-1 monocytes as target cells for ISS (Sanjuan et al., 2006; Kuo et al., 2005). Furthermore, addition of CpG sequences was demonstrated to attenuate growth of virulent *Mycobacteria tuberculosis* (Erdman) in human monocyte-derived macrophages (Wang et al., 2005). Our group had previously shown that that human monocyte-derived macrophages express TLR9. Here, we demonstrate that they are activated by treatment with bacterial DNA. Interestingly, we found that human macrophages respond far more vigorously to bacterial DNA than they do to CpG ODNs at the same concentration. Many of the published effects ascribed to specific CpG sequences were recently proven to be due to CpG-independent effects of phosphodiesterases (Roberts et al., 2005b). As shown by the employment of GpC ODN controls, such non-specific effects seem to be of little importance in human macrophages, leading to a weak activation by the use of phosphorothioate-modified ISS. In addition, multimerization of DNA has been reported crucial for optimal TLR9 activation, suggesting that genomic DNA has a higher potential of aggregation (Wu et al., 2004). This was confirmed by the observation that bacterial genomic DNA is much more efficient than oligonucleotides in activating mouse macrophages (Roberts et al., 2005a). Here, we show for the first time that such a difference can also be observed in human macrophages.

The differential activatory potential of CpG DNA preparations, either dissolved, oligonucleotide DNA or nanoparticulate genomic DNA, seems to be related to different uptake/interaction modes, as inhibition of actin polymerization by cytochalasin D attenuated BCG DNA-induced TNF- $\alpha$  expression. Ongoing work in our group supports this suggestion: first data demonstrate that exposure of macrophages to genomic nanoparticulate DNA induces stronger actin polymerisation than oligonucleotide treatment (Robert Zarbock, Saarland University, Pharmaceutical Biology, unpublished data).

Besides monocyte-derived macrophages, we also show TLR9-mediated activation of human AM after stimulation with bacterial DNA. This contrasts to the report by Suzuki et al. (2005) who described impaired TLR9 signalling in mouse alveolar macrophages despite detectable TLR9 expression. Like other publications that failed to find evidence of TLR9 signalling in human monocytes or macrophages (Hornung et al., 2002; Remer et al., 2006; Doyle et al., 2004), Suzuki et al. only tested the effect of CpG ODNs - not of larger, bacterial DNA. Thus, the use of the suboptimal stimulus might explain the lack of responsiveness. The use of bacterial DNA in fact seems to more adequately reflect the *in vivo* situation. This notion is largely supported by the demonstration of different responses of macrophages obtained from TLR9 deficient mice towards mycobacterial infection compared to cells from wild-type animals (Kierner et al., 2009). In addition, theoretical calculations indicate that the small volume of endosomes (the organelle known TLR9 signalling takes place in) promotes signalling even from a limited number of TLR agonists (Croizat and Beutler, 2004).

### **2.3.2 Differential activatory potential of mycobacterial DNA**

Previous studies done in our group in collaboration with The Scripps Research Institute (La Jolla, USA) and the University of California (Berkeley) indicated that macrophage TLR9 activation in fact plays a role in mycobacterial infection. When macrophages from wild-type (C57BL/6) or TLR9 deficient (TLR9<sup>CpG1/CpG1</sup>) mice (Tabeta et al., 2004) were infected with mycobacteria, there was no difference in intracellular replication of the virulent H37Rv strain between wild-type and TLR9-deficient macrophages. This result corroborates an *in vivo* study demonstrating that TLR9 deficient animals did not show differences in survival compared to wild-type animals when infected with a low dose of H37Rv (Bafica et al., 2005). In contrast, when macrophages were infected with the attenuated H37Ra strain, bacteria replicated much faster in TLR9<sup>CpG1/CpG1</sup> macrophages than in wild-type cells. The TLR9<sup>CpG1/CpG1</sup> macrophages also showed a distinct activation

pattern compared to wild-type macrophages one day after infection, indicating an impaired TLR9 activation. Interestingly, knockdown of TLR9 lead to completely different cytokine responses upon infection with H37Ra or H37Rv. Whereas TLR9<sup>CpG1/CpG1</sup> mice displayed reduced cytokine production after H37Ra infection, it was increased after H37Rv infection. This observation definitely shows differences in TLR9 activation between virulent and attenuated mycobacterial strains (Kierner et al., 2009).

Taken together, the infection data suggest that virulent H37Rv mycobacteria elicit an altered TLR9 response compared to attenuated H37Ra mycobacteria. Here, we stimulated AM with DNA preparations made from virulent (H37Rv) or attenuated (H37Ra and *M. bovis* BCG) mycobacteria to address the mechanism underlying this difference. We demonstrated that DNA from attenuated mycobacteria is more efficient in activating AM than DNA from virulent mycobacteria, thus confirming previous findings for monocyte derived macrophages (Kierner et al., 2009). These results might explain data from the literature reporting that the ability of mycobacteria to induce the secretion of TNF- $\alpha$  is inversely related to their virulence in murine macrophages (Falcone et al., 1994).

### **2.3.3 What distinguishes DNA from virulent and attenuated mycobacteria**

A recent genome-wide screening analyzed immunostimulatory sequences in genomic mycobacterial DNA (Lee et al., 2006). The data showed that not only the CpG motifs but also the context of the sequence surrounding the CpG motif are important for the immunostimulatory activities of genomic DNA of *M. bovis*. The generally higher CG content in *Mycobacteria* compared to other bacteria, such as *E. coli* (65% vs. 51%) together with an even higher frequency of CpG sequences in mycobacteria compared to *E. coli* suggested a specifically high potential of mycobacteria to activate TLR9. Since the different mycobacterial strains have a >99% DNA homology and possess a comparable CG content of about 65% (Baess et al., 1978; Garnier et al., 2003), one might wonder how differences in the extent of TLR9 activation can occur between genomic DNA from different strains. There are at least three possible explanations for the observed differences in the efficiency of TLR9 activation by different mycobacterial DNA: (I) attenuated strains might have a reduced frequency of activatory CpG sequences based on subtle differences in the surrounding DNA sequences; (II) virulent strains might have an increased number of immunosuppressive DNA sequences in their genomes; or (III) virulent strains may have developed strategies to mask their CpGs, such as by expressing DNA methylases. Since the genomes of attenuated strains have not been sequenced yet,

whole-genome sequence comparisons cannot be performed in order to check hypotheses (I) and (II). Most interestingly, however, data from the literature suggest that the virulent H37Rv strain is able to methylate cytosines whereas the H37Ra strain is not (Srivastava et al., 1981; Hemavathy et al., 1995). This observation might explain why DNA from virulent strains has a lower potential to activate TLR9 in human macrophages than DNA from attenuated strains.

Taken together, these studies establish that human macrophages express functional TLR9, and suggest suggest that signalling through TLR9 contributes to the innate macrophage response to infection by mycobacteria. Furthermore, the differences between the stimulatory activities of DNA from virulent *versus* attenuated mycobacteria indicate that TLR9-induced macrophage activation may influence the host's ability to limit and then kill intracellular mycobacteria. The altered TLR9 activation by virulent mycobacteria might represent a mechanism how they evade the host immune response.

Parts of the results presented in this chapter have been published in:

Attenuated activation of macrophage TLR9 by DNA from virulent mycobacteria.

Kiemer AK, Senaratne RH, Hoppstädter J, Diesel B, Riley LW, Tabet K, Bauer S, Beutler B, Zuraw BL. *J Innate Immun* 2009; 1:29-45.

### **3. Chapter II**

Differential cell reaction upon Toll-like receptor  
activation in human alveolar and lung interstitial  
macrophages



### 3.1 Introduction

AM play a central role in pulmonary innate immune response against inhaled particles and pathogens due to their localization in the lung alveoli. Besides their function in the defence against infectious diseases, they are known to play a role in inflammatory airway diseases, such as COPD (Barnes, 2004) and to participate in the dysregulation of immune responses in allergic disease (Vissers et al., 2004). In contrast to AM as a rather well-defined macrophage population commonly obtained by bronchoalveolar lavage (BAL), little is known about another potential macrophage-like cell population in human lungs, which are commonly referred to as interstitial macrophages (IM).

Studies using primary rat or mouse macrophages suggest that AM display a high microbicidal and phagocytic potential and produce numerous pro-inflammatory and chemotactic mediators upon activation. In contrast, rodent IM have been reported to be less effective in Fc-receptor-independent phagocytosis, production of cytokines such as TNF- $\alpha$  or interferon (IFN)- $\alpha/\beta$ , and production of reactive oxygen and nitrogen intermediates. In contrast, accessory function and MHCII expression have been suggested to be increased compared to AM (Lohmann-Matthes et al., 1994; Laskin et al., 2001; Ferrari-Lacraz et al., 2006; Bedoret et al., 2009). The relevance of these observations in humans has not been described in the literature. One of the very few studies investigating functional differences between human AM and IM describes a higher phagocytic activity of AM compared to IM (Fathi et al., 2001). Moreover, a higher production of matrix metalloproteinases in IM compared to AM has been reported (Ferrari-Lacraz et al., 2001), indicating that IM might play a more pronounced role in tissue remodelling.

Lung DC have recently gained marked scientific interest. This cell type resides in small numbers in the lung interstitial tissue in close proximity to both the large airways and the alveoli and is specialized for antigen presentation and accessory function (Lohmann-Matthes et al., 1994; Cochand et al., 1999). A study using mouse models only recently revealed that IM are able to inhibit maturation and migration of lung dendritic cells (Bedoret et al., 2009). This makes IM the cell type responsible for the suppression of allergic reactions towards harmless antigens. The relevance of these findings for humans, however, needs to be confirmed.

In order to investigate the role of AM and IM in the pathogenesis of human lung disease, aim of the present study was to characterize respective cell populations isolated from human lung tissue. Since TLRs represent key mediators of infectious as well as non-

infectious lung disease (Doffinger et al., 2006; Rohde et al., 2006; Opitz et al., 2010), a special focus was laid on potential differences in AM and IM with respect to activation *via* TLR4 and TLR9.

## 3.2 Results

### 3.2.1 Cell number and appearance

The AM and IM fractions obtained from 30 – 50 g of human non-tumor lung tissue from patients undergoing lung resection each contained  $2\text{-}20 \times 10^6$  cells, with the number of IM being equal to or exceeding the number of AM. The overall viability of cells obtained by washing or enzyme digestion of lung tissue was  $> 90\%$  as determined by trypan blue staining.

Both AM and IM preparations almost exclusively contained highly auto-fluorescent cells compared to low fluorescent cells like DC, as observed by flow cytometry and fluorescence microscopy (data not shown).

AM populations consisted mostly of large, round cells heterogeneous in size whereas IM appeared to be smaller, but more heterogeneous in shape compared to AM as observed by light microscopy (figure 11 A). FACS analysis assessing FSC confirmed the smaller size of IM (figure 11 B).

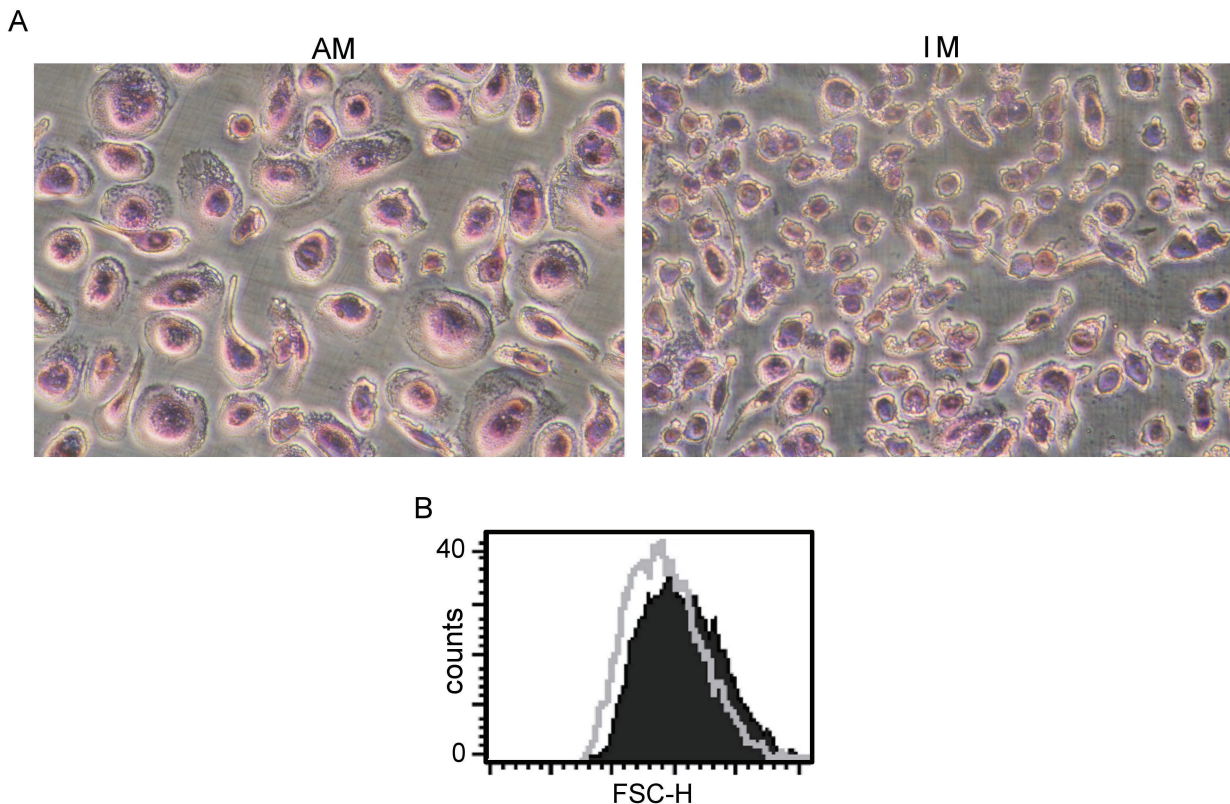


**Figure 11: Morphology of AM and IM** – A: Macrophage visualization by Pappenheim staining. Images are representative for cell preparations from at least two different donors. C: Comparison of macrophage sizes by forward scatter as measured by flow cytometry. Light grey line: IM; filled / dark grey: AM.

Phenotypic differences could be seen directly after isolation and persisted for at least 5 days. As tissue macrophages isolated by enzyme perfusion have been shown previously to require several days to recover surface receptor functionality (Kiemer et al., 2002), cells were cultured 3-4 days before use for further experiments.

Since the presence of fibroblasts can alter phagocyte functions (Chomarat et al., 2000; Oshikawa et al., 2003), we determined a potential contamination with this cell type. However, neither AM nor IM exhibited a significant contamination with fibroblasts as shown by immunostaining of CD90 (figure 12). This surface marker is highly expressed in fibroblasts (Kunisch et al., 2004; Pilling et al., 2009), as we confirmed for the human fibroblast cell lines MRC-5 and HSF-1. In contrast, CD90 is expressed only to a very low extent in macrophages, as was shown in the literature (Kunisch et al., 2004; Pilling et al., 2009) and confirmed by ourselves in human differentiated THP-1 macrophages. CD90 staining of AM and IM preparations revealed that mean percentages of CD90 positive cells were very low ( $0.9 \pm 0.5$  % in AM vs.  $1.3 \pm 0.5$  % in IM) and did not significantly differ between the two cell types.

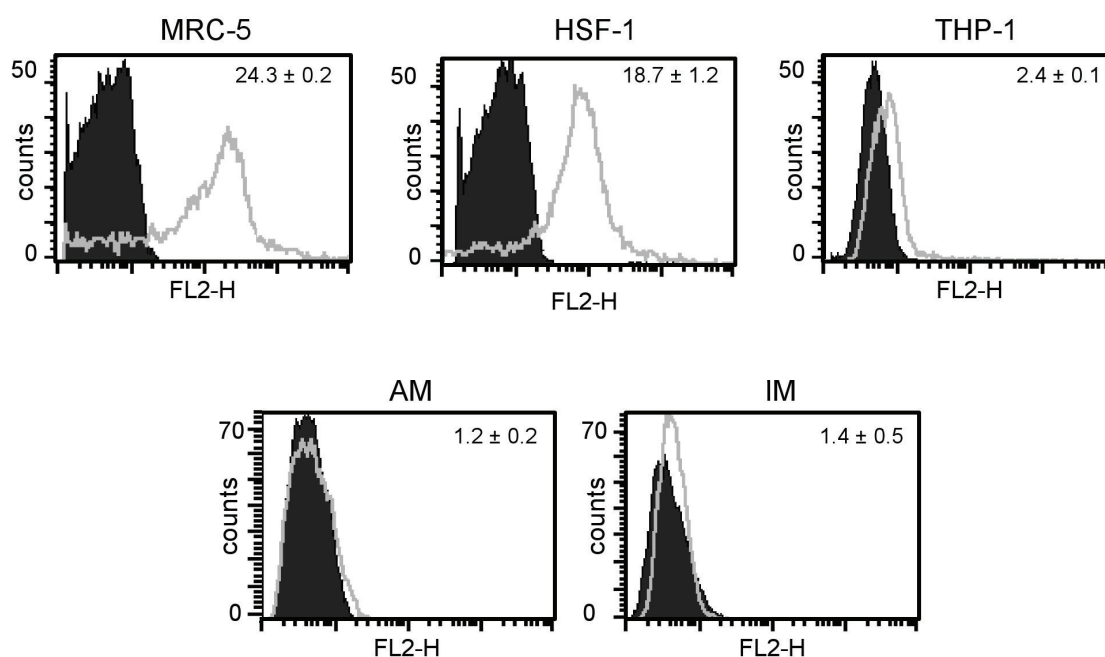


**Figure 12: CD90 surface expression of macrophages and fibroblasts** – AM, IM, fibroblasts (MRC-5 and HSF-1 cell lines) and macrophage-like PMA-differentiated THP-1 cells were stained for CD90 and analyzed by flow cytometry. Filled / dark grey: isotype control; light grey line: antibody staining. MFI values are given within graphs. Data show one representative out of three independent experiments. AM and IM were obtained from three different donors.

### 3.2.2 Expression of intracellular and surface markers

In order to define potential phenotypic differences between AM and IM, we analyzed their expression of the cell-surface molecules CD14 and human leukocyte-associated antigen-DR (HLA-DR). Moreover, the expression of surface markers CD83 and CD1a as well as intracellular CD68 in both populations was compared to *in vitro* differentiated immature and mature dendritic cells (iDC and mDC). Among the cell-surface molecules studied, only the expression of HLA-DR displayed significant differences between IM and AM, whereas CD14 expression was low or not detectable in both cell types. With respect to donor dependent differences in absolute mean fluorescence intensity (MFI) values, HLA-DR-expression in IM was almost 3-fold higher than in AM (figure 13 A and B).

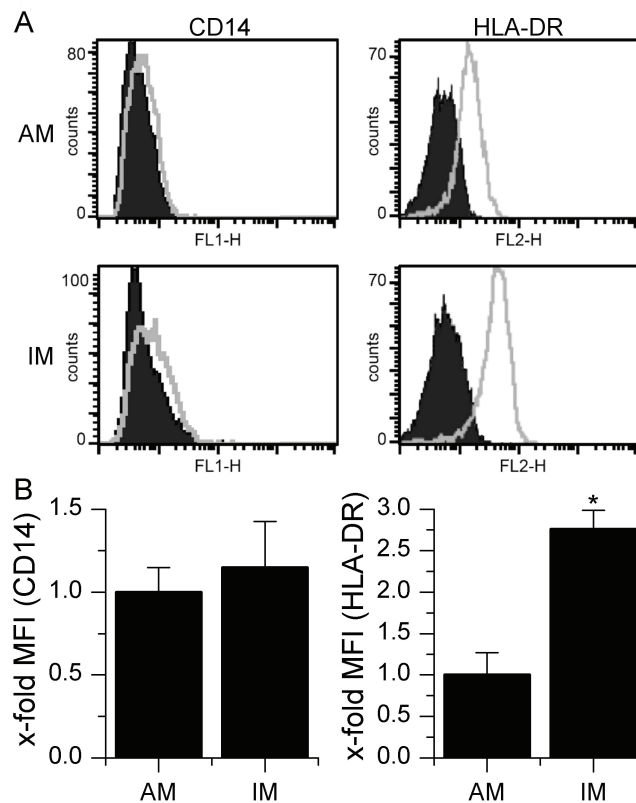


**Figure 13: CD14 and HLA-DR expression** – AM and IM were stained and analyzed by flow cytometry. A: Data show one representative out of four independent experiments. Filled / dark grey: isotype control; light grey line: antibody staining. B: Comparison of AM and IM concerning CD14 and HLA-DR expression. Data are expressed as MFI related to AM values. Data show means  $\pm$  SEM of independent experiments with cells derived from four different donors. \*  $P < 0.05$  compared to AM values.

CD68, often used as a specific marker for macrophages (Bedoret et al., 2009; Holness and Simmons, 1993; Kõhalmi et al., 1996) was highly expressed in both AM and IM, but could also be found in iDC as well as mDC. The dendritic cell markers CD1a and CD83

were not detectable in AM and IM (figure 14). These data suggest that IM share many phenotypic characteristics with AM, whereas no similarities to dendritic cells were observed.

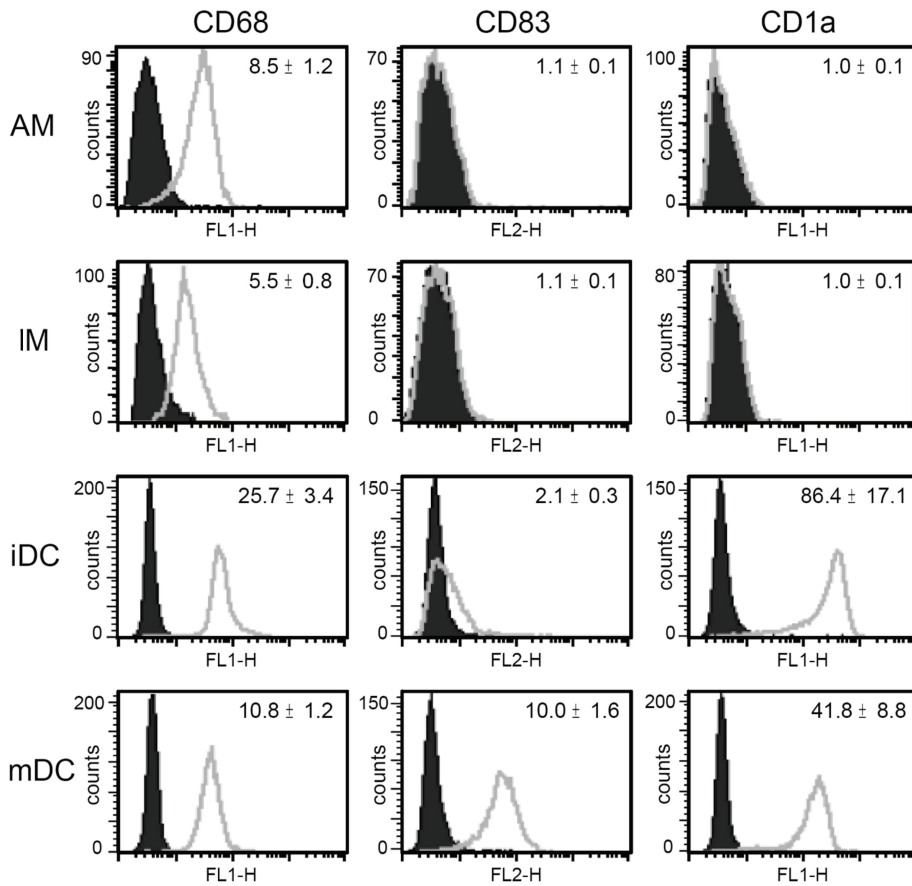


**Figure 14: Expression of CD68, CD83 and CD1a** – AM and IM as well as *in vitro* differentiated iDC and mDC were stained and analyzed by flow cytometry. Filled / dark grey: isotype control; light grey line: antibody staining. MFI values are given within graphs. Data show one representative out of three independent experiments with cells originating from different donors.

### 3.2.3 Phagocytosis

The internalization of fluorescent latex beads was quantified by flow cytometry. After incubation with fluorescent particles for 4 h, about two thirds of both macrophage populations had internalized fluoerespheres. Particle uptake was significantly lowered by pretreatment of the cells with cytochalasin D or incubation with fluorospheres at 4°C, but it was not abrogated completely (figure 15 A and B). This might be due to particle attachment to the cell surface, which can not be distinguished from internalization by flow cytometry. Therefore, fluorosphere uptake was visualized by confocal laser scanning microscopy. Upon incubation with the fluorescent particles for 4 h, most macrophages had

internalized several fluorospheres. As most of the particles were found to be internalized and not attached to the surface, quenching was supposed not to be necessary for flow cytometry analysis.

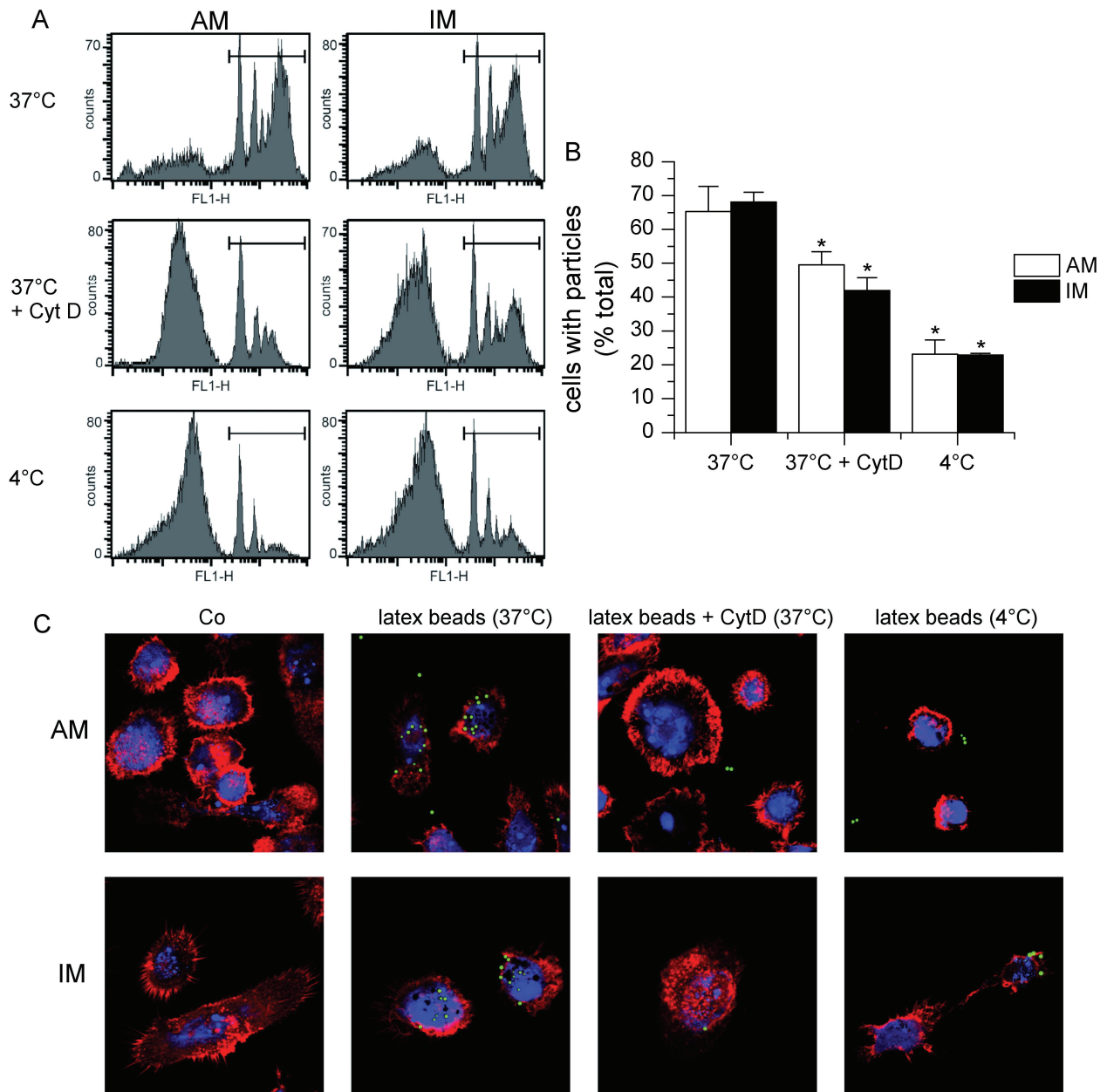


**Figure 15: Phagocytic Activity** – AM and IM were cultured with fluorescent FITC-labeled microspheres for 4 h at 37°C. As a control, cells were pretreated with cytochalasin D (10 µg/ml, CytD) for 1 h prior to particle addition. Alternatively, cells were preincubated at 4°C for 1 h and incubated with microspheres for 4 h at 4°C afterwards. Experiments were performed with cells derived from at least three different donors. A, C: representative results are shown. A: Fluoresphere-associated fluorescence (marked with black bars) was detected in AM and IM using flow cytometry. B: Average of percentage of macrophages positive for fluorosphere-associated fluorescence. Data represent mean ± SEM. \*  $P < 0.05$  as compared to cells left untreated at 37°C. C: Particle uptake in AM and IM was visualized by CLSM. F-actin was stained with rhodamin-phalloidine (red), nuclei with TOTO-3 iodide (blue). Latex beads are shown in green. Co: untreated cells. CLSM imaging was done by Robert Zarbock (Saarland University, Pharmaceutical Biology).

Pretreatment with cytochalasin D or incubation at 4 °C for 1 h prior to particle addition blocked particle uptake completely (figure 15 C). Pre-treatment of cells with DMSO, the solvent used for cytochalasin D, did not affect particle uptake (data not shown).

### 3.2.4 TLR expression

To investigate the expression of TLR1-10, we performed real time RT-PCR with samples from untreated AM and IM. TLR mRNA expression levels were not significantly different in AM and IM (figure 16). Among the TLRs recognizing bacterial patterns, TLR1, 2 and 4 were expressed strongest, whereas TLR8 as a sensor of viral infections showed highest expression of the RNA-responsive receptors.

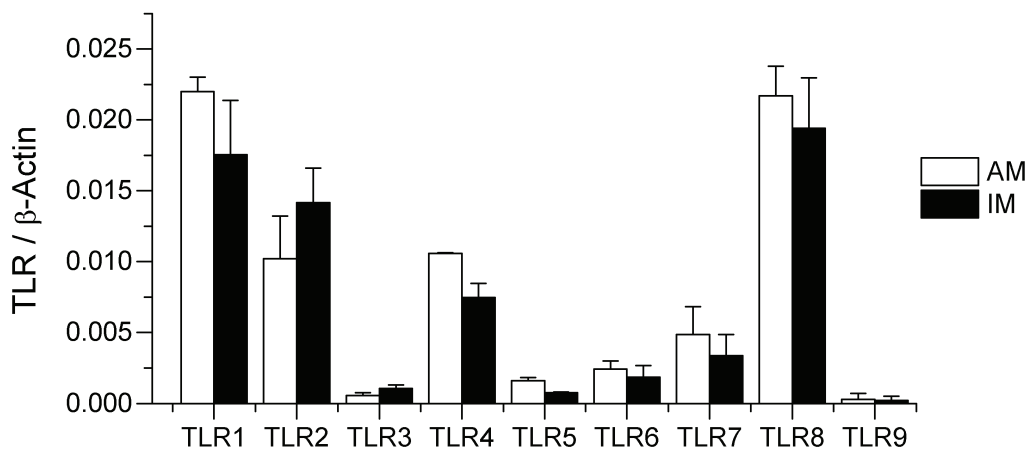


**Figure 16: TLR expression** – RNA was isolated from AM and IM and real-time RT-PCR analysis for TLR1-10 was performed. Data were normalized to  $\beta$ -actin values. Data show means  $\pm$  SEM of independent experiments performed with cells from 3 to 4 different donors.

### 3.2.5 Cell reaction upon TLR4 and TLR9 stimulation

As most comparative data for AM and IM focus on TLR4 activation, we treated respective cell populations with LPS and then determined induction of cytokine mRNA. Though we observed an increase in TNF- $\alpha$ , IL10 and IL6 mRNA in both cell types, the extent of TNF- $\alpha$  induction observed in IM was weak compared to the LPS-induced increase of TNF- $\alpha$  in AM. IM expressed both more IL6 and IL10 mRNA upon TLR4 activation than AM (figure 17). Interestingly, AM and IM differed also largely in basal IL10 and IL6 mRNA levels with IL10 expression in IM exceeding IL10 expression in AM 9.7-fold ( $\pm$  2.4) and IL6 expression in IM being 16.9-fold ( $\pm$  3.8) higher compared to AM (figure 17). These high basal

expression levels of IL6 and IL10 in IM are also the reason why x-fold cytokine mRNA inductions upon TLR4 activation compared to respective untreated controls were higher in AM for all cytokine mRNAs investigated (figure 17 D).

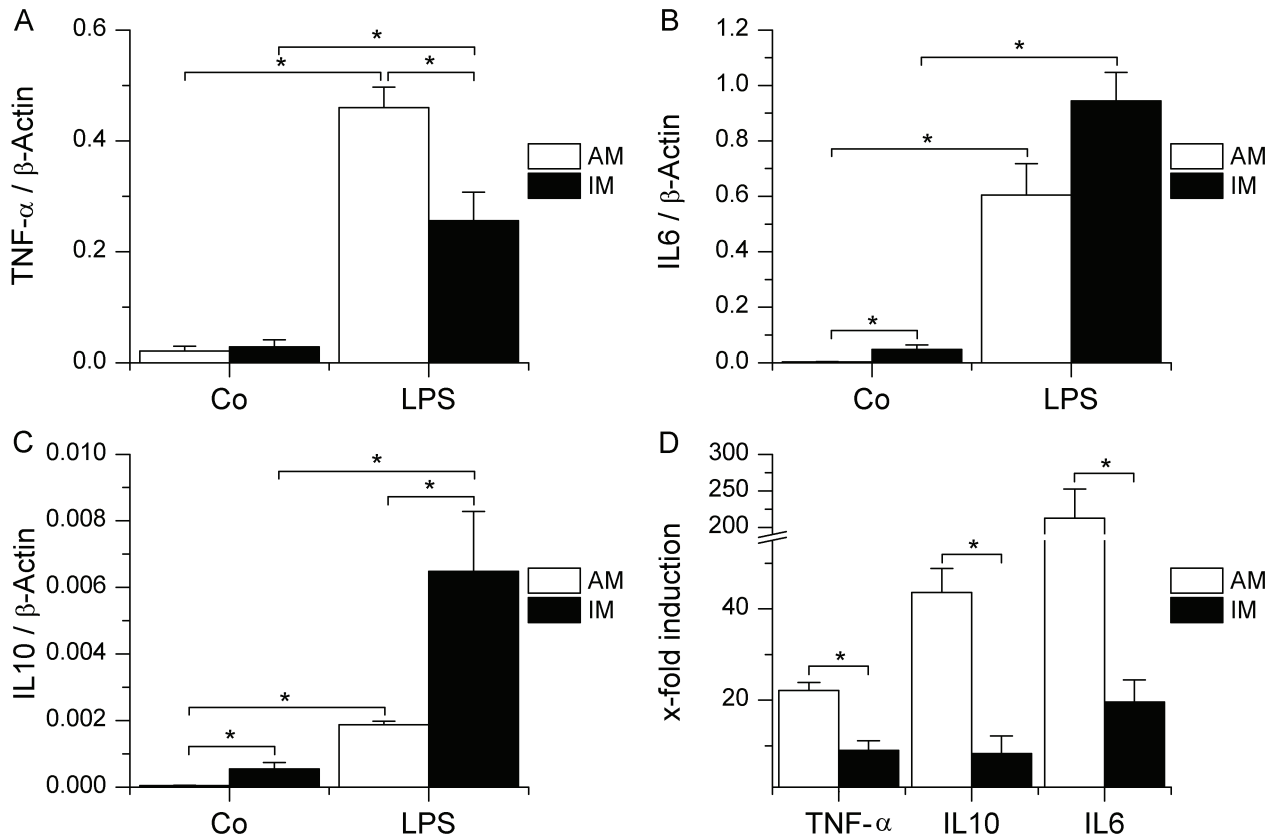


**Figure 17: Activation of AM and IM by LPS** – AM or IM were left untreated (Co) or treated with LPS (100 ng/ml) for 4 h, followed by RNA isolation and real-time PCR analysis for TNF- $\alpha$  (A), IL6 (B) or IL10 (C). Data are normalized to  $\beta$ -actin values. D: Comparison of x-fold cytokine mRNA inductions. Data show means  $\pm$  SEM of four independent experiments with cells derived from different donors. \* $P < 0.05$ .

AM have only recently been shown to be highly activated by BCG DNA as TLR9 ligand despite low TLR9 expression levels (Kierner et al., 2009; Chapter I). Due to this interesting fact, we decided to also test responsiveness of IM towards TLR9 ligands. Cells were treated with different stimuli including a CpG-containing oligonucleotide (phosphorothioate-modified immunostimulatory sequence ISS 1018) and genomic DNA isolated from the attenuated *M. bovis* BCG strain. In accordance with observations for monocyte-derived macrophages (Kierner et al., 2009; Chapter I), TNF- $\alpha$  induction by ISS was weak or absent in both cell types. Treatment with BCG DNA resulted in a markedly stronger TNF- $\alpha$  induction in AM, but an only moderate response in IM (figure 18 A). Interestingly, AM

completely lacked IL10 induction upon stimulation with BCG DNA, whereas IM showed a distinct IL10 induction upon TLR9 activation (figure 18 C). IL6 was induced in both cell types by BCG DNA (figure 18 E). In contrast, the extent of IL10 as well as IL6 induction by ISS was minimal in both AM and IM.

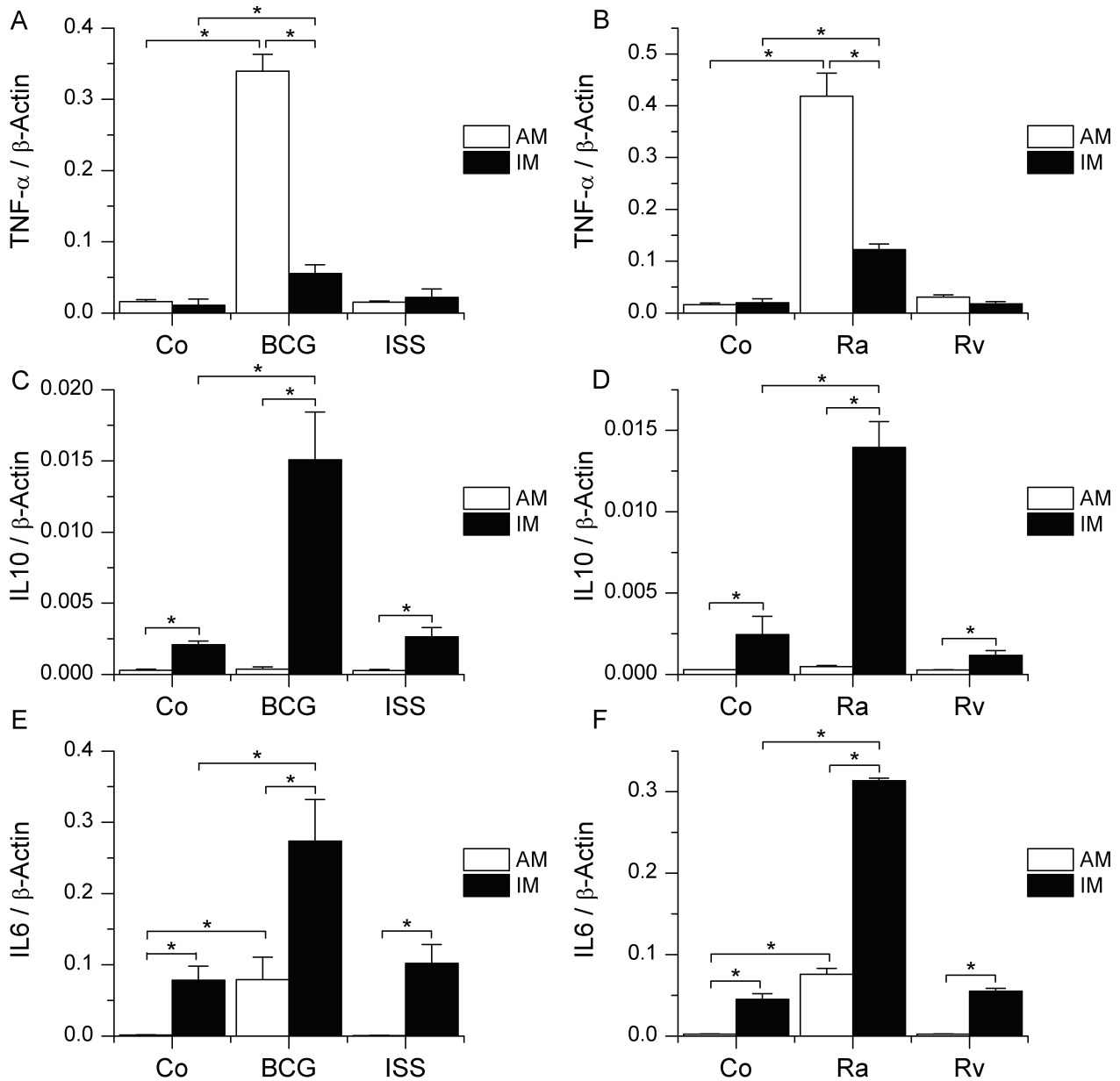


**Figure 18: Activation of AM and IM by TLR9 ligands** – AM or IM were left untreated (Co) or incubated with TLR9 ligands, followed by RNA isolation and real-time PCR analysis for TNF- $\alpha$  (A, B), IL10 (C, D) or IL6 (E, F). A, C, E: Cells were treated either with immunostimulatory sequences (ISS 1018 phosphorothioate-modified oligonucleotide, 20  $\mu$ g/ml) or genomic DNA from *M. bovis* BCG (20  $\mu$ g/ml) for 2 h. B, D, F: DNA isolated from virulent *M. tuberculosis* (H37Rv) or from the attenuated H37Ra strain (20  $\mu$ g/ml) was added to AM or IM for 2 h. Data show means  $\pm$  SEM of four experiments with cells derived from two different donors. \*  $P < 0.05$ .

Next, we examined cell reaction upon treatment with DNA from virulent (H37Rv) or attenuated (H37Ra) mycobacteria. Both AM and IM treated with DNA from virulent bacteria (H37Rv) showed a minimal induction of TNF- $\alpha$  compared to cells treated with DNA from non-virulent Mycobacteria (H37Ra, figure 19 B; BCG, figure 18 A). The lack of IL10 and IL6 induction by H37Rv DNA in both AM and IM confirmed its low activatory potential (figure 18 D, 18 F).

Observations for H37Ra DNA complied with the findings for BCG-DNA for both AM and IM, i.e. high TNF- $\alpha$  induction and absence of IL10 induction in AM contrasting a distinct IL10 response in IM.

Taken together, these data obtained on mRNA level suggested that the activation profiles of AM and IM upon TLR4 and TLR9 stimulation are markedly different, indicating that both cell types differ in their functional properties. We therefore extended cytokine mRNA profiling to protein quantification using a fluorescent bead-based immunoassay and additionally determined the cytokine levels of IL1 receptor antagonist (IL1ra), granulocyte-colony stimulating factor (G-CSF), interferon-inducible protein 10 (IP10), IL1 $\beta$ , IL12p40, IL12p70, and IFN $\gamma$  at baseline and after LPS activation in AM and IM (figure 19). These data revealed that AM and IM constitutively produced IL10, IL6, and IL1ra. Most remarkably, the baseline production of these anti-inflammatory and regulatory cytokines was markedly higher in IM than in AM. In detail, IL10 production was 1.9-fold ( $\pm$  0.2), IL6 secretion 3.3-fold ( $\pm$  0.4), and IL1ra secretion 2.5-fold ( $\pm$  0.4) higher in IM compared to AM (figure 19 A-C). Moreover, granulocyte-colony stimulating factor (G-CSF) was only detectable in IM at baseline (figure 19 D). Upon LPS treatment, IM still produced significantly more IL10 as well as IL1ra than AM. In contrast, production of the proinflammatory cytokines IL1 $\beta$  and IL12p40 following LPS activation was significantly higher in AM compared to IM. IFN $\gamma$  and IL12p70 were actually only secreted by AM, but not by IM, upon LPS challenge (figure 19 E). The concentrations of IP10 and TNF- $\alpha$  were both above detection limit in LPS-treated cells.

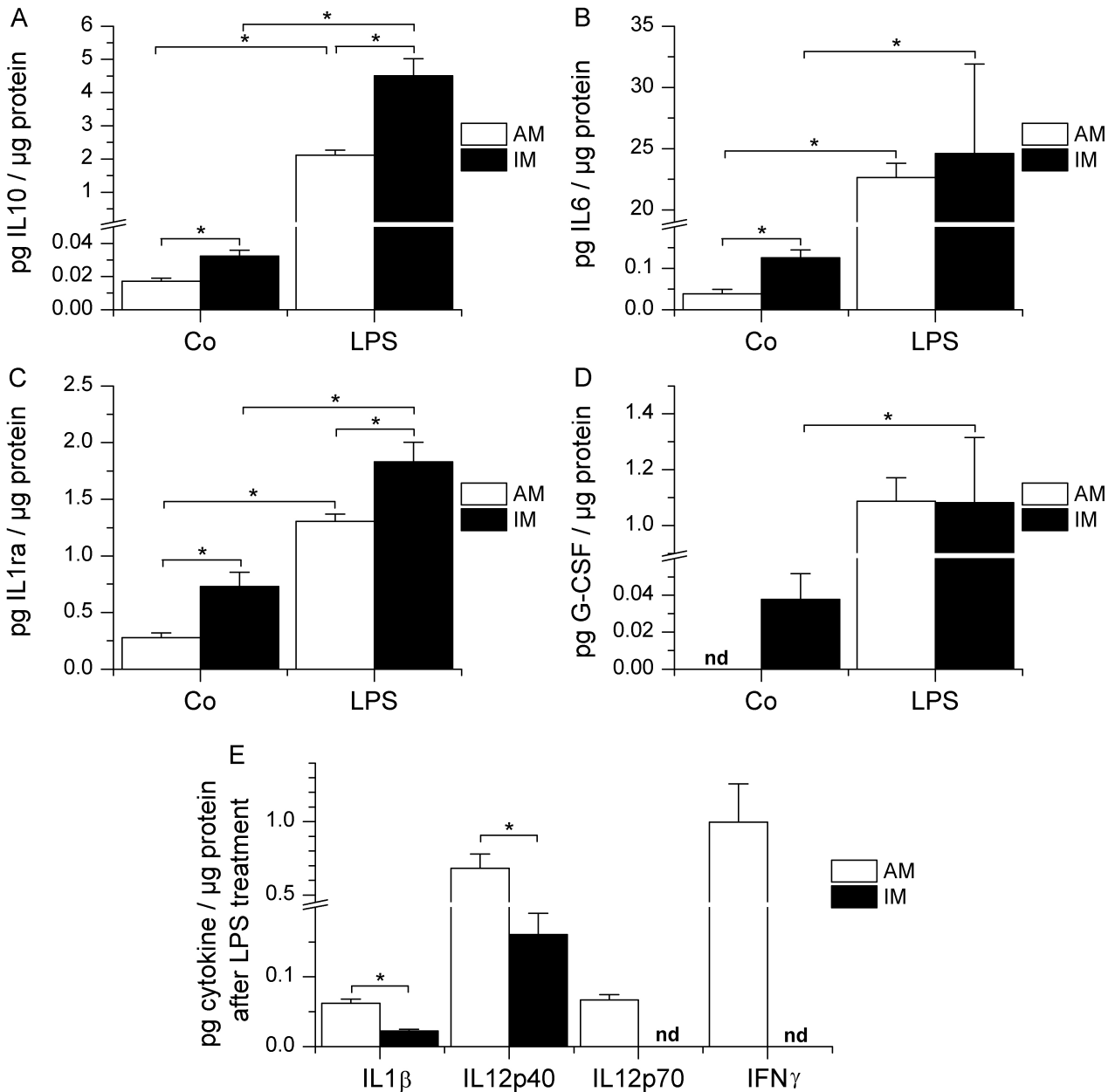


**Figure 19: LPS-induced cytokine secretion** – AM or IM were left untreated (Co) or treated with LPS (100 ng/ml) for 6 h. Supernatants were removed and used for measurement of cytokine protein production. Data are normalized to total cellular protein values. Data show means  $\pm$  SEM of 2-4 independent experiments performed in triplicate with cells derived from different donors. \*  $P < 0.05$ . nd: not detectable. IP10 and TNF- $\alpha$  were above detection limit. The multiplex cytokine assay was performed by Dominik Monz (Department of Neonatology, Saarland University Hospital).

### 3.2.6 Response to MyD88-dependent and -independent TLR activation

As the differential activatory potential of LPS in AM and IM might be related to a distinct utilization of MyD88-dependent and -independent pathways (Andreaskos et al., 2004), we also examined cytokine levels in response to Pam<sub>3</sub>CSK<sub>4</sub> (TLR1/2 agonist) and Poly(I:C) (TLR3 agonist).

Induction patterns of IL1ra, IL10, IL12p40, IL1 $\beta$  and IFN $\gamma$  upon Pam<sub>3</sub>CSK<sub>4</sub> treatment were found to be quite similar to those observed in response to LPS (figure 20). In contrast to the data obtained for TLR4 activation, however, the Pam<sub>3</sub>CSK<sub>4</sub>-induced secretion of IL6 as well as G-CSF was markedly stronger in AM than in IM (figure 20 B and C). In addition, AM produced significantly more TNF- $\alpha$  in response to Pam<sub>3</sub>CSK<sub>4</sub> than IM, which also resembled the findings for TLR3 activation (figure 20 E). Remarkably, IP10 was not inducible by Pam<sub>3</sub>CSK<sub>4</sub> (figure 20 F), but solely by Poly(I:C) treatment (figure 20 F) in both cell types. Besides IP10, only TNF- $\alpha$  was significantly upregulated by Poly(I:C) in both macrophage populations, suggesting that the induction of IL10 and IL12p40 is largely MyD88 dependent. The same might be true for IL1 $\beta$ , although we only detected negligible amounts of this cytokine upon Pam<sub>3</sub>CSK<sub>4</sub> treatment (Figure 20 I). Moreover, an increase in IL6, G-CSF and IFN $\gamma$  secretion occurred in AM, but not in IM, upon Poly(I:C) treatment. Interestingly, both the MyD88-dependent as well as the -independent agonist induced IL1ra in IM to about the same extent (Figure 20 D). Similarly, IFN $\gamma$  was equally inducible by both Poly(I:C) and Pam<sub>3</sub>CSK<sub>4</sub> in AM (Figure 20 H).

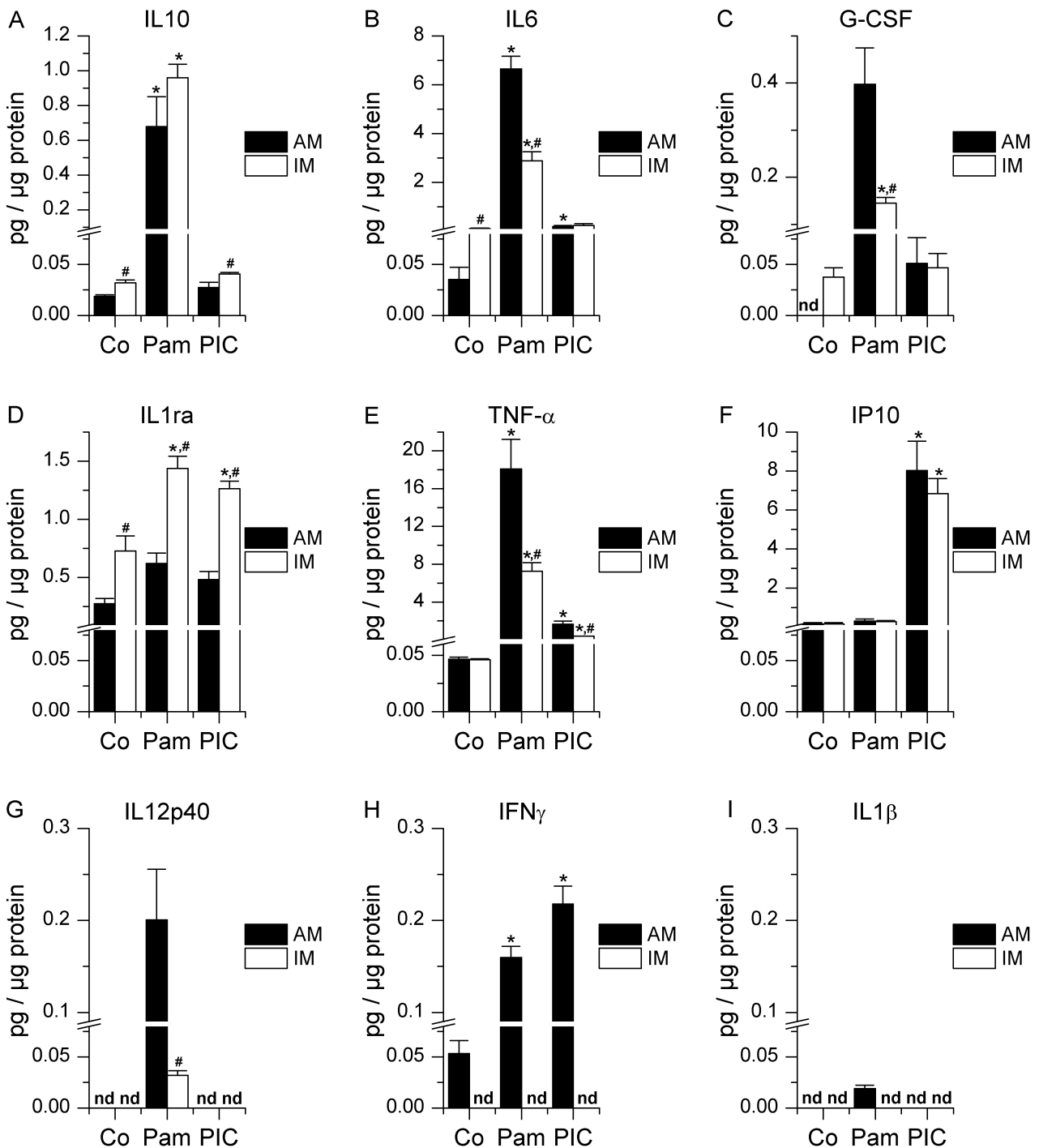


**Figure 20: Cytokine secretion upon TLR1/2 (MyD88 dependent) or TLR3 (MyD88 independent) activation** – AM or IM were left untreated (Co) or treated with Pam<sub>3</sub>CSK<sub>4</sub> (100 ng/ml) or Poly (I:C) (10 µg/ml) for 6 h. Supernatants were removed and used for measurement of cytokine protein production. Data are normalized to total cellular protein values. Data show means ± SEM of 2-4 independent experiments performed in triplicate with cells derived from different donors. \*  $P < 0.05$  compared to Co; #  $P < 0.05$  compared to similarly treated AM. The multiplex cytokine assay was carried out by Dominik Monz (Department of Neonatology, Saarland University Hospital).

## 3.3 Discussion

### 3.3.1 Isolation procedure

Human IM are less accessible than AM, which is why IM have in the past mostly been characterized using animal models (Lohmann-Matthes et al., 1994; Laskin et al., 2001). Our approach for macrophage isolation from human lung interstitial was based on a previously described method for isolation of epithelial cells (Elbert et al., 1999) and allows parallel isolation of AM, IM and epithelial cells. The digestion procedure we used slightly differed from those previously described for isolation of human IM (Fathi et al., 2001; Ferrari-Lacraz et al., 2001).

We are aware that donor specifics, such as medication or smoking behaviour might alter macrophage functions. In fact, smoking has been shown previously to increase basal levels of TNF- $\alpha$ , IL1 or IL8 in human AM (Ito et al., 2001) and to cause changes in morphology and surface molecule expression in rat AM (Lohmann-Matthes et al., 1994). Nevertheless, our results reveal many similarities of AM from lung tissue compared to AM from bronchoalveolar lavage described in the literature, as detailed below.

### 3.3.2 Morphology

Human as well as rat AM were previously described as large, mature cells, which closely resemble other tissue macrophages (Fathi et al., 2001; Laskin et al., 2001). In contrast, IM of human, rat or hamster origin were shown to be smaller than AM, more uniform in size and to generally resemble more closely peripheral blood monocytes (Bedoret et al., 2009; Laskin et al., 2001; Lavnikova et al., 1993; Kobzik et al., 1988). Our findings were similar to those described in the literature, which indicates that we were able to successfully separate macrophage populations.

### 3.3.3 CD14 and HLA-DR expression

Studies using primary rat AM and IM suggest that AM and IM do not differ in CD14 expression (Lohmann-Matthes et al., 1994). We were able to show that CD14 is marginally expressed in human AM as well as IM. Low CD14 expression was reported previously for human AM obtained from bronchoalveolar lavage (Lensmar et al., 1999; Haugen et al., 1998). CD14 expression by human IM is not described in the literature, but our results resemble findings reported for other tissue macrophage populations (Lensmar et al., 1999).

Several studies using rat, mouse as well as human macrophages reported a higher MHC-II expression in IM compared to AM (Bedoret et al., 2009; Ferrari-Lacraz et al., 2001; Lohmann-Matthes et al., 1994; Zetterberg et al., 1998). Our own results resemble those findings, indicating that IM are more involved in acquired immune responses than AM.

### **3.3.4 Comparison to dendritic cells**

Lung DC are a small subset of pulmonary mononuclear cells, which exhibit low autofluorescence and are known to be loosely adherent (Cochand et al., 1999; Demedts et al., 2005; Van Haarst et al., 1994; Havenith et al., 1993). Moreover, this cell type possesses an immature phenotype along with a rather weak CD83 expression (Cochand et al., 1999). Subsets of lung DC are known to express CD1a (Demedts et al., 2005). Our macrophage preparations displayed high autofluorescence, were highly adherent and shared no phenotypic characteristics with DC regarding CD83 or CD1a expression. Therefore, the presence of DC in our cell preparations can be excluded for the most part.

### **3.3.5 Phagocytic Activity**

Both macrophage types displayed phagocytic activity, which underlines the macrophage phenotype of IM. Phagocytic activity was comparable in AM and IM. This finding resembles observations for Fc $\gamma$ -dependent phagocytosis in the animal model (Lohmann-Matthes et al., 1994). Differences in phagocytic activity have been shown previously for human AM and IM phagocytosing *Saccharomyces cerevisiae* (Fathi et al., 2001). As this process is Fc $\gamma$ -independent, these findings can not be compared to our results.

### **3.3.6 TLR expression**

In the present study, expression of TLR1-10 mRNA levels were examined in both AM and IM for the first time. TLR1-10 mRNA expression by AM obtained from bronchoalveolar lavage was previously described by Maris et al. (2006). According to this study, TLR1, TLR4, TLR7, TLR8 are strongly and TLR2, TLR6 weakly expressed, whereas TLR3, TLR5, TLR9 and TLR10 were not detectable. Our results for TLR1, TLR4, TLR6, TLR8 and TLR10 expression by AM resemble those observations. In contrast to Maris et al., we observed a strong expression of TLR2 mRNA, which is in line with results by Suzuki et al. (2005) as well as ourselves (Kierner et al., 2009). Contrary to Maris et al., we were able to detect TLR3, TLR5 and TLR9 mRNA, suggesting a higher sensitivity of our assay. In fact,

our real time PCR analysis is linear over 8 orders of magnitude, down to a concentration of  $10^{-6}$  attomole /  $\mu\text{l}$ .

No significant differences between AM and IM concerning the TLR mRNA expression profile were found. Still, we can not exclude that TLR protein expression or localization differs in the different macrophage populations, which might both cause a differential cell reaction upon ligand binding.

### **3.3.7 Baseline cytokine expression and response to LPS**

#### *TNF- $\alpha$*

Previous studies using rat macrophages revealed that AM express higher amounts of the proinflammatory cytokine TNF- $\alpha$  compared to IM in response to LPS (Lohmann-Matthes et al., 1994; Franke-Ullmann et al., 1996). Our data suggest that this is also true for human AM and IM. Moreover, the effect was not restricted to TLR4 activation, as TLR1/2 and TLR3 activation gave equivalent results.

#### *IL10, IL6 and G-CSF*

Although IL10 is one of the most important anti-inflammatory mediators in human immune response (Opal and DePalo, 2000; Moore et al., 2001), its expression by human AM and IM has not been investigated before. AM display low basal IL10 levels, which might allow efficient defence against inhaled particles and pathogens, whereas the fast induction of IL10 upon LPS treatment suggests an autoregulatory mechanism. As for IM, basal IL10 mRNA and protein levels were found to be significantly higher than in AM and to increase after LPS treatment. A recently published study comparing murine AM and IM showed that IL10 levels were markedly higher in IM (Bedoret et al., 2009). Our data demonstrate that this is also true for human IM. In the animal model, IM were shown to inhibit lung DC maturation and migration in an IL10-dependent manner, thereby preventing Th2 sensitization to harmless inhaled antigens (Bedoret et al., 2009). Our findings suggest that this regulatory function might also be exhibited by human IM, indicating that IM play a crucial role in immune homeostasis.

IL6 has proinflammatory as well as anti-inflammatory properties. Studies using knockout mice demonstrated that in innate immunity IL6 acts predominantly as an antiinflammatory cytokine by attenuating the synthesis of proinflammatory cytokines (Libert et al., 1994; Xing et al., 1998). Exogenous IL6 was also shown to reduce the extent of pulmonary inflammation caused by hemorrhagic shock in rats, possibly by attenuating NF- $\kappa$ B activity

(Meng et al., 2000). Furthermore, IL6 is involved in the specific immune response by upregulating B-cell differentiation, T-cell proliferation, and antibody secretion (Xing et al., 1998). The high constitutive expression of IL6 we found in IM both on mRNA and protein level indicates that IM display a pronounced immunoregulatory capacity and suggests that they are more involved in specific immune responses than AM.

Additional to its ability to promote increased release of granulocytes from the bone marrow, G-CSF prolongs the life-span of neutrophils in the air spaces by delaying their apoptosis (Matute-Bello et al., 2000). Accordingly, G-CSF is associated with severity of pulmonary neutrophilia in acute respiratory distress syndrome and hemorrhagic shock (Aggarwal et al., 2000; Meng et al., 2000). Both AM and IM secrete G-CSF in response to LPS. Baseline expression of G-CSF, however, was only detected in IM. Interestingly, a recently published study revealed that MyD88-dependent IL10, IL6 and G-CSF induction is involved in the up-regulation of arginase 1 during mycobacterial infection in murine macrophages (Qualls et al., 2010). Macrophage arginase 1 exerts its anti-inflammatory action by competing with NO synthases for arginine, a substrate common to both types of enzymes, to inhibit NO production and prevent tissue damage (Munder et al., 1998). Qualls et al. demonstrated that arginase 1 expression was controlled by IL6, IL10 and G-CSF in a STAT3 dependent manner, and only the combined blockade of all three cytokines was sufficient to completely inhibit the induction of arginase 1 upon mycobacterial infection, suggesting that IL6, IL10 and G-CSF share some of their autocrine-paracrine functions. Thus, one could assume that IM express higher levels of arginase 1 than AM, which may explain the impaired NO production upon TLR4 activation previously described for rat IM (Franke-Ullmann et al., 1996). Interestingly, arginase 1 is also considered to be a marker for the anti-inflammatory M2 macrophage phenotype in the mouse model, although the relevance of this association for human macrophages remains controversial (Stempin et al., 2010).

#### *IL1ra, IL12, IL1 $\beta$ and IFN $\gamma$*

IL1ra is a major antiinflammatory cytokine that functions as a specific inhibitor of the two other functional members of the IL-1 family, IL-1 $\alpha$  and IL-1 $\beta$  (Opal and DePalo, 2000; Arend et al., 2008). Our data demonstrate that IM secrete higher amounts of IL1ra when compared to AM, both at baseline and upon TLR4 activation. In contrast, LPS induced secretion of proinflammatory cytokines was low in IM when compared to AM (IL1 $\beta$ , IL12p40) or even completely absent (IL12p70 and IFN $\gamma$ ). These findings clearly underline

the anti-inflammatory phenotype of IM previously described in the literature based on data obtained from murine or rat macrophages (Lohmann-Matthes et al., 1994; Franke-Ullmann et al., 1996; Laskin et al., 2001; Bedoret et al., 2009).

### **3.3.8 Differential response to TLR1/2, TLR3 and TLR4 activation**

Upregulation of cytokine levels by TLR4 activation was markedly stronger than observed after treatment with the TLR3 ligand Poly(I:C), which correlates with the observation that TLR3 mRNA expression was low in both cell types. Moreover, we also found that cells were more responsive towards LPS than Pam<sub>3</sub>CSK<sub>4</sub>. As TLR4 mRNA levels did not largely differ from TLR1 and TLR2 mRNA levels, a higher expression of TLR4 on protein level, distinct trafficking mechanisms and/or suboptimal ligand concentrations are suggested to cause the differences observed in the activatory potential of LPS vs. Pam<sub>3</sub>CSK<sub>4</sub>.

Additionally, LPS might amplify cytokine induction due to synergistic effects of MyD88-dependent and -independent pathways (Kawai and Akira, 2006). Of all mediators examined, however, IL1ra and IFN $\gamma$  were the only cytokines, which were inducible *via* both the MyD88- and the TRIF-related pathway.

IP10 was the only cytokine exclusively induced by TRIF signalling. A cell-type specific restriction of IP10 upregulation to the TRIF-dependent pathway was reported before for the myeloid lineage (Lundberg et al., 2007). Accordingly, both AM and IM secreted IP10 in response to TLR3 activation to about the same extent, indicating the presence of functional TLR3. Apart from IP10, cytokine induction upon Poly(I:C) treatment was low when compared to LPS and Pam<sub>3</sub>CSK<sub>4</sub> or even absent. As the activation of intracellular TLR3 might follow kinetics different from those of extracellular TLR1/2 and TLR4 and we did not perform studies on time- and dose-dependency, the relevance of this finding presently remains elusive.

We observed marked differences between AM and IM concerning both TLR1/2 as well as TLR3 activation. In detail, we observed a higher induction of IL6 and G-CSF in AM than in IM after Pam<sub>3</sub>CSK<sub>4</sub> treatment, which contrasts our findings of a similar expression of these two cytokines in both cell populations upon LPS challenge. The upregulation of IL6 and G-CSF occurred in a largely MyD88 dependent manner, as previously described in the literature for murine macrophages (Qualls et al., 2010). However, IL6 and G-CSF were also induced by Poly(I:C) to a moderate extent, although the induction was restricted to AM. This suggests that TLR1/2 and TLR3 protein expression / localization and/or downstream signalling differ largely between AM and IM. As for TLR3, differential

downstream effects seem more likely, as the IP10 response was comparable in both cell types.

### **3.3.9 Cell reaction upon TLR9 activation**

Despite the weak expression of TLR9 in AM and IM, cells reacted strongly upon stimulation with mycobacterial DNA. Methylation or digestion of mycobacterial DNA as well as chloroquine pretreatment lead to an abrogation of the macrophage response (Chapter I), which indicates that gene expression upon treatment with isolated DNA is not due to contaminants in DNA preparations, but due to TLR9 activation. It has been shown previously for human monocyte-derived macrophages as well as a mouse macrophage cell line that TLR9 activation is higher upon treatment with bacterial DNA than after oligonucleotide treatment, which might be due to oligonucleotide structure (Kiemer et al., 2009; Kerkmann et al., 2005; Roberts et al., 2005a). Moreover, it has been reported for human *in vitro* differentiated macrophages as well as for AM from BAL that DNA from virulent strains has a lower potential to activate macrophage TLR9 than DNA from attenuated strains (Kiemer et al., 2009). Several studies indicate that the virulent H37Rv strain is able to methylate cytosines, whereas the H37Ra strain is not (Hemavathy et al., 1995; Srivastava et al., 1981), which might explain why H37Rv DNA fails to activate TLR9. We were able to show that IM are less responsive to bacterial DNA than AM concerning TNF- $\alpha$  induction, which resembles our findings for TLR4 activation. Similar to the results of the TLR4 activation experiments, IL6 as well as IL10 expression were much higher in IM compared to AM, which once again emphasizes the immunoregulatory function of IM. Moreover, IL10 was only induced in IM, but not in AM, upon mycobacterial DNA treatment. Absence of IL10 induction after TLR9 activation by mycobacterial DNA has been reported before (Juarez et al., 2010) and might be part of a mechanism of AM to overcome the immunosuppressive environment of the alveoli. Lung epithelial cells have been shown to constitutively express IL10, which is accompanied by an impaired responsiveness of AM towards IL10 (Fernandez et al., 2004). In the same study, it was also observed that activation of human AM through TLR2, TLR4 or TLR9 leads to inhibition of IL10 receptor function associated with a reduced ability to activate STAT3. IL10 is known to induce its own transcription *via* several positive feedback loops involving STAT3 (Staples et al., 2007; Lang et al., 2002). A low capacity of AM to activate STAT3, as previously reported for murine AM (Jose et al., 2009), might explain the lack of IL10 induction in AM upon TLR9 activation as well as to the low basal levels of IL10 in comparison to IM. In this

manner, the higher baseline production of the STAT3 activating cytokines IL6 and G-CSF in IM compared to AM possibly also contributes to the higher expression of IL10 in unstimulated IM.

Taken together, the present results confirm and extend limited data obtained with murine and human AM and IM characterizing phenotypic differences. We were able to demonstrate functional and morphological differences as well as similarities between AM and IM from human lung tissue, leading to the conclusion that the heterogeneity of lung macrophages should be taken into consideration in future studies on their role in TLR-mediated inflammatory response.

Parts of the results presented in this chapter have been published in:

Differential cell reaction upon Toll-like receptor 4 and 9 activation in human alveolar and lung interstitial macrophages.

Hoppstädter J, Diesel B, Zarbock R, Breinig T, Monz D, Koch M, Meyerhans A, Gortner L, Lehr CM, Huwer H, Kierner AK.

*Respir Res* 2010;11:124.

Subsets of data shown within this chapter were previously presented as diploma thesis.



## 4. Chapter III

Downregulation of the  
glucocorticoid-induced leucine zipper (GILZ)  
upon Toll-like receptor activation in human alveolar  
macrophages



## 4.1 Introduction

Glucocorticoid-induced leucine zipper (GILZ) was originally identified as a dexamethasone-responsive gene by comparing mRNA species expressed in dexamethasone-treated and untreated murine thymocytes (D'Adamio et al., 1997). Glucocorticoids influence the regulation of various physiological processes, including inflammation, immune response, metabolism, cell growth and development. Glucocorticoids exert their immunosuppressive and anti-inflammatory effects via their action on innate and adaptive immunity. They are of extraordinary value for the therapy of inflammatory and autoimmune diseases.

Similar to dexamethasone treatment, GILZ overexpression in macrophages was reported to inhibit the production of inflammatory mediators as well as TLR2 expression (Berrebi et al., 2003). Many of these functions are under control of the transcription factor NF- $\kappa$ B, whose nuclear translocation is inhibited by GILZ. Accordingly, overexpression of GILZ in epithelial cells was shown to impair NF- $\kappa$ B activation in response to IL1 receptor and TLR activation, whereas knockdown of GILZ inhibits the ability of dexamethasone to suppress IL1 $\beta$ -induced chemokine expression (Eddleston et al., 2007). The induction of GILZ has also been proven crucial for the mediation of anti-inflammatory actions of glucocorticoids in other cell types, such as T cells, mast cells and dendritic cells (Ayroldi et al., 2001; Berrebi et al., 2003; Godot et al., 2006; Hamdi et al., 2007; Mittelstadt and Ashwell, 2001).

Despite the well-studied role of GILZ upon glucocorticoid treatment, hardly anything is known about the regulation of GILZ during the immune response in the absence of pharmacological intervention. Recently, however, Eddleston et al. reported that cytokines involved in airway inflammation, namely TNF- $\alpha$ , IL1 $\beta$  and IFN $\gamma$ , can reduce GILZ mRNA levels in epithelial cells (Eddleston et al., 2007). In line with those findings, GILZ was found to be downregulated in granulomas of tuberculosis patients and nasal explant cultures from patients suffering from chronic rhinosinusitis (Berrebi et al., 2003; Zhang et al., 2009). Interestingly, knockdown of GILZ in airway epithelial cells resulted in elevated baseline levels of the chemokine IL8 (Eddleston et al., 2007), suggesting that the mere absence of GILZ provokes an inflammatory response.

The lung is the organ with the highest GILZ expression, and macrophages have been reported to be the major source of human GILZ (Berrebi et al., 2003; Cannarile et al., 2001). This indicates that GILZ plays a pivotal role in respiratory immune homeostasis.

Therefore, the aim of this chapter was to investigate mechanisms regulating GILZ expression in human alveolar macrophages under inflammatory conditions.

## 4.2 Results

### 4.2.1 Constitutive and dexamethasone-induced GILZ expression in AM

As limited data is available in the literature on expression levels and regulatory actions of GILZ in AM, we determined constitutive expression of GILZ in this cell type. We assessed GILZ mRNA expression by using quantitative real-time RT-PCR with human *in vitro* differentiated macrophages as well as THP-1 monocytic cells as positive controls. Additionally, we examined GILZ expression in IM, which represent another pivotal lung macrophage cell population (Bedoret et al., 2009; Chapter II). GILZ mRNA levels were 3-fold higher in both AM and IM compared to blood monocyte-derived macrophages as well as differentiated and non-differentiated THP-1 cells (figure 21 A). As reported for other cell types (Eddleston et al., 2007; D'Adamio et al., 1997), GILZ mRNA and protein amounts were increased in AM by dexamethasone treatment in a time- and dose-dependent manner (figures 21 B – D).

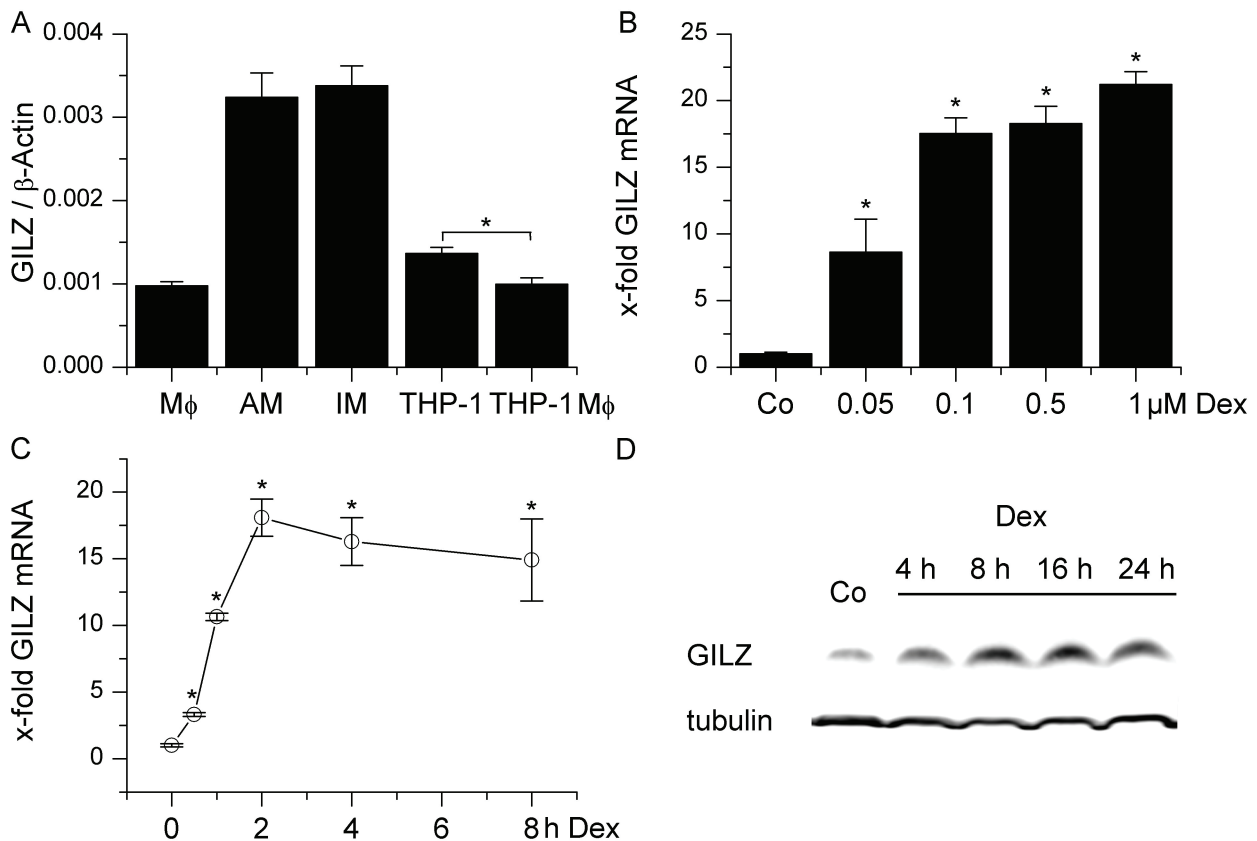


**Figure 21: Constitutive expression and induction of GILZ by dexamethasone** – A: RNA was isolated from AM, IM, *in vitro* differentiated macrophages (M $\Phi$ ), THP-1 cells and PMA-differentiated THP-1 macrophage like cells (THP-1 M $\Phi$ ) and real-time RT PCR analysis for GILZ was performed. Data were normalized to  $\beta$ -Actin. Data show means  $\pm$  SEM of at least 5 independent experiments. Primary cells were from at least 5 different donors. \* $P < 0.05$ . B, C: AM were left untreated (Co) or treated with dexamethasone

(Dex) for 4 h at the indicated concentrations (B) or with 100 nM Dex for the indicated time points (C) followed by real-time RT-PCR analysis for GILZ. Data are normalized to  $\beta$ -actin and represent means  $\pm$  SEM of two independent experiments performed in triplicate with cells derived from two different donors. \*  $P < 0.05$  compared to Co. D: Western Blot analysis of AM treated with Dex (1  $\mu$ M) for the indicated time points. Tubulin protein expression served as a loading control. One representative out of three independent experiments with cells originating from different donors is shown.

#### **4.2.2 TLR9 activation attenuates GILZ expression**

Within the project investigating the reaction of human AM upon treatment with mycobacterial DNA as a TLR9 ligand (see also Chapter II), the effects on the expression of pro- and anti-inflammatory mediators was investigated. In this context, we aimed to determine whether TLR9 ligands affect GILZ expression. When we treated AM with DNA from *M. bovis* BCG as natural TLR9 ligand, we found a rapid and dose-dependent decrease of GILZ mRNA and protein (figure 22 A and B). Determination of TNF- $\alpha$  mRNA levels demonstrated a strong activation of the cells. Also the synthetic oligonucleotide ODN2006 as TLR9 ligand activating AM (as assessed by TNF- $\alpha$  mRNA induction) attenuated GILZ mRNA levels already 2 h after treatment (figure 22 C and D). As observed previously, however, the synthetic oligonucleotide showed weaker effects on macrophages than genomic bacterial DNA.

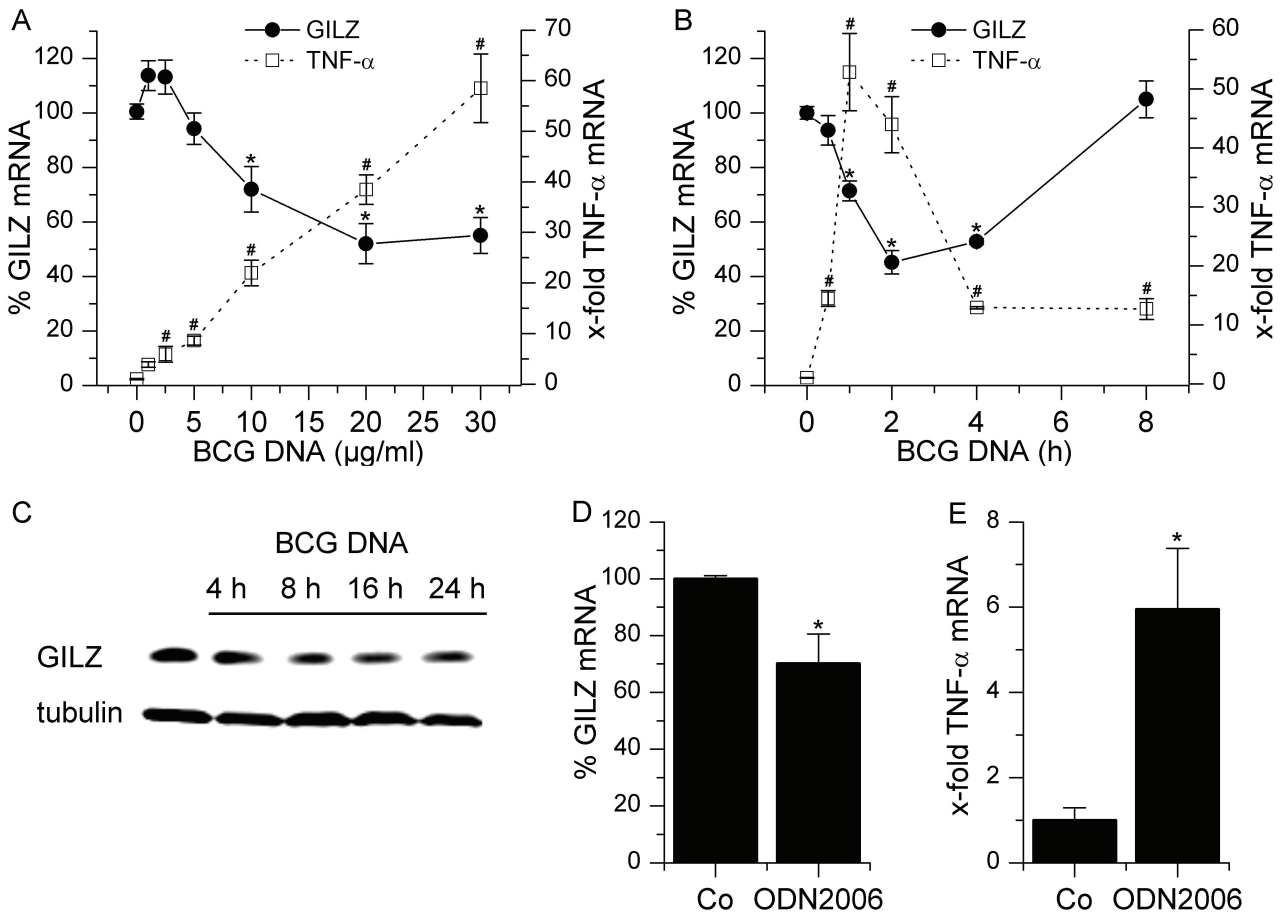


**Figure 22: Downregulation of GILZ upon TLR9 activation** – A, B: AM were treated with BCG DNA for 2 h at the indicated concentrations (A) or with 20 μg/ml BCG DNA for the indicated time points (B) followed by real-time RT-PCR analysis for GILZ and TNF-α. Data are normalized to β-actin and represent means ± SEM of 3-4 independent experiments with cells from different donors. \*  $P < 0.05$  compared to GILZ in untreated controls, #  $P < 0.05$  compared to TNF-α in untreated controls. C: AM were treated with BCG DNA (20 μg/ml) for the indicated time points. Western blot analysis was performed using tubulin as a loading control. Data show one representative out of two independent experiments performed in triplicate with cells from different donors. D, E: AM were treated with ODN2006 oligonucleotides (40 μg/ml) for 2 h followed by real-time RT-PCR for GILZ and TNF-α. Data are normalized to β-actin and represent means ± SEM of 3 independent experiments with cells from different donors. \*  $P < 0.05$  compared to Co.

#### 4.2.3 GILZ downregulation in response to TLR4 activation

In order to determine whether downregulation of GILZ was an effect specific for TLR9 activation, we used LPS as a ligand for TLR4. GILZ was quickly downregulated after LPS addition. This was accompanied by activation of AM, as indicated by a significant induction of TNF-α mRNA upon LPS challenge (figures 23 A and B). GILZ mRNA levels were already downregulated to 20% of untreated controls at a LPS concentration of 10 ng/ml and were not further decreased by increasing LPS concentrations (figure 23 A). Maximal LPS-mediated reduction of GILZ mRNA occurred at 2 h (figure 23 B). Similar results were

obtained with *in vitro* differentiated macrophages (figure 23 C) as well as the THP-1 cell line (data not shown).

Next, we tested whether the transient decrease of GILZ mRNA levels attenuates GILZ protein in AM. In fact, LPS reduced GILZ protein very quickly (figure 23 D). Interestingly, GILZ protein levels were decreased for up to 24 h, even though GILZ mRNA showed to rise again after reaching a minimum after 2 h of treatment. These results suggested that GILZ downregulation might not solely be mediated by alteration of mRNA levels, but might involve attenuated translation or protein stability.

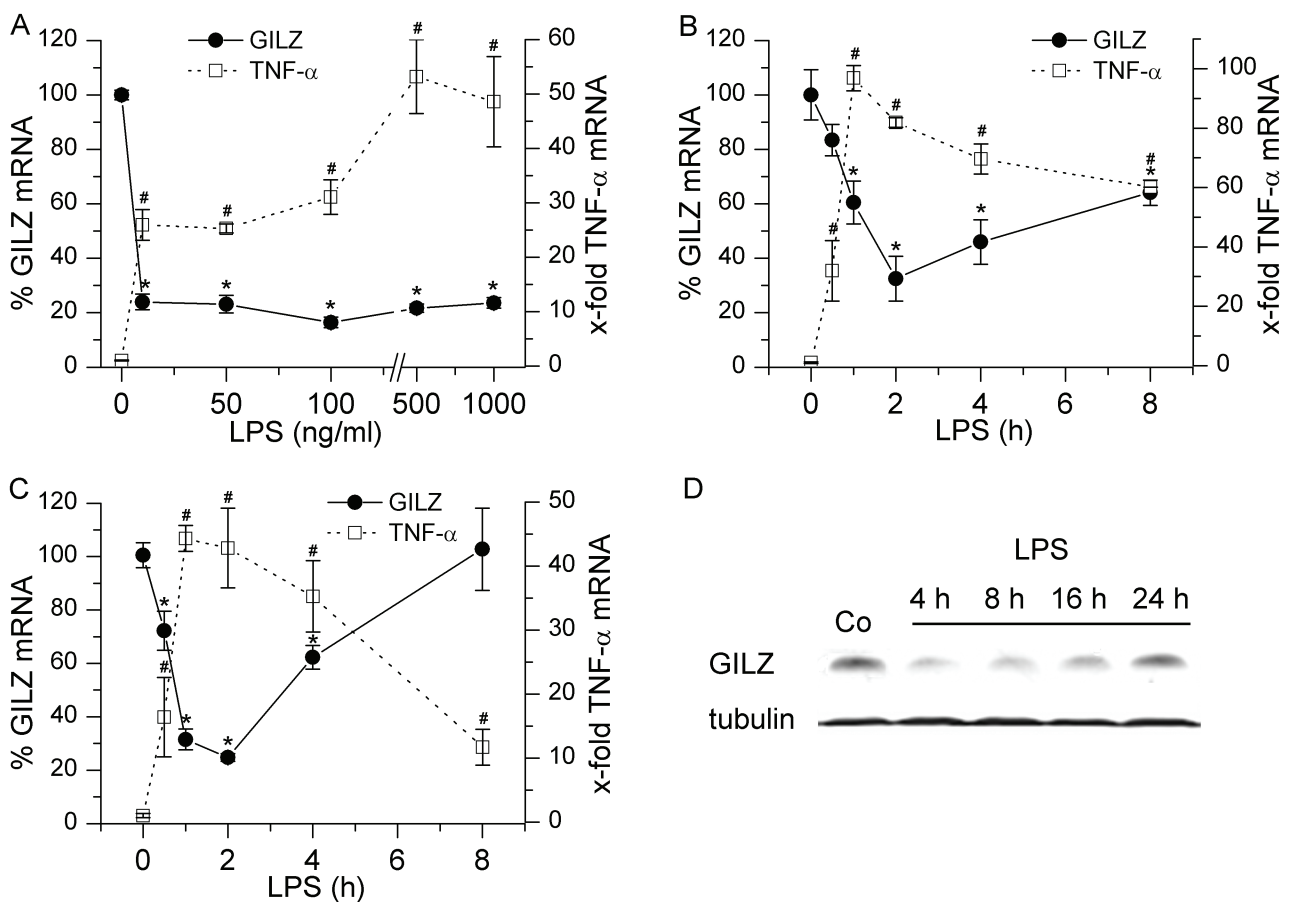


**Figure 23: Downregulation of GILZ by LPS** – A-C: AM (A, B) or *in vitro* differentiated macrophages (C) were treated with LPS for 2 h at the indicated concentrations (A) or with 100 ng/ml LPS for the indicated time points (B, C) followed by real-time RT-PCR analysis for GILZ and TNF- $\alpha$ . Data are normalized to  $\beta$ -actin and represent means  $\pm$  SEM of 4 independent experiments with cells from different donors. \*  $P < 0.05$  compared to GILZ in untreated controls, #  $P < 0.05$  compared to TNF- $\alpha$  in untreated controls. D: AM were treated with LPS (100 ng/ml) for the indicated time points. Western blot analysis was performed using tubulin as a loading control. Data show one representative out of three independent experiments with cells from different donors.

We then sought to check for an *in vivo* relevance for these findings. GILZ protein as well as mRNA levels were significantly decreased in lungs of LPS-treated mice compared to control animals (figure 24), which corroborated our *in vitro* findings.

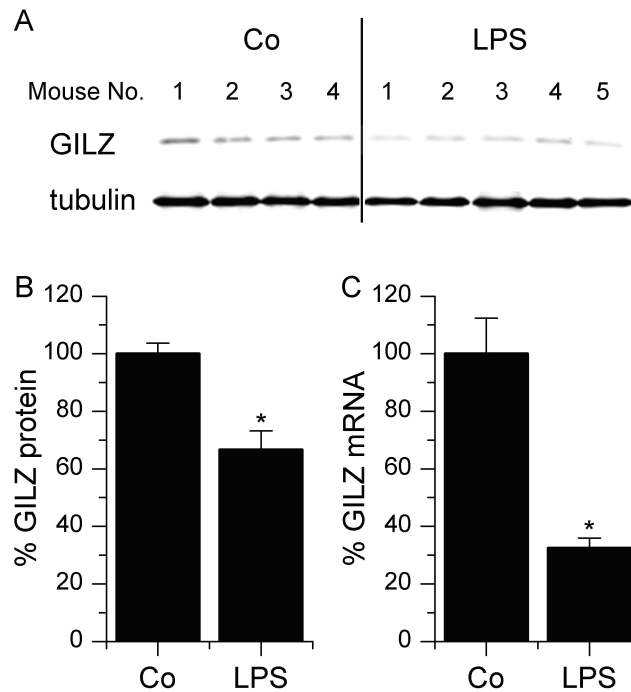


**Figure 24: In vivo downregulation of GILZ under inflammatory conditions** - C57BL/6 mice were injected intraperitoneally with 50 µg LPS diluted in physiological salt solution (n = 5) or the equal amount of salt solution only (Co, n = 4). 4 h after injection, mice were sacrificed and the lungs were removed to determine GILZ levels. A: Lung tissue was lysed, and equal protein amounts were assessed by Western Blot analysis using tubulin as a loading control. B: Relative GILZ protein signal intensities were quantified and normalized to tubulin values. Data are expressed as percentage of Co values. \*  $P < 0.05$  compared to Co. C: RNA was isolated from lung tissue and real-time RT-PCR analysis for GILZ was performed. Data are normalized to  $\beta$ -actin and show means  $\pm$  SEM. \*  $P < 0.05$  compared to Co.

#### 4.2.4 Enhanced expression of proinflammatory cytokines due to reduced GILZ levels

To determine the functional implications of GILZ downregulation, GILZ knockdown using siRNA was performed. As shown in figure 25 A, transfection of THP-1 cells with siGILZ resulted in reduced GILZ protein expression compared to both control siRNA transfected and untransfected cells. We then treated siGILZ cells or the respective control transfected cells with LPS and measured IL8 as well as TNF- $\alpha$  mRNA levels (figure 25 B and C). As expected, LPS treatment for 0.5 and 1 h induced IL8 as well as TNF- $\alpha$  mRNA in untransfected THP-1 cells. Transfection with control siRNA did not alter IL8 or TNF- $\alpha$

expression compared to untransfected cells, both at baseline and upon LPS stimulation. In contrast, knockdown of GILZ resulted in a small but significant increase in basal IL8 mRNA levels (figure 25 B). Moreover, LPS-induced IL8 as well as TNF- $\alpha$  mRNA expression was significantly enhanced in GILZ knockdown cells.

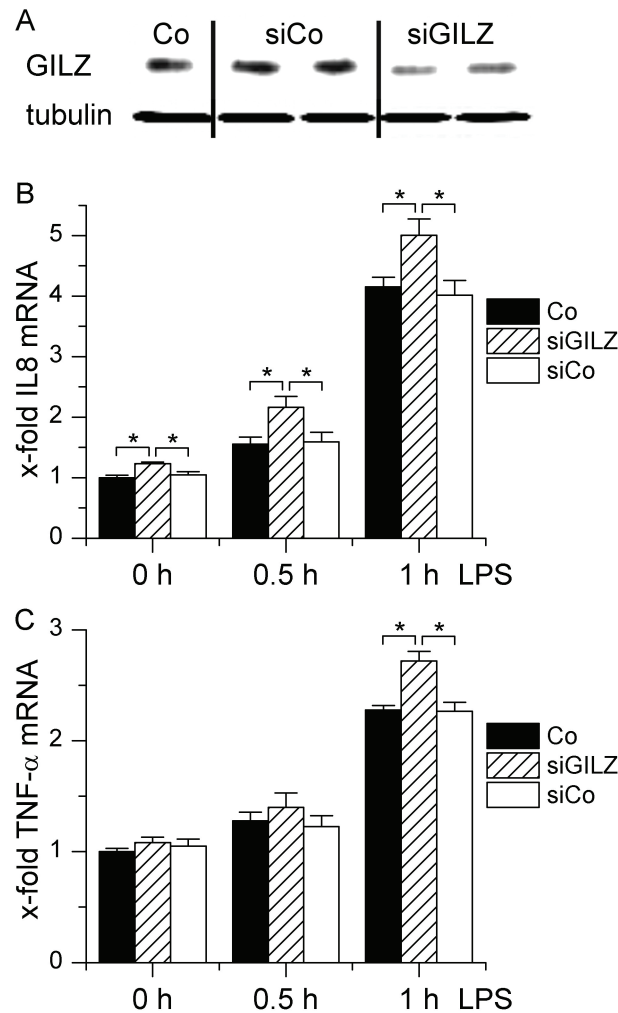


**Figure 25: Knockdown of GILZ drives proinflammatory responses** – THP-1 cells were transfected with either control siRNA (siCo) or GILZ siRNA (siGILZ) or left untreated (Co) for 24 hours. A: Western Blot analysis for GILZ using tubulin as a loading control. Data show one representative out of four independent experiments. B, C: siGILZ, siCo or Co cells were treated with LPS for the indicated time points, and IL-8 (B) and TNF- $\alpha$  (C) expression was measured by real-time RT PCR. Data are normalized to  $\beta$ -actin and represent means of four independent experiments performed in triplicate  $\pm$  SEM. \*  $P < 0.05$

#### 4.2.5 GILZ downregulation upon MyD88-dependent and –independent TLR activation

Reduced GILZ expression following TLR4 and TLR9 activation suggested that cell activation *via* TLRs generally decreased GILZ levels. In order to test this assumption, we employed other TLR ligands and determined GILZ mRNA levels. TLR ligands mimicking bacterial or viral molecular patterns, i.e. Pam<sub>3</sub>CSK<sub>4</sub> (TLR1/2 ligand), flagellin (TLR5 ligand), FLS-1 (TLR2/6 ligand), imiquimod (TLR7 ligand), ssRNA40 (TLR8 ligand), and bacterial DNA (TLR9 ligand, see 4.2.2), reduced GILZ mRNA levels after 2 h in AM (figure 26 A). GILZ downregulation was paralleled by a marked activation of cells, as assessed by TNF- $\alpha$  induction (figure 26 B). We also determined the influence of TLR1/2 activation on GILZ protein expression. In fact, GILZ protein amounts were reduced after Pam<sub>3</sub>CSK<sub>4</sub> addition (figure 26 C), which resembled our observations for LPS.

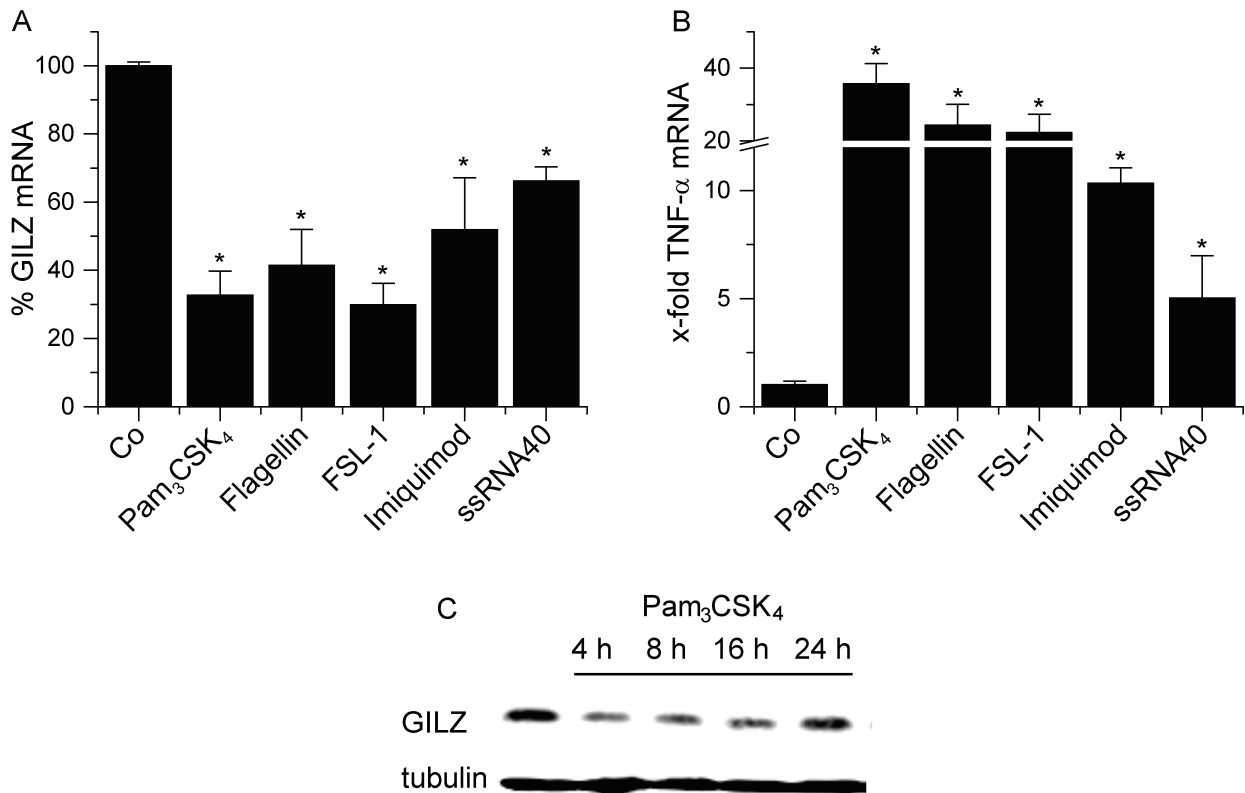


**Figure 26: GILZ downregulation upon MyD88-dependent TLR activation** – A, B: AM were left untreated (Co) or treated with either Pam<sub>3</sub>CSK<sub>4</sub> (250 ng/ml), flagellin (250 ng/ml), FSL-1 (250 ng/ml), imiquimod (7.5  $\mu$ g/ml), ssRNA40 (7.5  $\mu$ g/ml) or bacterial DNA (20  $\mu$ g/ml), followed by real-time RT-PCR analysis for GILZ (A) or TNF- $\alpha$  (B). Data are normalized to  $\beta$ -actin and represent means  $\pm$  SEM of four independent experiments performed with cells derived from four different donors. \*  $P < 0.05$  compared to Co. C: AM were treated with Pam<sub>3</sub>CSK<sub>4</sub> (100 ng/ml) for the indicated time points. Western blot analysis was performed using tubulin as a loading control. Data show one representative out of two independent experiments with cells from different donors

Treatment of AM with the synthetic analogue of double-stranded RNA and TLR3 ligand Poly(I:C) also increased TNF- $\alpha$  mRNA levels after 2 h (figure 27 A). TNF- $\alpha$  induction was not due to activation of cytosolic Poly(I:C) responsive elements (Barral et al., 2009), as inhibition of TLR3-dependent signalling by chloroquine completely abrogated cell activation (figure 27 A). Interestingly, TLR3 activation was not paralleled by GILZ mRNA downregulation (figure 27 B), and Poly(I:C) did not alter GILZ mRNA expression at 2 h at any of the concentrations tested (figure 27 C). As the lack of effect of Poly(I:C) on GILZ mRNA might be due to a different time course transmitted via the MyD88-independent TLR3 pathway compared to the other TLR ligands utilizing MyD88 as an adapter molecule, we performed time-course studies with the TLR3 ligand for up to 8 h. Although TNF- $\alpha$  mRNA levels were markedly increased one to eight hours after treatment, no decrease in GILZ mRNA could be observed at any time point (figure 27 D). Similar to AM, Poly(I:C) did not decrease GILZ mRNA in THP-1 cells (data not shown). This observation suggests that GILZ mRNA downregulation is mediated *(I)* independent of MyD88 and *(II)* independent of TNF- $\alpha$ . Most interestingly, however, Western blot analysis showed that GILZ protein levels are in fact reduced after treatment with Poly(I:C) despite a lack of effect on GILZ mRNA (figure 27 E). GILZ protein downregulation was mediated via TLR3 activation, as it was inhibited by chloroquine pretreatment. These findings let us hypothesize that GILZ is regulated on two levels, i.e. on mRNA and protein level.

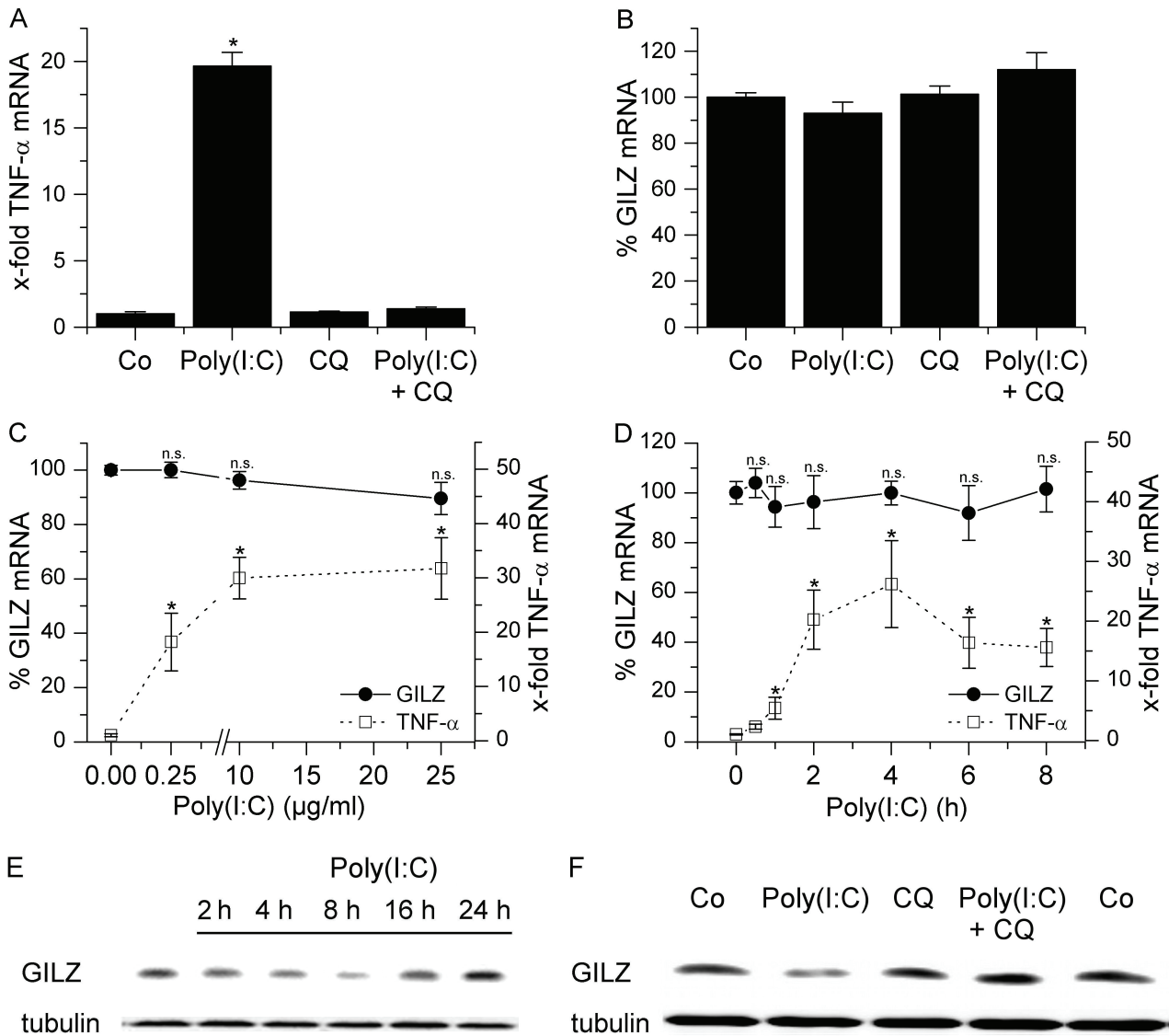


**Figure 27: TLR3 activation reduces GILZ protein, but not mRNA levels** – A, B: AM were either left untreated (Co), or treated with chloroquine (CQ, 10  $\mu$ M), Poly(I:C) (10  $\mu$ g/ml, 2 h) or a combination of both whereby CQ was added to the cells 1 h before Poly(I:C). Real-time RT-PCR analysis for TNF- $\alpha$  (A) or GILZ (B) was performed. Data are normalized to  $\beta$ -actin and represent means  $\pm$  SEM of three independent experiments performed with cells derived from different donors. \*  $P < 0.05$  compared to Co. C, D: AM were left untreated (Co) or treated with Poly(I:C) for 2 h at the indicated concentrations (C) or with 10  $\mu$ g/ml Poly(I:C) for the indicated time points (D) followed by real-time RT-PCR analysis for GILZ and TNF- $\alpha$ . Data are normalized to  $\beta$ -actin and represent means  $\pm$  SEM of six independent experiments with cells obtained from six different donors. \*  $P < 0.05$  compared to Co values. n.s.: not significant. E: AM were treated with Poly(I:C) (10  $\mu$ g/ml) for the indicated time points, followed by immunoblotting for GILZ using tubulin as a loading control. Data show one representative out of three independent experiments with cells from different donors. F: AM were either left untreated (Co) or treated with CQ (10  $\mu$ M) and/or Poly(I:C) (10  $\mu$ g/ml, 8 h). CQ was added to cells 1 h prior to Poly(I:C) challenge, and Western blot analysis for GILZ was performed. Tubulin served as a loading control. One representative out of three independent experiments with cells from different donors is shown.

#### **4.2.6 MyD88-dependent GILZ mRNA downregulation**

Our findings indicated that downregulation of GILZ mRNA requires the adapter molecule MyD88. To specify the role of MyD88, we performed an siRNA-mediated MyD88 knockdown and checked the ability of LPS and Pam<sub>3</sub>CSK<sub>4</sub> to decrease GILZ mRNA levels. MyD88 protein levels were effectively knocked down in PMA-differentiated THP-1 cells by MyD88 siRNA 72 h post transfection when compared with levels seen in cells transfected with control siRNA (figure 28 A). Treatment of control siRNA cells with LPS or Pam<sub>3</sub>CSK<sub>4</sub> reduced GILZ mRNA levels. Effects were comparable to those detected in untransfected control cells: GILZ mRNA decreased by 70 % at 2 h after treatment. This effect was significantly abrogated in MyD88 siRNA cells. Under these conditions LPS and Pam<sub>3</sub>CSK<sub>4</sub> only reduced GILZ mRNA levels by 30 % (figure 28 B). Employment of a MyD88 inhibitory peptide resulted in similar effects, although inhibition of MyD88 was not as efficient as the knockdown procedure (figure 28 C). Taken together, these data demonstrate that GILZ mRNA downregulation upon TLR activation requires the adapter molecule MyD88.

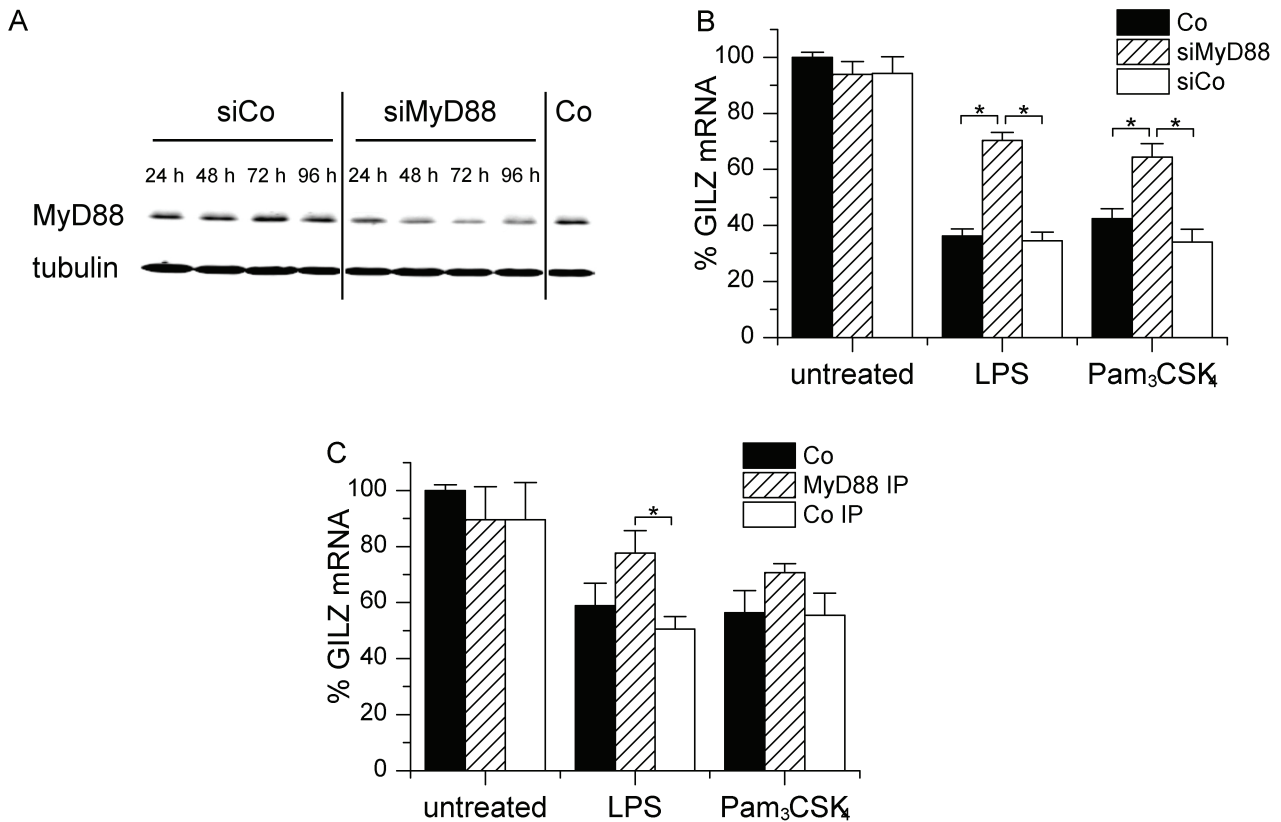


**Figure 28: *GILZ* mRNA downregulation requires *MyD88*** – A: Differentiated THP-1 cells were transfected with either control siRNA (siCo) or MyD88 siRNA (siMyD88) or left untreated (Co) for up to 96 h, followed by immunoblotting for MyD88 using tubulin as a loading control. Data show one representative out of 4 independent experiments. B: siMyD88, siCo or Co cells were treated with LPS (100 ng/ml) or Pam<sub>3</sub>CSK<sub>4</sub> (100 ng/ml) 70 h after transfection for 2 h, and *GILZ* mRNA was assessed by real-time RT-PCR. Data are normalized to  $\beta$ -actin and represent means of three independent experiments performed in triplicate  $\pm$  SEM. \*  $P < 0.05$ . C: Differentiated THP-1 cells were treated with either MyD88 inhibitory peptide (MyD88 IP, 10  $\mu$ g/ml) or control peptide (Co IP, 10  $\mu$ g/ml) or left untreated for 24 h, followed by addition of LPS (100 ng/ml) or Pam<sub>3</sub>CSK<sub>4</sub> (100 ng/ml) for 2 h. *GILZ* mRNA was quantified by real-time RT-PCR. Values are normalized to  $\beta$ -Actin and represent means of two independent experiments performed in triplicate. \*  $P < 0.05$ .

#### 4.2.7 Decrease of *GILZ* mRNA half life in response to LPS

*GILZ* mRNA downregulation might either occur on the level of transcription or on the level of mRNA stability. Since effects on *GILZ* mRNA were very rapid, we hypothesized a destabilization of *GILZ* mRNA upon TLR activation. In order to determine potential changes in *GILZ* mRNA half-life, we incubated AM with the transcription inhibitor actinomycin D in the presence or absence of LPS and determined changes in *GILZ* mRNA levels. Control cells displayed a  $t_{1/2}$  of *GILZ* mRNA of 2.3 h, whereas *GILZ* mRNA half-life was only 1.3 h in LPS-treated cells (figure 29 A), confirming the hypothesis of a reduced mRNA stability in TLR-activated AM. Similar results were obtained when repeating the actinomycin D experiments with *in vitro* differentiated macrophages (figure 29 B),

indicating that the shortening of GILZ mRNA half life after LPS treatment is not restricted to a single macrophage type.

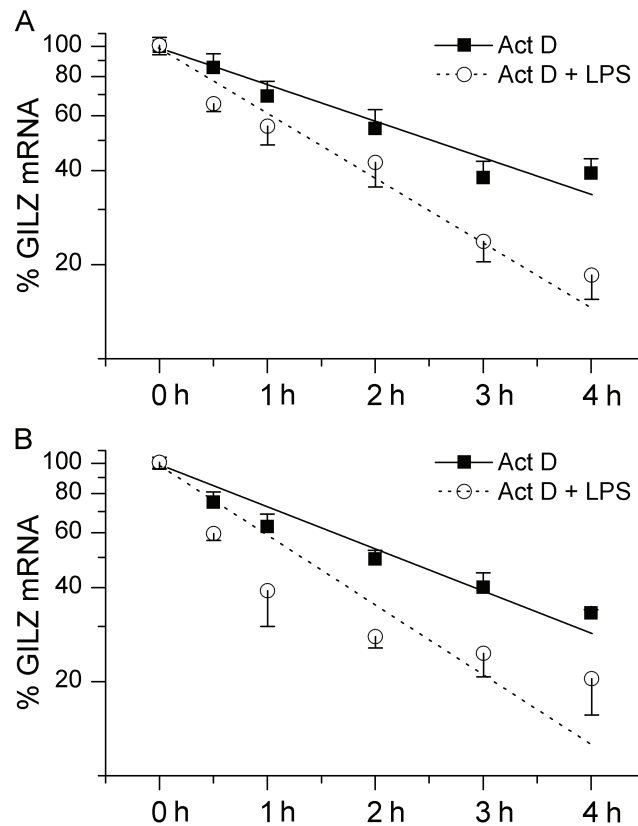


**Figure 29: GILZ mRNA destabilization upon TLR activation** – AM (A) or *in vitro* differentiated macrophages (B) were either left untreated or treated with actinomycin D (10  $\mu$ g/ml) in the absence or presence of LPS (100 ng/ml). RNA was isolated at the indicated time points, and real-time PCR analysis for GILZ was performed. Data are normalized to  $\beta$ -Actin and represent means  $\pm$  SEM of five (A) or three (B) independent experiments with cells obtained from different donors. Curve fitting was done using Origin software.

#### 4.2.8 Involvement of TTP in GILZ mRNA destabilization

A prime mechanism of 3'UTR dependent mRNA destabilization is mediated *via* RNA binding proteins (Eberhardt et al., 2007). Tristetraprolin (TTP) is an RNA binding protein critically involved in the regulation of many inflammation-associated mediators. Our data indicate that TTP is induced in AM in a MyD88-dependent fashion, since its upregulation was only seen after LPS or Pam<sub>3</sub>CSK<sub>4</sub>, but not after Poly(I:C) treatment (figure 30 A).

To evaluate whether TTP plays a role in regulating GILZ expression, we transiently overexpressed TTP mRNA in THP-1 cells. As shown in figure 30 C, Western blot analysis

revealed enhanced TTP protein expression in TTP vector transfected cells, whereas no change of TTP protein expression was seen in control vector (CoV) transfected cells as compared to untransfected controls.

We then determined expression of TNF- $\alpha$  mRNA, whose regulation by TTP is well described (Carballo et al., 1998), similar to the recently identified TTP target IL10 mRNA (Stoecklin et al., 2008; Tudor et al., 2009). Overexpression of TTP significantly decreased TNF- $\alpha$  and IL10 mRNA, thus confirming TTP functionality (figure 30 B). Interestingly, these findings were accompanied by decreased GILZ expression both at mRNA and protein level, indicating a TTP-mediated GILZ downregulation (figure 30 B and C).

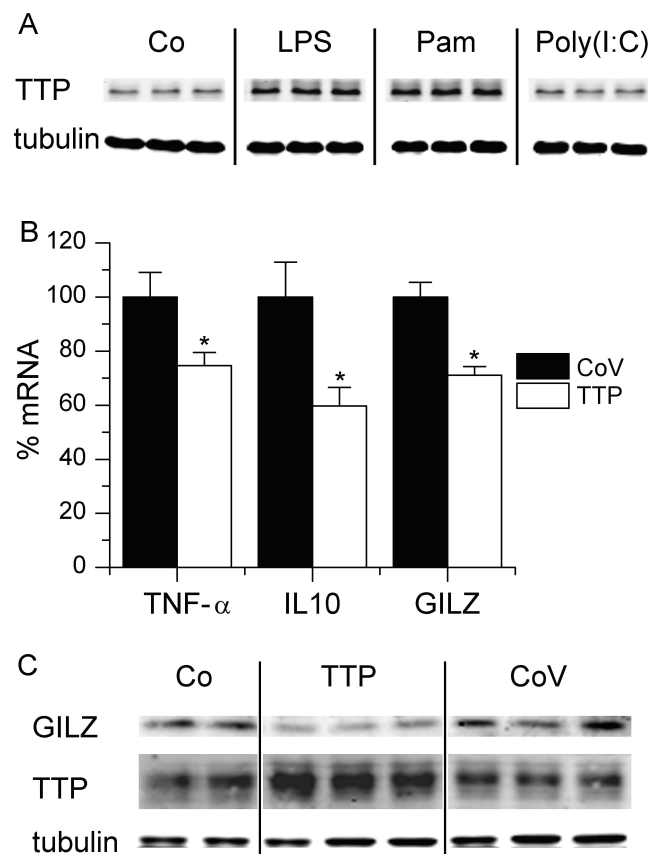


**Figure 30: MyD88 dependent TTP induction and influence of TTP overexpression on GILZ expression** – A: AM were either left untreated or treated with LPS (100 ng/ml), Pam<sub>3</sub>CSK<sub>4</sub> (100 ng/ml) or Poly(I:C) (10  $\mu$ g/ml) for 8 h. Western blot analysis for TTP was performed using tubulin as a loading control. One representative out of two independent experiments performed in triplicate with cells obtained from different donors is shown. B: THP-1 cells were transfected with either control (CoV) or TTP expression (TTP) vector and harvested after 24 h, followed by real-time RT-PCR analysis for TNF- $\alpha$ , IL10 and GILZ. Data are normalized to  $\beta$ -actin and represent means  $\pm$  SEM of four independent experiments performed in triplicate. \*  $P < 0.05$  compared to CoV. C: Total protein was isolated from CoV or TTP transfected and untransfected (Co) THP-1 cells and assessed by Western blot analysis for GILZ and TTP. Tubulin served as a loading control. One representative out of four independent experiments is shown.

To support these results and assess the influence of TTP on TLR-mediated GILZ regulation, we knocked down TTP expression using shRNA. We transfected THP-1 cells with two different shRNA constructs directed against the human TTP mRNA (shTTP1 and shTTP2). As a control, cells were transfected with a construct expressing an shRNA, which targets the luciferase gene (shLuc). Subsequently, cells were treated with Pam<sub>3</sub>CSK<sub>4</sub> in order to induce MyD88-dependent GILZ downregulation.

TTP was efficiently knocked down by both shRNAs 24 h post transfection (figure 31 A). As previously seen in AM, LPS and Pam<sub>3</sub>CSK<sub>4</sub> treatment induced TTP in control transfected shLuc THP-1 cells, whereas TTP induction upon TLR activation was undetectable in either shTTP1 or shTTP2 cells (figure 31 E). As expected, Pam<sub>3</sub>CSK<sub>4</sub> upregulated TNF- $\alpha$  as well as IL10 mRNA, which was significantly enhanced by the knockdown of TTP when compared to mRNA induction in shLuc cells (figure 31 B and C).

shRNA-mediated downregulation of TTP also abrogated GILZ downregulation upon activation with Pam<sub>3</sub>CSK<sub>4</sub> both at mRNA and protein level (figures 31 D and E). We also detected similar effects for GILZ protein when challenging cells with LPS (figure 31 E), further supporting the role of TTP in GILZ downregulation.

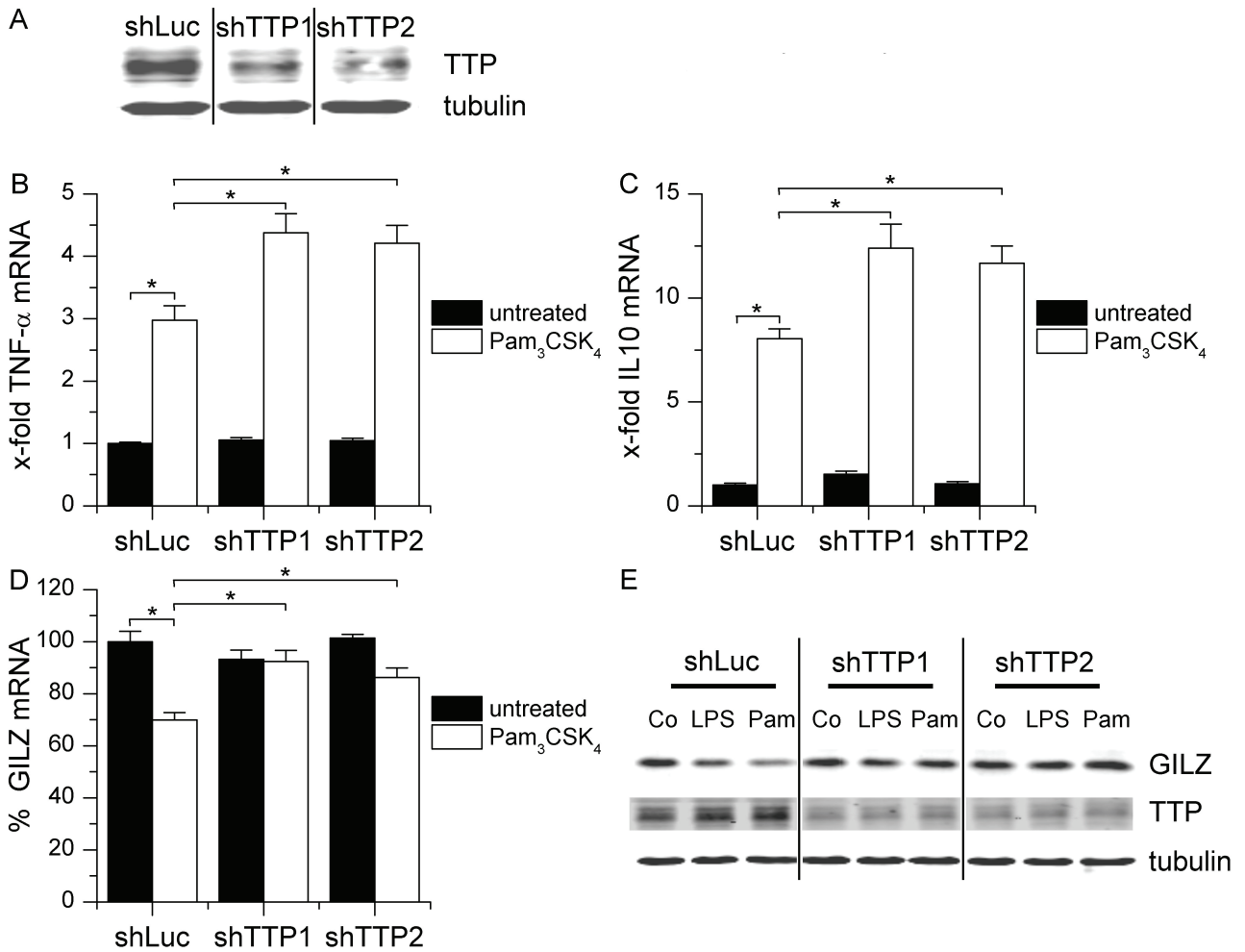


**Figure 31: Impact of TTP knockdown on TLR-mediated decrease in GILZ expression** – THP-1 cells were transfected with a control shRNA construct (shLuc) or one of two shRNA vectors targeting TTP (shTTP1, shTTP2). A: Cells were lysed 24 h after transfection, and TTP was assessed by Western blot analysis using tubulin as a loading control. One representative out of four independent experiments is shown. B, C, D: 22 h after transfection, shLuc, shTTP1 or shTTP2 cells were either treated with Pam<sub>3</sub>CSK<sub>4</sub> (100 ng/ml) or left untreated for 2 h and real-time RT-PCR for TNF- $\alpha$  (B), IL10 (C) or GILZ (D) mRNA was performed. Values are normalized to  $\beta$ -actin and represent means of four independent experiments performed in triplicate  $\pm$  SEM. Data are expressed as x-fold (B, C) or percentage (D) of values for untreated shLuc cells. \*  $P < 0.05$ . E: 20 h after transfection, shLuc, shTTP1 or shTTP2 cells were treated with Pam<sub>3</sub>CSK<sub>4</sub> (100 ng/ml) for 4 h or left untreated. Western blot analysis for GILZ and TTP was performed using tubulin as a loading control. One representative out of four independent experiments is shown.

#### 4.2.9 Proteasome-dependent GILZ downregulation

As the MyD88-independently acting Poly(I:C) is capable of reducing GILZ mRNA, but not protein levels, we hypothesized that GILZ protein might be downregulated in a proteasome-dependent fashion in response to TLR3 activation. Thus, we employed the proteasome inhibitor MG-132 prior to Poly(I:C) addition. As shown in figure 32 A, MG-132 pretreatment completely abrogated GILZ downregulation upon stimulation with Poly(I:C) in AM. DMSO, the solvent for MG-132, did not influence GILZ protein expression (data not shown). Interestingly, MG-132 treatment also inhibited MyD88-facilitated, i.e Pam<sub>3</sub>CSK<sub>4</sub>- and LPS-mediated downregulation of GILZ protein (figure 32 B and C).

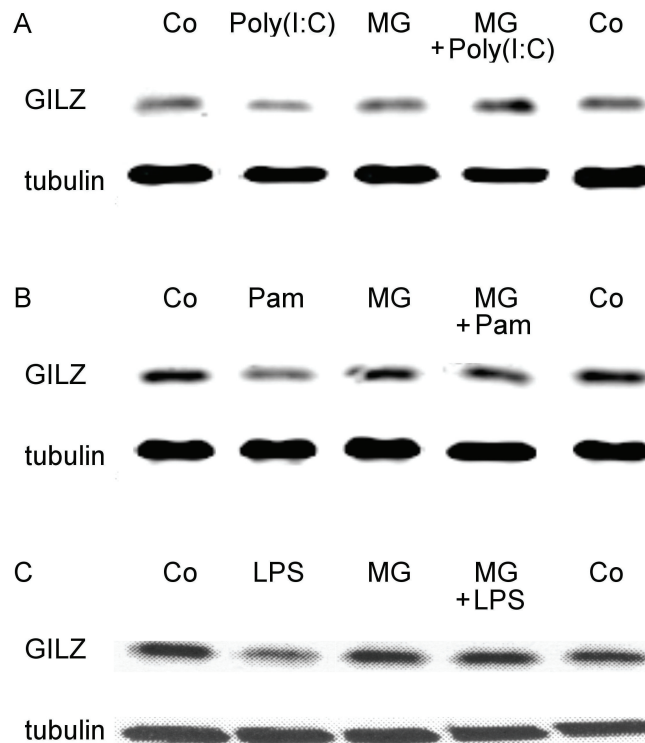


**Figure 32: Abrogation of GILZ protein downregulation by MG-132** – AM were treated with MG-132 (10  $\mu$ M) 1 h prior to addition of either (A) Poly(I:C) (10  $\mu$ g/ml), (B) Pam<sub>3</sub>CSK<sub>4</sub> (100 ng/ml) or (C) LPS (100 ng/ml) for 4 h. Western blot analysis for GILZ was performed using tubulin as a loading control. One representative out of 2-4 independent experiments with cells from different donors is shown.

Since Myd88-dependent GILZ downregulation was shown to be regulated on mRNA level, we wondered whether MG-132 also affected GILZ mRNA levels upon LPS treatment.

In fact, LPS treatment failed to decrease GILZ mRNA amounts when AM or *in vitro* differentiated macrophages were pretreated with MG-132 (figure 33 A and C). This was

paralleled by an inhibition of TNF- $\alpha$  induction, most likely via inhibition NF- $\kappa$ B activation. DMSO did neither influence GILZ nor TNF- $\alpha$  mRNA expression (figure 33 B and D).

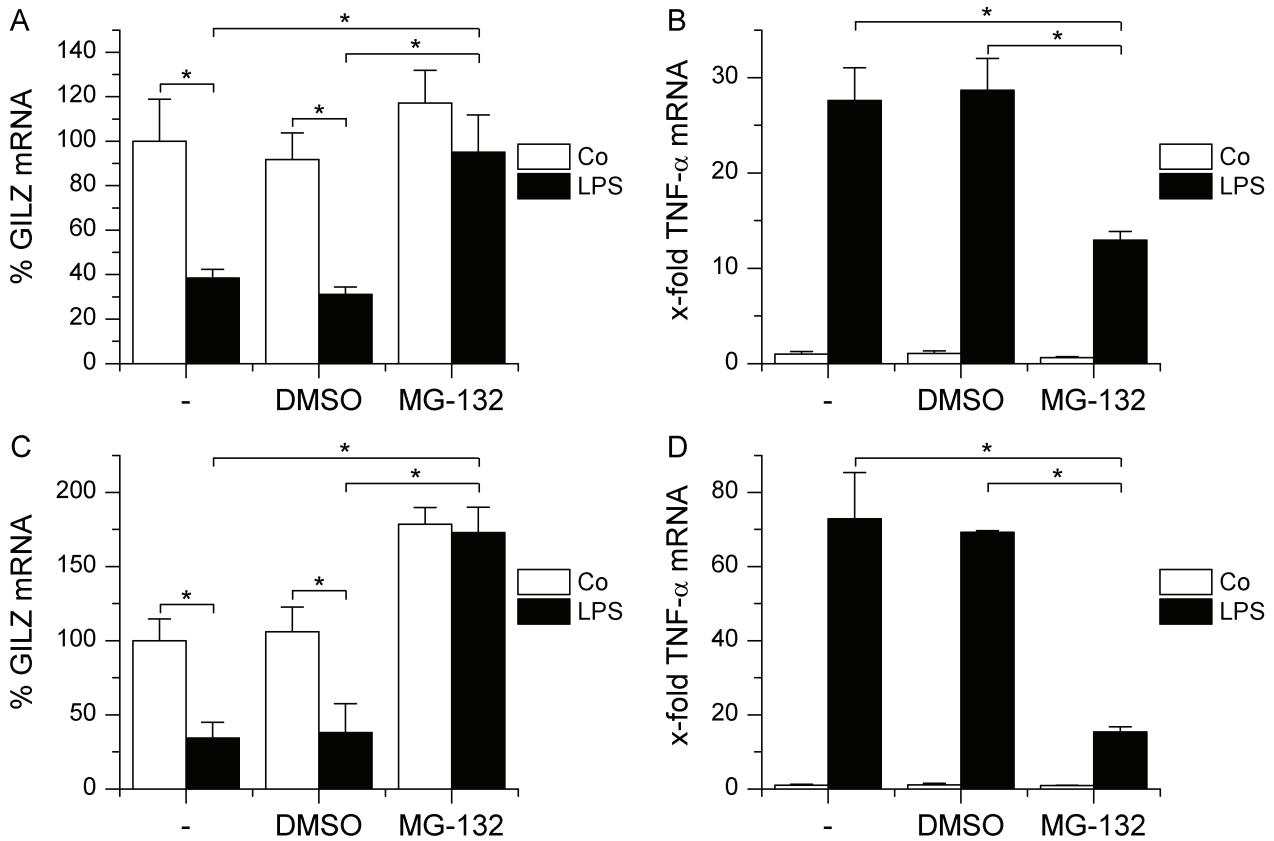


**Figure 33: Inhibition of GILZ mRNA downregulation by MG-132** – AM (A, B) or in vitro differentiated macrophages (C, D) were either left untreated (-) or pretreated with MG-132 (10  $\mu$ M, 1h) or an equal volume of DMSO as a solvent control. Cells were incubated for an additional 2 h in absence (Co) or presence of LPS (100 ng/ml), followed by real-time RT-PCR analysis for GILZ (A, C) and TNF- $\alpha$  (B, D). Data are normalized to  $\beta$ -actin and represent means  $\pm$  SEM of two (A, B) or three (C, D) independent experiments with cells from different donors. \*  $P < 0.05$ .

#### 4.2.10 TNF- $\alpha$ -mediated GILZ downregulation

As TNF- $\alpha$  has previously been reported to reduce GILZ levels in epithelial and endothelial cells (Eddleston et al., 2007; Hirschfelder et al., 2010), we speculated that TNF- $\alpha$  induction might contribute to the effects observed after TLR activation. Thus, we incubated AM with TNF- $\alpha$  (10 ng/ml) and determined GILZ mRNA and protein expression. TNF- $\alpha$  treatment decreased GILZ mRNA as well as protein levels (figure 34).

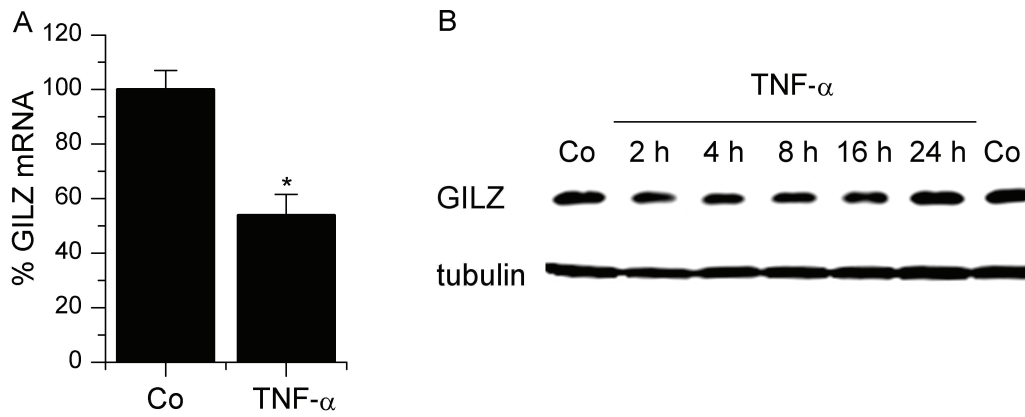


**Figure 34: *TNF- $\alpha$*  decreases *GILZ* expression** – A: AM were either left untreated or treated with *TNF- $\alpha$*  (10 ng/ml) for 2 h, followed by real-time RT-PCR for *GILZ*. Values are normalized to  $\beta$ -actin and represent means of two independent experiments performed in triplicate with cells from different donors. \*  $P < 0.05$ . B: AM were left untreated (Co) or treated with *TNF- $\alpha$*  (10 ng/ml) for the indicated time points. Western blot analysis for *GILZ* was performed using tubulin as a loading control. One representative out of three independent experiments is shown.

#### 4.2.11 *GILZ* mRNA expression in endotoxin tolerance

Macrophages exposed to LPS show reduced responses to a second stimulation with LPS, which is termed endotoxin or LPS tolerance. We wondered whether *GILZ* downregulation might be affected in LPS tolerant cells. When AM were stimulated with 1  $\mu$ g/ml LPS for 2 h, these cells displayed a significant increase in production of *TNF- $\alpha$*  mRNA. However, when the cells were preincubated with 100 ng/ml LPS for 24 h, *TNF- $\alpha$*  mRNA induction was dramatically reduced. In fact, *TNF- $\alpha$*  mRNA levels did not exceed those observed in cells that were only pretreated, indicating that the cells were LPS tolerant (Figure 35 A). Remarkably, desensitized cells lost their ability to reduce *GILZ* mRNA levels in response to LPS, suggesting that *GILZ* might play a role in macrophage desensitization. We also observed that *GILZ* mRNA amounts were slightly increased by the initial LPS treatment, although data did not reach statistical significance (figure 35 B).

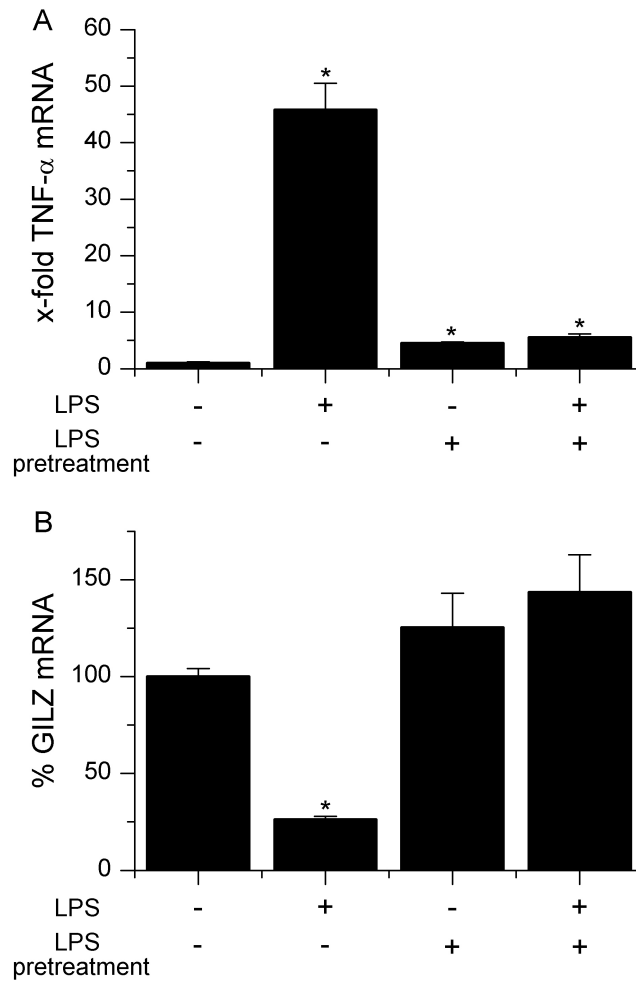


**Figure 35: LPS tolerant AM fail to decrease GILZ levels** – AM were left untreated (-) or pretreated with 100 ng/ml LPS for 24 h. Cells were washed and then incubated in the absence or presence of 1  $\mu$ g/ml LPS for an additional 2 h. Real-time RT-PCR was performed for TNF- $\alpha$  (A) and GILZ (B). Data are normalized to  $\beta$ -actin and represent means of three independent experiments performed in triplicate with cells obtained from different donors. \*  $P < 0.05$  compared to untreated cells.

## 4.3 Discussion

Lung macrophages represent key players in pulmonary inflammation as associated with asthma, chronic obstructive pulmonary disease (COPD) or allergic diseases (Sabroe et al., 2007; O'Donnell et al., 2006). Whereas the scientific interest in reducing macrophage activation mostly focuses on the reduction of inflammatory mediators (Gordon, 2007), few is known about the regulation of anti-inflammatory regulators, such as GILZ. Glucocorticoids are currently the most widely used class of anti-inflammatory drugs in the treatment of inflammatory lung diseases, and they are considered to exert their actions to a significant extent *via* induction of GILZ (Eddleston et al., 2007; Ayroldi and Riccardi, 2009). GILZ mediates its anti-inflammatory properties mainly *via* inhibition of the NF- $\kappa$ B pathway (Ayroldi et al., 2001; Eddleston et al., 2007). Moreover, GILZ was reported to inhibit AP-1 activation and to interfere with Raf / Ras signalling (Ayroldi et al., 2002; Mittelstadt and Ashwell, 2001; Ayroldi et al., 2007; Ayroldi and Riccardi, 2009). Thus, GILZ expression affects signalling pathways, which are pivotal to inflammatory processes.

### 4.3.1 Constitutive and dexamethasone-induced GILZ expression in pulmonary macrophages

Here we present the first report of constitutive GILZ expression in primary human lung macrophages, both in AM and in IM. Interestingly, although IM express higher levels of IL10 than AM (Bedoret et al., 2009; Chapter II), and IL10 is able to induce GILZ expression (Berrebi et al., 2003), expression levels do not differ between AM and IM. As expected, we found that GILZ is upregulated by the glucocorticoid dexamethasone in AM on mRNA as well as protein level. GILZ upregulation by glucocorticoids was originally reported for murine lymphocytes and thymocytes (D'Adamio et al., 1997) and is mediated *via* activation of the glucocorticoid receptor, which subsequently interacts with the three glucocorticoid response element sites found in the promoter region of the GILZ gene (Ayroldi and Riccardi, 2009). Glucocorticoid-induced GILZ upregulation was also observed in human cells, such as epithelial cells (Eddleston et al., 2007), monocytes (Berrebi et al., 2003), mast cells (Godot et al., 2006), and dendritic cells (Cohen et al., 2006). Our findings demonstrate that a rapid and persistent glucocorticoid-mediated GILZ induction also occurs in AM, suggesting that the induction of GILZ is crucial for the mediation of anti-inflammatory actions of glucocorticoids in this cell type.

### 4.3.2 TLR-mediated GILZ downregulation

The regulation of GILZ in inflammatory conditions is poorly understood. TLRs play a key role in both infectious and noninfectious inflammatory lung diseases, as they are capable of sensing different microbial as well as endogenous molecules whereby the latter are released after cell damage (Opitz et al., 2010). We assessed the effect of TLR activation on the level of GILZ expression in AM. When we treated AM with the TLR4 agonist LPS or mycobacterial DNA as a ligand of TLR9, both GILZ mRNA and protein levels were quickly decreased. Most interestingly, we also detected severely decreased GILZ mRNA and protein levels in lungs of LPS-exposed mice. Along with reports of decreased GILZ levels in inflammatory bowel disease, tuberculosis and chronic rhinosinusitis (Berrebi et al., 2003, Zhang et al., 2009), these observations demonstrate the *in vivo* relevance of our findings.

To assess the functional implications of GILZ downregulation, we used siRNA to knock down GILZ in THP-1 monocytic cells and then examined TNF- $\alpha$  and IL8 levels in the presence or absence of LPS. Although GILZ knockdown cells displayed significantly enhanced levels of TNF- $\alpha$  as well as IL8 upon TLR4 activation, the effects we observed were quite small. This might be due to the fact that the effects of GILZ knockdown merely add to TLR-mediated GILZ downregulation. Thus, the knockdown procedure might only be able to affect inflammatory processes to a limited extent. Interestingly, we also detected slightly increased IL8 expression levels in GILZ siRNA cells in the absence of any other stimulation, which is in accordance with findings previously described for airway epithelial cells (Eddleston et al., 2007) and might be caused by an increased nuclear translocation of NF- $\kappa$ B (Hirschfelder et al., 2010). In contrast, lung epithelial cells with a stable GILZ knockdown did not display increased cytokine levels compared to GILZ expressing cells (Gomez et al., 2010). It has to be noted, however, that the early cellular response upon decreased GILZ expression can not be detected in stably transfected cells. Since activation of NF- $\kappa$ B results in a functional feedback loop, e.g. *via* diminished degradation of  $\kappa$ B (Medvedev et al., 2000), an activation induced by GILZ knockdown is considered to be only transient.

When we explored the effects of other TLR ligands, we found that activation of all TLRs with the exception of TLR3 leads to diminished GILZ mRNA amounts in AM. Our data show that GILZ protein levels are reduced after treatment with Poly(I:C) despite a lack of effect on GILZ mRNA. These findings let us hypothesize that GILZ is regulated *via* distinct pathways affecting either mRNA or protein levels.

### 4.3.3 MyD88- and TTP-dependent GILZ mRNA downregulation

As TLR3 represents the only TLR that does not utilize the adaptor molecule MyD88 for signal transduction (Kawai and Akira, 2006), we examined the role of MyD88 in GILZ mRNA regulation by MyD88 knockdown. GILZ mRNA downregulation upon TLR activation was markedly abrogated in MyD88 knockdown cells, indicating that the effect does in fact require functional MyD88.

MyD88 was reported to be critically involved in the recognition of bacterial as well as viral infections in the respiratory tract, mainly *via* the TLR pathway (Opitz et al., 2010). MyD88 knockout mice show an impaired expression of proinflammatory mediators and a reduced pathogen clearance after infection with *Klebsiella pneumoniae* (Cai et al., 2009). Mice lacking MyD88 are also highly susceptible towards *Legionella pneumophila*, *Streptococcus pneumoniae* as well as *Haemophilus influenzae* infections (Hawn et al., 2006; Wieland et al., 2005; Albiger et al., 2005). The potential inability to downregulate the expression of the anti-inflammatory factor GILZ might contribute to an insufficient host response in those mice. Interestingly, a MyD88-independent upregulation of the anti-inflammatory S100A8 protein has been reported in macrophages (Endoh et al., 2009) supporting the notion of MyD88 as a critical determinant for a differential activation profile.

Gene expression can be regulated by both transcriptional and post-transcriptional mechanisms. Post-transcriptional modulation of gene expression is commonly procured by changes in mRNA stability, which can be modulated by various extracellular stimuli. Regulation of mRNA stability permits cells to rapidly decrease or increase mRNA levels, and therefore provides a mechanism for fast and tight regulation of protein production. In this manner, cells are enabled to dynamically change gene expression profiles depending on environmental challenges (Wilusz et al., 2001; Wilusz and Wilusz, 2004). Thus, we wondered whether mRNA destabilization might account for TLR-mediated GILZ mRNA downregulation and found that GILZ mRNA half life was indeed significantly shortened after LPS treatment.

The rate of mRNA decay is often determined by cis-regulatory elements containing AU-rich elements (ARE) found in the 3'UTR. These AREs mostly induce a destabilization of the respective mRNA and were found in mRNAs coding for numerous cellular regulators, such as COX-2, IL10, and a number of cytokines involved in the inflammatory response (Lasa et al., 2001; Bakheet et al., 2001; Stoecklin et al., 2008). Since GILZ mRNA is regulated *via* mRNA stability, we analyzed its 3'UTR sequence. This approach revealed one copy of the AUUUA pentamer and a U-rich region, which both represent potential

binding sites for destabilizing RNA binding proteins (Chen and Shyu, 1995). Therefore, we assessed the effect of this region on GILZ mRNA stability by transfecting THP-1 cells with a luciferase construct containing the GILZ 3'UTR and observed that GILZ 3'UTR-luciferase mRNA was in fact significantly destabilized upon TLR activation (Hopstädter et al., 2010b).

Several proteins are known to bind to AREs (Hollams et al., 2002), and many of them have been shown to regulate mRNA stability. These include the tristetraprolin (TTP) family of Zinc-finger RNA binding proteins (Lai et al., 1999). LPS has been shown previously to increase TTP mRNA and protein levels, e.g. in THP-1 cells (Baseggio et al., 2002; Fairhurst et al., 2003, Brooks et al., 2004) or human primary monocytes (Carrick and Blackshear, 2007). Our data show for the first time that this is also true for AM. Moreover, our observations reveal that TTP induction upon TLR activation occurs in a MyD88-dependent manner, which gave us a first hint of a possible involvement of TTP in GILZ mRNA decay. Both TTP overexpression and knockdown experiments in THP-1 cells confirmed this assumption.

IL10 mRNA has only recently been shown to be regulated by TTP in murine macrophages (Stoecklin et al., 2008; Tudor et al., 2009), although these observations have not been described for human cells yet. TNF- $\alpha$  mRNA represents the best characterized TTP target (Taylor et al., 1996; Carballo et al., 1998; Lai et al., 1999). IL10 and TNF- $\alpha$  were both downregulated when overexpressing TTP. *Vice versa*, knockdown of TTP and subsequent treatment with Pam<sub>3</sub>CSK<sub>4</sub> led to higher induction of TNF- $\alpha$  as well as IL10 in shTTP cells compared to control cells. Most importantly, TTP overexpression also resulted in decreased GILZ amounts, both on mRNA and protein level. In addition, our results demonstrate that attenuation of TTP expression by the use of RNAi abrogates TLR1/2- as well as TLR4-mediated GILZ downregulation. These observations document an involvement of TTP in the regulation of GILZ expression, suggesting that GILZ mRNA might be degraded due to direct interaction with TTP. However, it is also possible that GILZ mRNA interacts with additional RNA-binding proteins that are antagonistic to the destabilizing function of TTP, such as Human Antigen R (HuR) (Anant and Houchen, 2009). Our observation that overexpression of TTP enhances the degradation of GILZ mRNA in the absence of any other stimulus supports the notion that GILZ mRNA is sensitive to the balance of different ARE-binding proteins. Thus, the composition of the entire RNA-protein complex rather than the binding of an individual protein might determine the fate of GILZ mRNA in accordance with the concept of post-transcriptional

operon networks in eukaryotic systems. These networks are considered to be regulated by groups of RNA-binding proteins, whose binding in addition may be modulated by miRNAs (Keene and Tenenbaum, 2002; George and Tenenbaum, 2006). Interestingly, analysis of GILZ 3'-UTR by [www.mirorna.org](http://www.mirorna.org) revealed 40 potential miRNA binding sites. The presence of the binding site for miR-16 might be of special importance, since it has been shown to be involved in TTP-mediated mRNA turnover (Jing et al., 2005).

#### **4.3.4 Proteasome-dependent GILZ downregulation**

The 26S proteasome plays a central role in the maintenance of cellular homeostasis, as it represents the major extralysosomal degradative machinery in eukaryotic cells. Generally, the proteasome degrades proteins tagged by ubiquitin for destruction. Many substrates are regulatory proteins that must be tightly regulated, such as transcription factors and proteins involved in the cell cycle (Hochstrasser, 2009). A recently published study by Delfino et al. (2010) delivered evidence for polyubiquitination and proteosomal degradation of GILZ in thymocytes. Interestingly, GILZ was found to be protected from degradation by inhibition of ubiquitination in glucocorticoid treated cells, suggesting that a prolonged GILZ protein half-life contributes to the increase of GILZ expression upon glucocorticoid treatment.

Our results employing the proteasome inhibitor MG-132 also suggest that GILZ protein might be regulated by proteasome degradation upon TLR activation: Poly(I:C)-induced downregulation of GILZ protein was abrogated by treatment with the proteasome inhibitor. It is also possible, however, that an NF- $\kappa$ B dependent reduction of GILZ was abrogated by the proteasome inhibitor, since MG-132 treatment also prevents I $\kappa$ B from degradation. Potential NF- $\kappa$ B dependent mechanisms of GILZ downregulation might include the induction of miRNAs, resulting in decreased mRNA stability and/or translational repression. As Poly(I:C)-mediated decrease of GILZ protein levels was not paralleled by a reduction of GILZ mRNA amounts and Poly(I:C) is known to activate NF- $\kappa$ B (Blasius and Beutler, 2010), a repression of GILZ translation seems most likely.

Most interestingly, LPS- and Pam<sub>3</sub>CSK<sub>4</sub> mediated GILZ mRNA and protein reduction was completely inhibited by MG-132 pretreatment, indicating that the proteasome is not only involved in TRIF-dependent GILZ protein downregulation, but also in MyD88-dependent downregulation of GILZ mRNA and protein. In accordance with our findings, Deleault et al. (2008) reported that MG-132 stabilizes TTP target mRNAs in monocytes and macrophages, since TTP function requires the proteasome. The mechanisms underlying

TTP/proteasome interactions in mRNA decay are as yet unknown. It seems likely that the proteasomal degradation of TTP represents one step in a process involving several cellular components, such as the exosome or P-Body (Lykke-Andersen and Wagner, 2005; Mukherjee et al., 2002; Kedersha et al., 2005; Stoecklin et al., 2004) and possibly the RNA induced silencing complex (RISC) (Jing et al., 2005).

An overview of potential TLR activation-induced GILZ downregulation mechanisms as suggested by our data and the literature is given in figure 36. Further studies are needed to clarify the role of the proteasome and miRNA in this regulatory network.

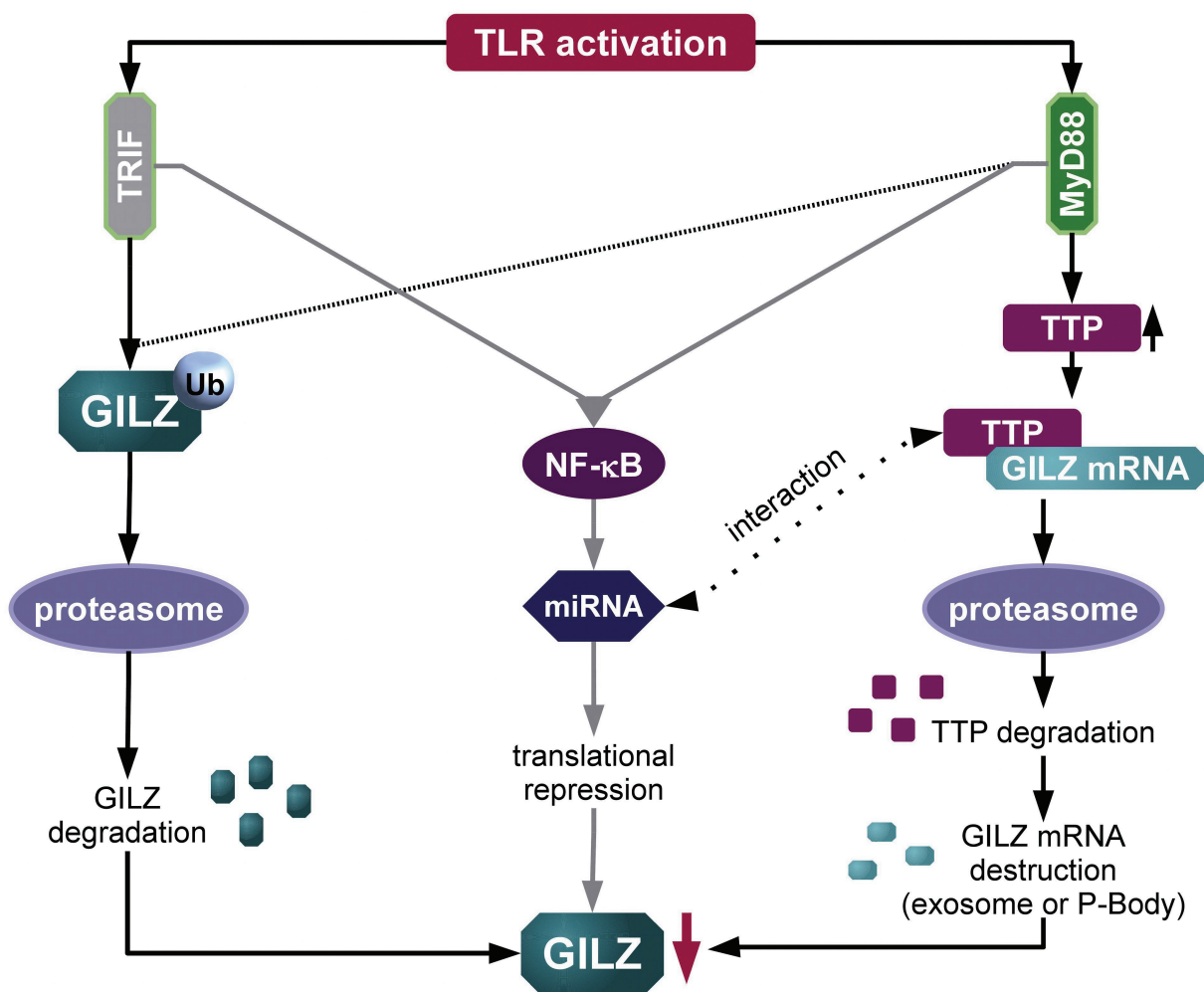


**Figure 36: Potential mechanisms of GILZ downregulation.** Ub: ubiquitin. See text for additional details.

#### 4.3.5 TNF- $\alpha$ mediated GILZ downregulation

TNF- $\alpha$  has previously been shown to reduce GILZ levels in epithelial cells (Eddleston et al., 2007), which is in accordance with our findings for TNF- $\alpha$  treated AM. TNF- $\alpha$  might act in several ways to decrease GILZ similar to those suggested for TLR activation, i.e. *via* TTP-induction, NF- $\kappa$ B dependent miRNA induction and/or promotion of proteasomal GILZ degradation. TNF- $\alpha$  was previously shown to increase TTP protein levels in primary mouse macrophages (Carballo et al., 1998), THP-1 cells (Fairhurst et al., 2003) and human glioma cell lines (Suswam et al., 2008), thereby inducing its own downregulation. In addition, NF- $\kappa$ B activation by TNF- $\alpha$  is well described for many cell types including or human AM (Li et al., 2006). Thus, NF- $\kappa$ B- or TTP- dependent GILZ downregulation could be expected to not only occur after TLR activation, but also upon TNF- $\alpha$  challenge. However, endogenous TNF- $\alpha$  is unlikely to play a major role in GILZ downregulation in our *in vitro* system, as an increase in TNF- $\alpha$  production did not induce GILZ mRNA destabilization upon Poly(I:C) treatment. This assumption was confirmed by our finding that GILZ downregulation was inhibited by TTP knockdown, although TNF- $\alpha$  levels were increased. Nevertheless, we can not exclude a contribution of endogenous TNF- $\alpha$  to GILZ downregulation upon TLR activation at the time being.

#### 4.3.6 GILZ in endotoxin tolerance

Endotoxin tolerance describes the phenomenon that previous exposure to a low level of LPS induces a transient period of hyporesponsiveness after subsequent challenge with LPS (Biswas and Lopez-Collazo, 2009). Clinically, this state is associated with monocytes/macrophages in sepsis patients where it contributes to a high risk of secondary infections and increased mortality (Monneret et al., 2008). Numerous molecules have been identified to contribute to attenuated TLR signalling in tolerant cells, including IRAK-M, suppressor of cytokine-signaling-1 (SOCS-1), Src homology 2-containing inositol-5'-phosphatase (SHIP), and I $\kappa$ B isoforms. At the nuclear level, increase in the NF- $\kappa$ B subunit p50 homodimer expression and increased activation of peroxisome-proliferator activated receptors- $\gamma$  (PPAR $\gamma$ ) have been linked to the tolerance phenotype (Fan and Cook, 2004; Biswas and Lopez-Collazo, 2009). In addition, miRNAs like miR-155, miR-146, and miR-9 induced by TLR4 signalling act in a negative feedback fashion, inhibiting various levels of the MyD88 or TRIF signaling pathway (Baltimore et al., 2008).

Thus, it seemed likely that GILZ regulation is altered in endotoxin tolerance. We found that GILZ mRNA downregulation was indeed completely abrogated in LPS-tolerant AM. In fact, GILZ expression was even slightly, but not significantly, enhanced. The inability to downregulate the expression of the anti-inflammatory factor GILZ might contribute to an insufficient immune response in tolerant cells, suggesting that increased GILZ expression may contribute to the tolerant phenotype. However, additional experiments are needed to elucidate the role of GILZ in endotoxin tolerance.

In summary, we present the first observation of GILZ expression in primary human lung macrophages. We also show that the expression of GILZ in AM is actively regulated, being induced by glucocorticoids and downregulated by TLR activation in a MyD88-dependent fashion. The RNA binding protein TTP and the proteasome are critically involved in TLR-mediated GILZ downregulation. Finally, we suggest that GILZ might play a role in endotoxin tolerance. GILZ has emerged as a potential target for treatment of inflammatory lung diseases, and an understanding of its regulation under inflammatory conditions might help to develop strategies to influence its expression.

Parts of the results presented in this chapter have been submitted for publication as:

Downregulation of Glucocorticoid-Induced Leucine Zipper in alveolar macrophages upon Toll-like receptor activation occurs MyD88-dependently.

Hopstädter J, Diesel B, Eifler LK, Schmid T, Brüne B, Kiemer AK.



## **5. Experimental procedures**



## 5.1 Materials

Cell media, fetal calf serum (FCS), penicillin, streptomycin and glutamine were from PAA (Pasching, Austria). TLR ligands (Pam<sub>3</sub>CSK<sub>4</sub>, Poly(I:C), LPS, flagellin, FLS-1, imiquimod, ssRNA40, ODN2006 and ODN2006 GC control) were obtained from Invivogen (San Diego, CA, USA) and diluted and stored according to the manufacturer's guidelines. Immunostimulatory sequences (ISS1018) were purchased from Dynavax (Berkeley, CA, USA). Chloroquine (CQ, diphosphate salt) was obtained from Sigma-Aldrich (St. Louis, MO, USA). CQ was dissolved in water at a stock concentration of 100 mM, syringe-filtered (0.2 µM), aliquoted, and stored at -20 °C until use. MG-132 (Calbiochem, Nottingham, UK) and cytochalasin D (Sigma-Aldrich, St. Louis, MO, USA) were diluted in DMSO (stock concentrations: 10 mM and 10 mg/ml, respectively) under sterile conditions, aliquoted and stored at -20°C. Real Time RT-PCR primers and dual-labelled probes were obtained from Eurofins MWG Operon (Ebersberg, Germany). *Taq*-Polymerase (5 U/µl), 10 x *Taq* buffer and the dNTP mix (containing dATP, dCTP, dGTP and dTTP at a concentration of 10 mM, each) were from Genscript (Piscataway, NJ, USA). SMART pool siRNA targeting GILZ or MyD88 mRNA as well as control siRNA were purchased from Dharmacon (Chicago, IL, USA) and diluted in DEPC-treated PBS as recommended by the supplier. Lipofectamine LTX reagent, Lipofectamine 2000 and Opti-MEM I reduced serum medium were obtained from Invitrogen (Carlsbad, CA, USA). The MyD88 inhibitor peptide and the respective control peptide were from Imgenex (San Diego, CA, USA). Goat anti-GILZ antibody (sc-26518) was obtained from Santa Cruz Biotechnology (Santa Cruz, CA, USA), rabbit anti-MyD88 (ab2064) and rabbit anti-TTP (ab36558) antibodies were purchased from Abcam (Cambridge, MA, USA). Mouse anti-tubulin (T9026) was from Sigma-Aldrich (St. Louis, MO, USA). IRDye<sup>®</sup> 800 conjugated anti-goat antibodies (605-7352-125) were obtained from Rockland (Gilbertsville, PA, USA). IRDye<sup>®</sup> 680 or 800 conjugated anti-mouse (926-32220) and anti-rabbit (926-32221) antibodies were from LI-COR Biosciences (Lincoln, NE, USA). FITC-labelled anti-CD14 (11014973) and FITC-IgG1 (114714) were obtained from eBioscience (San Diego, CA, USA), PE-labelled anti-HLA-DR (R7267), FITC-labelled anti-CD68 (F7135), FITC-labelled anti-CD1a (F7141) as well as PE-IgG2a $\kappa$  (X 0950), FITC-IgG2a $\kappa$  (X933) and PE-IgG1 $\kappa$  (X928) isotype controls were purchased from Dako (Carpinteria, CA, USA). PE-labelled anti-CD83 (556855), PE-labelled anti-CD90 (555596), and PE-IgG1 $\kappa$  (554680) were from BD Biosciences (San Jose, CA, USA).

Restriction enzymes were obtained from New England Biolabs (Ipswich, MA, USA). Other chemicals were purchased either from Sigma-Aldrich (St. Louis, MO, USA) or Roth (Karlsruhe, Germany) unless marked otherwise.

## 5.2 Mice

C57BL/6 mice were kept under controlled conditions in terms of temperature, humidity, day /night rhythm and food delivery. Animals were 5 weeks of age when experiments were done. All animal procedures were performed in accordance with the local animal welfare committee.

Mice were injected intraperitoneally either with 50 µg LPS diluted in saline or the equal amount of salt solution only. 4 h after injection, mice were sacrificed and the lungs were removed to determine GILZ levels. Murine lung tissue was kindly provided by Sonja M. Keßler (Saarland University, Pharmaceutical Biology).

## 5.3 Cell culture

### 5.3.1 Alveolar macrophages (AM)

Alveolar macrophages were isolated from human non-tumor lung tissue, which was obtained from patients undergoing lung resection. The use of human material for isolation of primary cells was reviewed and approved by the local Ethics Committees (State Medical Board of Registration, Saarland, Germany). Isolation was performed referring to a protocol for the recovery of type II pneumocytes previously described by Elbert et al. (1999). After visible bronchi were removed, the lung tissue was sliced into small pieces of about 1 cm<sup>3</sup> and washed at least three times with BSS (balanced salt solution; 137 mM NaCl, 5 mM KCl, 0.7 mM Na<sub>2</sub>HPO<sub>4</sub>, 10 mM HEPES, 5.5 mM glucose, pH 7.4). The washing buffer was collected and cells were obtained by centrifugation (15 min, 350 x g). Remaining erythrocytes were lysed by incubation with hypotonic buffer (155 mM NH<sub>4</sub>Cl, 10 mM KHCO<sub>3</sub>, 1 mM Na<sub>2</sub>EDTA) and the cell suspension was washed with PBS (137 mM NaCl, 2.7 mM KCl, 10.1 mM Na<sub>2</sub>HPO<sub>4</sub>, 1.8 mM KH<sub>2</sub>PO<sub>4</sub>, pH 7.4) three times. Subsequently, cells were resuspended in AM/IM medium (RPMI 1640, 5 % [v/v] FCS, 100 U/ml penicillin G,

100 µg/ml streptomycin, 2 mM glutamine), seeded at a density of  $0.5-1 \times 10^6$  cells/well in a 12- or 6-well plate and incubated at 37 °C for 2 h. Adherent cells were washed at least 5 times with PBS and cultivated with medium for 3-4 days. Medium was changed every two days.

### **5.3.2 Lung interstitial macrophages (IM)**

After recovering alveolar macrophages, lung tissue was chopped into pieces of 0.6 mm thickness using a McIlwain tissue chopper. To remove remaining alveolar macrophages and blood cells, the tissue was washed with BSS over a 100 µm cell strainer until the filtrate appeared to be clear. The tissue was then digested using a combination of 150 mg trypsin type I (T-8003, Sigma-Aldrich, St. Louis, MO, USA) and 0.641 mg elastase (LS022795, CellSystems, Remagen, Germany) in 30 ml BSSB for 40 min at 37°C in a shaking water bath. After partial digestion, the tissue was brought to DMEM/F12 medium containing 25 % FCS and 350 U/ml DNase I (D5025, Sigma-Aldrich, St. Louis, MO, USA). Remaining undigested lung tissue in the solution was disrupted by repeatedly pipetting the cell suspension slowly up and down. After filtration through gauze and a 40 µm cell strainer, cells were incubated in a 1:1 mixture of DMEM/F12 medium and SAGM (Cambrex, East Rutherford, NJ, USA), containing 5% [v/v] FCS and 350 U/ml DNase I in Petri dishes in an incubator at 37°C and 5% CO<sub>2</sub> for 90 min in order to let macrophages attach to the plastic surface. Afterwards, non-adherent cells were removed by washing with PBS, remaining cells were detached from plates by treatment with trypsin/EDTA solution (PAA, Pasching, Austria) and seeded at a density of  $0.5-1 \times 10^6$  cells/well in a 12- or 6-well plate. As surface receptor expression might be influenced by different isolation procedures, cells were cultured with AM/IM medium for 3-4 days to restore receptors as shown previously for tissue macrophages isolated by enzyme perfusion (Kiemer et al., 2002b). Medium was changed every other day.

### **5.3.3 Monocyte-derived macrophages**

Peripheral blood mononuclear cells (PBMC) were obtained from healthy adult blood donors (Blood Donation Center, Saarbrücken, Germany) using Percoll (GE Healthcare, Munich, Germany) as described previously (Kiemer et al., 2009). Briefly, the buffy coat was diluted with PBS at a ratio of 2:1. Subsequently, the Percoll solution (density 1.077 g/ml; 55 % [v/v] Percoll in PBS) was overlaid with an equal amount of the buffy coat mixture, followed by centrifugation (30 min, 500 x g, w/o break). The cell layer containing

mononuclear cells was removed and washed twice with PBS. Subsequently, erythrocytes were lysed by addition of sterile water, and lysis was instantly stopped by PBS addition. Cells were washed twice with PBS and resuspended in medium (RPMI1640 supplemented with 20 % [v/v] FCS, 100 U/ml penicillin G, 100 µg/ml streptomycin, 2 mM glutamine). Thereafter, cells were allowed to adhere to culture flasks for 2 h at 37°C. Non-adherent cells were removed by washing, and the adherent monocytes were harvested by trypsin/EDTA treatment. After 5 min, digestion was stopped with RPMI containing 20 % [v/v] FCS, penicillin (100 U/ml), and streptomycin (100 µg/ml). Monocytes were then seeded at a density of  $0.5-1 \times 10^6$  cells/well in a 12- or 6-well plate and differentiated into macrophages in RPMI-1640 containing 20 % FCS [v/v] for 7 days. Medium was changed every other day.

#### **5.3.4 Monocyte-derived immature and mature dendritic cells (iDC, mDC)**

Monocytes were obtained as described by Schütz et al. (2006). In brief, PBMC were isolated from buffy coats using Ficoll-Paque (GE Healthcare, Munich, Germany). The mononuclear cell layer was removed and washed with PBS. Erythrocytes were lysed in hypotonic buffer (see 5.2.4) and washed twice with PBS. Subsequently, cells were allowed to adhere to culture flasks for 2 h at 37 °C. Non-adherent cells were removed by washing, and the adherent monocytes were harvested as described above. To generate immature DCs (iDC), monocytes were cultured for 5 d in RPMI 1640 containing 10 % [v/v] FCS, penicillin (100 U/ml), and streptomycin (100 µg/ml) in the presence of GM-CSF (800 U/ml, Berlex Bioscience Inc., Richmond, CA, USA) and IL4 (20 U/ml, Strathmann Biotec, Hamburg, Germany) with one-quarter of the medium being replaced by fresh cytokine-containing medium on day 2 post-isolation. Mature dendritic cells (mDC) were generated by adding 100 ng/ml LPS (Sigma-Aldrich, St. Louis, MO, USA) to iDC cultures for an additional 48 h. iDC and mDC were kindly provided by Tanja Breinig (Saarland University, Department of Virology).

#### **5.3.5 Cell lines**

##### *THP-1 cells*

THP-1 cells were cultivated in RPMI-1640 with 10 % [v/v] FCS and kept at a density of  $2 \times 10^5 - 1 \times 10^6$  cells / ml. For differentiation, cells were treated with 100 nM PMA (Sigma-

Aldrich, St. Louis, MO, USA), seeded at a density of  $0.2-0.5 \times 10^5$  cells / well in a 12- or 6-well plate and incubated for 48 h.

#### *MRC-5 and HSF-1 cells*

The fibroblast cell lines MRC-5 and HSF-1 were cultured in Dulbecco's modified Eagle's medium (DMEM) supplemented with 10 % [v/v] FCS, penicillin (100 U/ml), and streptomycin (100 µg/ml) at 37 °C and 5 % CO<sub>2</sub>. Upon reaching confluence, cells were washed with PBS and detached from culture flasks by treatment with trypsin/EDTA solution (PAA, Pasching, Austria). After 10 min, digestion was stopped with DMEM containing 20 % FCS [v/v], penicillin (100 U/ml), and streptomycin (100 µg/ml). The suspension was centrifuged and resuspended in DMEM with 10 % [v/v] FCS, penicillin (100 U/ml), and streptomycin (100 µg/ml) and appropriate aliquots of the cell suspension were added to new culture vessels.

#### *Freezing and thawing of cells*

For freezing, cell suspensions were washed with PBS and cells were resuspended in ice cold freezing medium (70 % [v/v] RPMI 1640, 20 % [v/v] FCS, 10 % [v/v] DMSO). After cells were transferred into cryovials, they were stored at -80 °C for 2 d and afterwards in liquid nitrogen at -196 °C.

To minimize the cytotoxic effects of DMSO, cells were rapidly thawed for 2 or 3 min and instantly transferred into the respective pre-warmed cell growth medium. After centrifugation, cells were resuspended in growth medium and cultured as described above.

### **5.3.6 Determination of cell viability**

Viable cell counts were assessed using a hemocytometer and trypan blue (0.5 % [v/v] in PBS) exclusion.

Additionally, MTT assays were performed in order to determine potential cytotoxic effects of cell treatment. Cells were seeded at a density of  $2 \times 10^4$  cells per well in a 96-well plate and treated as indicated. Afterwards, cells were washed and 200 µl medium containing MTT (0.5 µg/ml, Sigma-Aldrich, St. Louis, MO, USA) were added for 2 h. After medium was removed, cells were lysed and the water-insoluble purple formazan was solubilized by the addition of 80 µl DMSO. Absorbance was detected at a wavelength of 550 nm using a Sunrise absorbance reader (Tecan, Grödig, Austria).

## 5.4 Bacterial culture

### 5.4.1 *Escherichia coli* (*E.coli*) strains

#### Culture

The following strains were used as host organisms for plasmid amplification:

- XL1 Blue (Stratagene, Santa Clara, CA, USA), genotype *endA1 gyrA96(nal<sup>R</sup>) thi-1 recA1 relA1 lac glnV44 F'[::Tn10 proAB<sup>+</sup> lacI<sup>q</sup> Δ(lacZ)M15] hsdR17(rκ<sup>-</sup> mκ<sup>+</sup>)*
- TOP10 (Invitrogen, Carlsbad, CA, USA), genotype *F- mcrA Δ(mrr-hsdRMS-mcrBC) φ80lacZΔM15 ΔlacX74 nupG recA1 araD139 Δ(ara-leu)7697 galE15 galK16 rpsL(Str<sup>R</sup>) endA1 λ<sup>-</sup>*
- GT116 (Invivogen, San Diego, CA, USA), genotype *F<sup>-</sup> mcrA Δ(mrr-hsdRMS-mcrBC) φ80lacZΔM15 ΔlacX74 recA1 endA1 Δdcm ΔsbcC-sbcD*.

*E.coli* GT116 were employed to amplify shRNA encoding plasmids, as this strain is more compatible with hairpin structures. For all other vectors, the XL1 Blue or TOP10 strains were used.

Bacteria were either grown in Luria-Bertani (LB; 10% tryptone [w/v], 5% yeast extract [w/v], 5% [w/v] NaCl, diluted in H<sub>2</sub>O, pH 7.5) medium supplemented with ampicillin (100 μg/ml) or Low Salt LB (10 % tryptone [w/v], 5 % yeast extract [w/v], 2.5 % [w/v] NaCl, pH 7.5) containing zeocin (25 μg/ml, Invivogen) at 37°C and 5% CO<sub>2</sub>. For selection of single clones, LB<sub>amp</sub> or Low salt LB<sub>zeo</sub> agar (30 % [w/v] agar in LB containing the respective antibiotic) plates were used.

#### Generation of competent *E.coli*

Competent *E.coli* were generated using the CaCl<sub>2</sub> method. Briefly, 100 ml of an overnight culture (OD<sub>650</sub> = 0.4) were incubated on ice for 30 min, centrifuged (2,000 x g, 5 min, 4°C) and resuspended in 2.5 ml ice cold CaCl<sub>2</sub> solution containing 75 mM CaCl<sub>2</sub> and 15% glycerol. Another 20 ml ice cold CaCl<sub>2</sub> were added, and the mixture was incubated on ice for 20 min. Cells were obtained by centrifugation (2,000 x g, 5 min, 4°C), resuspended in 2.5 ml CaCl<sub>2</sub>, aliquoted and stored at -80 °C.

### *Transformation*

Transformation was carried out by adding 50-150 ng plasmid DNA to 100 µl competent bacteria. After incubation on ice for 20 min, bacteria were heat-shocked for 2 min at 42 °C and 900 µl prewarmed LB were added, followed by incubation at 37 °C for 1.5 h. 100 µl of the suspension were plated on LB<sub>amp</sub> or LB<sub>zeo</sub> plates and incubated at 37 °C and 5 % CO<sub>2</sub> over night.

#### **5.4.2 Culture of mycobacteria**

Mycobacteria (*M. bovis* BCG Pasteur ATCC 27289, wild-type *M. bovis* ATCC19210, H37Rv ATCC 27294, H37Ra ATCC 25177) were grown in Middlebrook 7H9 broth containing 10 % [v/v] ADC, 0.2 % [v/v] glycerol and 0.05 % [v/v] Tween 80 (7H9-ADCT) or on Middlebrook 7H10 agar containing OADC (Becton Dickinson, Franklin Lake, NJ, USA), 0.5 % glycerol and antifungal cycloheximide (100 µg/ml). Medium was replaced once a week. Antibiotics included hygromycin (50 µg/ml) and kanamycin (25 µg/ml). Mycobacteria were grown by the group of Prof. Lee W. Riley (UC Berkeley).

## **5.5 Plasmid generation**

### **5.5.1 Vectors for mammalian cell transfections**

#### *shRNA vectors*

Two shRNA plasmids termed shTTP1 and shTTP2 encoding different siRNAs directed against the human TTP mRNA were created by cloning double-stranded oligonucleotides into the *BbsI* sites of psiRNA-h7SKGFPzeo (Invivogen, San Diego, CA, USA) according to the manufacturer's instructions. After cloning, insert sequences were checked using the Eurofins MWG sequencing service.

Oligonucleotide sequences (5' → 3'):

shTTP1:

ACCTCGGGATCCGACCCTGATGAATATCAAGAGTATTCATCAGGGTCGGATCCCTT

shTTP2 as described by Fechir et al. (2005):

ACCTCACAAGACTGAGCTATGTCGGATCAAGAGTCCGACATAGCTCAGTCTTGTTT

Sequence of the small interfering RNA (siRNA) repeats directed against the human tristetraprolin mRNA are underlined.

#### *TTP expression vector*

The plasmids pZeo-hTTP-sense and -antisense (CoV) were derived from the pZeoSV2(-) expression plasmid (Invitrogen, Carlsbad, CA, USA) and were a kind gift of Hartmut Kleinert (Department of Pharmacology, Johannes Gutenberg University, Mainz, Germany).

### **5.5.2 Real-Time RT-PCR standard plasmids**

Standards of the PCR product of the gene of interest were cloned into the pGEM-T Easy vector (Promega, Madison, WI, USA) according to the manufacturer's guidelines. Standard plasmids were provided by Prof. Dr. Alexandra K. Kiemer (Saarland University, Pharmaceutical Biology). See 5.9.2 for primer sequences.

## **5.6 Isolation of bacterial DNA**

### **5.6.1 Plasmid purification**

Plasmid DNA was isolated from overnight cultures by using the Mini or Midi plasmid isolation kit (Qiagen, Hilden, Germany) according to the manufacturer's instructions. Plasmids for transfections were purified using the EndoFree Maxi Plasmid isolation kit (Qiagen, Hilden, Germany) in order to avoid endotoxin contaminations of the plasmid preparations.

### **5.6.2 Isolation, digestion and methylation of mycobacterial DNA**

Before DNA isolation, mycobacteria were centrifuged and boiled for 10 min. DNA was isolated according to a previously published method (Santos et al., 1992). Briefly, bacteria from cultures at  $OD_{600} = 1$  were pelleted and resuspended in TE (10 mM Tris, 1 mM EDTA, pH 8). TE-saturated phenol pH 8 and glass beads were added and the suspension was vortexed for 3 min. The phenol phase was re-extracted with TE, followed by the addition of 0.2 vol 5 % [w/v] sodium deoxycholate and incubation at 56 °C for 90 min. Protein was removed by at least three cycles of extraction with phenol:chloroform:isoamyl. DNA was precipitated by the addition of sodium acetate/ethanol, washed in 70% ethanol, and resuspended in Tris buffer. Any residual RNA was digested with RNase (Qiagen, Hilden,

Germany) and residual protein was removed by chloroform:isoamyl extraction. DNA was again precipitated, washed, and resuspended in Tris buffer. The isolation was performed under sterile conditions in order to avoid bacterial contamination from the surrounding area. DNA was kindly provided by Prof. Dr. Alexandra K. Kiemer (Saarland University, Pharmaceutical Biology). Additional precipitation and washing steps including purification with Triton X-114 were included to assure purity of the DNA (Cotten et al., 1994). We checked all DNA preparations with a commercially available LAL assay (Cambrex, East Rutherford, USA) in order to exclude LPS contaminations.

For further control experiments, DNA was either digested with DNase or cytosine residues (C5) were methylated by the Sssl methyltransferase (Buryanov et al., 2005).

DNA was digested with DNase (500 µg/ml, D-4513, Sigma-Aldrich, St. Louis, MO, USA) for 2 h at 37 °C under sterile conditions. After digestion, DNase was heat-inactivated and the required volume of the reaction relative with the amount of DNA digested was added to a culture of monocyte-derived macrophages. In addition, appropriate volumes of a mock reaction (w/o DNA) as well as mock-treated H37Ra-DNA, which was homologously treated in the absence of DNase, were added to cells.

Cytosine residues of BCG DNA were methylated by Sssl methyltransferase under sterile conditions according to the manufacturer's instructions. In order to determine whether methylation in fact occurred, digestion was performed with HpaI as a restriction enzyme sensitive to CG methylation. After methylation, Sssl was heat-inactivated and the required volume of the reaction relative with the amount of DNA methylated as well as a suitable volume of a mock reaction (w/o DNA) was added to a culture of monocyte-derived macrophages. In addition, BCG DNA, which was homologously treated in the absence of Sssl, was added to cells.

### **5.6.3 Determination of DNA concentrations**

DNA concentrations were determined by measuring the extinction of the DNA solutions at 260 nm, whereas an extinction of 1 equates a concentration of 50 µg/ml. The purity of the DNA preparations was checked by absorption measurement at 280 nm, the characteristic absorption maximum of aromatic amino acids. Measurements were done with a BioMate UV-Vis spectrophotometer (ThermoElectron, Oberhausen, Germany).

## 5.7 Agarose gel electrophoresis

### 5.7.1 Detection of DNA

Depending on the DNA size, 0.5 – 2 % [w/v] agarose gels containing 0.04 % [v/v] ethidium bromide were used for DNA detection. Upon addition of a suitable volume of 6 x loading buffer (18 % Ficoll, 0.5 M EDTA, 60 ml 10 x TBE, 0.04 % bromphenol blue, 0.04 % xylencyanol, H<sub>2</sub>O ad 100 ml), DNA was loaded onto a gel and separated in TBE (89.1 mM Tris, 89.1 mM boric acid, 2.21 mM EDTA in H<sub>2</sub>O) at 100 V. To determine the size of the DNA, a 50 bp ladder (Fermentas, St. Leon-Rot, Germany) or a 1 kb ladder (Invitrogen, Carlsbad, CA, USA) were used. Detection of the DNA bands was carried out using a UV transilluminator and the software ArgusX1 (Biostep, Stollberg, Germany).

### 5.7.2 Detection of RNA

In contrast to DNA gels, RNA gels contained 1 % formaldehyde to ensure denaturation of the samples and were prepared with MOPS buffer (0.02 M MOPS, 5 mM sodium acetate, 0.5 mM EDTA in DEPC-treated H<sub>2</sub>O, pH 7) instead of TBE with 1% [w/v] agarose. Prior to loading onto the gels, RNA was boiled at 65 °C for 5 min in an appropriate volume of loading buffer (10 ml formamide, 3.5 ml formaldehyde, 1.5 ml 10 x MOPS). Samples were separated in MOPS buffer at 100 V and detected as described in 4.7.1.

## 5.8 RNA isolation and reverse transcription

### 5.8.1 RNA isolation

Total RNA was extracted using either RNeasy mini or micro kit columns (Qiagen, Hilden, Germany) according to the manufacturer's instructions. DNA was digested during the RNA isolation procedure using the RNase-Free DNase1 kit (Qiagen, Hilden, Germany). RNA integrity was checked using agarose gel electrophoresis.

### 5.8.2 Measurement of RNA concentrations

Photometric determination of RNA concentrations at 260 nm was carried out using a BioMate UV-Vis spectrophotometer (ThermoElectron, Oberhausen, Germany). An extinction of 1 equates a concentration of 40 µg/ml.

### 5.8.3 Alu PCR

To confirm the absence of DNA in our RNA preparations, a PCR for Alu elements, which occur in large numbers throughout the human genome, was performed using the following primer: 5'-TCATGTCGACGCGAGACTCCATCTCAA A-3'.

One reaction consisted of:

<i>Taq</i> -Polymerase	2.5 U
dNTPs	800 $\mu$ M
10 x <i>Taq</i> -buffer	2.5 $\mu$ l
MgCl <sub>2</sub> (50 mM)	5 mM
primer (50 $\mu$ M)	100 nM
template	100 ng RNA
H <sub>2</sub> O	ad 25 $\mu$ l

5 ng THP-1 DNA (provided by Christoph Meyer, formerly Saarland University, Pharmaceutical Biology) served as a positive control.

The PCR was carried out in a Thermocycler PX2 (ThermoElectron, Oberhausen, Germany) using the following conditions:

denaturation	5 min 94 °C	} 30 cycles
denaturation	1 min 94 °C	
annealing	1 min 56 °C	
elongation	1 min 72 °C	
final elongation	10 min 72 °C	

Products were detected by agarose gel electrophoresis. RNA was considered to be DNA - free when no product was visible.

### 5.8.4 Reverse transcription

250 - 500 ng of RNA were denatured at 65 °C for 5 min, placed on ice, and then reverse transcribed in a total volume of 20  $\mu$ l using oligo-dT primers (5'-TTT TTT TTT TTT TTT TTT-3') and the High-Capacity cDNA Reverse Transcription Kit (Applied Biosystems, Foster City, CA, USA) according to the manufacturer's instructions. The resulting cDNA was diluted by addition of 80  $\mu$ l TE buffer (AppliChem, Darmstadt, Germany) and used for real-time RT-PCR.

## 5.9 Real-time RT-PCR

### 5.9.1 Primer and probe sequences

Table1: *Primer sequences as used for real-time RT PCR.*

mRNA	primer sense, 5' → 3'	primer antisense, 5' → 3'
huGILZ	TCCTGTCTGAGCCCTGAAGAG	AGCCACTTACACCGCAGAAC
huIL6	AATAATAATGGAAAGTGGCTATGC	AATGCCATTTATTGGTATAAAAAC
huIL8	TGCCAGTGAACTTCAAGCA	ATTGCATCTGGCAACCCTAC
huIL10	CAACAGAAGCTTCCATTCCA	AGCAGTTAGGAAGCCCCAAG
huTNF- $\alpha$	CTCCACCCATGTGCTCCTCA	CTCTGGCAGGGGCTCTTGAT
huIP10	GAGCCTACAGCAGAGGAACC	AAGGCAGCAAATCAGAATCG
hu $\beta$ -actin	TGCGTGACATTAAGGAGA AG	GTCAGGCAGCTCGTAGCTCT
muGILZ	GGGATGTGGTTTCCGTTAAA	ATGGCCTGCTCAATCTTGTT
mu18S	GCGCTTCTCTTTCCGCCA	AGCTCTCCGACACCTCTT
huTLR1	AGCAAAGAAATAGATTACACATCA	TTACCTACATCATACTCACAAT
huTLR2	GCAAGCTGCGGAAGATAATG	CGCAGCTCTCAGATTTACCC
huTLR3	GAATGTTTAAATCTCACTGC	AAGTGCTACTTGCAATTTAT
huTLR4	ATGAAATGAGTTGCAGCAGA	AGCCATCGTTGTCTCCCTAA
huTLR5	GTACAGAAACAGCAGTATTTGAG	TCTGTTGAGAGAGTTTATGAAGAA
huTLR6	TTTACTTGGATGATGATGAATAGT	AGTTCCCCAGATGAAACATT
huTLR7	CCATACTTCTGGCAGTGTCT	ACTAGGCAGTTGTGTTTTGC
huTLR8	AAGAGCTCCATCCTCCAGTG	CCGTGAATCATTTTCAGTCAA
huTLR9	GGGACAACCACCACTTCTAT	TGAGGTGAGTGTGGAGGT
huTLR10	CAACGATAGGCGTAAATGTG	GAACCTCGAGACTCTTCATTT

**Table 2: Probe sequences as used for real-time RT-PCR.**

<b>mRNA</b>	<b>probe, 5' FAM → 3' BHQ1</b>
huGILZ	CCCGAATCCCCACAAGTGCCCGA
huIL6	TCCTTTGTTTCAGAGCCAGATCATTCT
huIL8	CAGACCCACACAATACATGAAGTGTTGA
huIL10	AGCCTGACCACGCTTTCTAGCTGTTGAG
huTNF- $\alpha$	CACCATCAGCCGCATCGCCGTCTC
huIP10	TCCAGTCTCAGCACCATGAATCAA
hu $\beta$ -actin	CACGGCTGCTTCCAGCTCCTC
huTLR1	ATTCCTCCTGTTGATATTGCTGCTTTTG
huTLR2	ATGGACGAGGCTCAGCGGGAAG
huTLR3	TTCAGAAAGAACGGATAGGTGCCTT
huTLR4	AAGTGATGTTTGATGGACCTCTGAATCT
huTLR5	AGGATCTCCAGGATGTTGGCTG
huTLR6	GTCGTAAGTAACTGTCZGGAGGTGC
huTLR7	ATAGTCAGGTGTTCAAGGAAACGGTCTA
huTLR8	TGACAACCCGAAGGCAGAAGGCT
huTLR9	ACTTCTGCCAGGGACCCACGG
huTLR10	ATTAGCCACCAGAGAAATGTATGAACTG

### 5.9.2 Standard dilution series

To confirm real-time RT-PCR efficiency and to quantify target mRNAs in a cDNA sample, standards from 10 to 0.0001 attomoles of the PCR product cloned into pGEM-T Easy (Promega, Madison, WI, USA), were run alongside the samples to generate a standard curve. Plasmids were isolated as described in 5.6.1 and diluted in TE-buffer (AppliChem, Darmstadt, Germany). The required amount of plasmid DNA was calculated as follows:

$$c(\text{target-DNA}) [\mu\text{mol/ml}] = c(\text{plasmid}) [\mu\text{g/ml}] / \text{MW} * L$$

with MW = molecular weight of the DNA (approx. 660 g/mol) and L = length of plasmid and insert in bp.

### 5.9.3 Experimental procedure

#### *Real-time RT-PCR using dual-labelled probes*

Reaction mixtures were assembled on ice and 20  $\mu$ l of the mixture were added to 5  $\mu$ l template cDNA or standard plasmid solutions in a 96 well plate. dNTP-, probe- and  $MgCl_2$ -concentrations for each target gene are listed in table 3.

The iCycler iQ5 (Bio-Rad, Richmond, CA, USA) was used for real-time RT-PCR. Primer and probe sequences are given in table 1 and 2. All samples and standards were analyzed in triplicate. The starting amount of cDNA in each sample was calculated using the iCycler iQ5 software package (Bio-Rad, Richmond, CA, USA). Absolute mRNA amounts were normalized to  $\beta$ -actin mRNA levels.

A reaction mixture for one sample consisted of:

<i>Taq</i> -Polymerase	2.5 U
10 x <i>Taq</i> -buffer	2.5 $\mu$ l
Primer sense	500 nM
Primer antisense	500 nM
dNTPs	200 or 800 $\mu$ M
dual-labelled probe	60 or 100 nM
$MgCl_2$	3-9 mM
Template	5 $\mu$ l
H <sub>2</sub> O	ad 25 $\mu$ l

The reaction conditions were as follows:

denaturation	8 min 95 °C	} 40 cycles
denaturation	15 s 95 °C	
annealing	15 s 57-60 °C	
elongation	15 s 72 °C	
final elongation	25 s 25 °C	

Target gene specific annealing temperatures are given in table 3.

**Table 3: dNTP-, dual-labelled probe-, MgCl<sub>2</sub>. and annealing temperatures as used for real-time RT-PCR.**

<b>mRNA</b>	<b>dNTPs</b>	<b>probe</b>	<b>MgCl<sub>2</sub></b>	<b>annealing</b>
<b>huTLR1</b>	800 µM	60 nM	9 mM	57 °C
<b>huTLR2</b>	800 µM	100 nM	6 mM	60 °C
<b>huTLR3</b>	800 µM	60 nM	7 mM	59 °C
<b>huTLR4</b>	800 µM	100 nM	5 mM	58 °C
<b>huTLR5</b>	800 µM	60 nM	7 mM	59 °C
<b>huTLR6</b>	800 µM	100 nM	8 mM	57 °C
<b>huTLR7</b>	800 µM	60 nM	5 mM	58 °C
<b>huTLR8</b>	800 µM	60 nM	5 mM	58 °C
<b>huTLR9</b>	800 µM	60 nM	7 mM	58 °C
<b>huTLR10</b>	800 µM	60 nM	9 mM	59 °C
<b>huGILZ</b>	200 µM	100 nM	4 mM	60 °C
<b>huIL6</b>	200 µM	100 nM	4 mM	57 °C
<b>huIL8</b>	200 µM	100 nM	4 mM	59 °C
<b>huIL10</b>	200 µM	100 nM	4 mM	60 °C
<b>huTNF-α</b>	200 µM	100 nM	3 mM	60 °C
<b>huIP10</b>	200 µM	60 nM	4 mM	60 °C
<b>hu β-actin</b>	200 µM	60 nM	4 mM	60 °C

*Real-time RT-PCR using SYBR Green*

For murine GILZ and 18S PCR, the Dynamo Flash SYBR Green qPCR kit (Finnzymes) was used according to the manufacturer's guidelines. The reaction conditions resembled those described above. An annealing temperature of 60 °C was used for both muGILZ and 18S. The starting cDNA quantity was calculated using the iCycler iQ5 software (Bio-Rad Richmond, CA, USA). Absolute muGILZ mRNA amounts were normalized to 18S mRNA levels.

## 5.10 Western Blot analysis

### 5.10.1 Preparation of protein samples

Cells were lysed in SB lysis buffer (50 mM Tris-HCl, 1 % [m/v] SDS, 10 % [v/v] glycerol, 5 % [v/v]  $\beta$ -mercaptoethanol, 0.004 % [m/v] bromphenol blue) supplemented with a protease inhibitor mixture (Complete<sup>®</sup>, Roche Diagnostics, Basel, Switzerland) according to the manufacturer's instructions. Murine lung tissue was disrupted using a Kontes tissue grinder and lysed accordingly. In general, 100  $\mu$ l lysis buffer were employed for lysis of  $2 \times 10^5$  cells or 1 mg of tissue. Subsequently, samples were sonicated for 5 s and centrifuged (10 min, 20,000 x g, 4 °C). Supernatants were removed and stored at -80 °C.

### 5.10.2 SDS-polyacrylamide gel electrophoresis (SDS-PAGE)

*Composition of 15 % gels:*

resolving gel		stacking gel	
H <sub>2</sub> O	4.6 ml	H <sub>2</sub> O	6.8 ml
30 % acrylamide / 0.8 % bisacrylamide solution	10 ml	30 % acrylamide / 0.8 % bisacrylamide solution	1.7 ml
Tris (1.5 M, pH 8.0)	5 ml	Tris (1 M, pH 6.8)	1.25 ml
SDS (10 % [w/v])	200 $\mu$ l	SDS (10 % [w/v])	100 $\mu$ l
APS (10 % [w/v])	200 $\mu$ l	APS (10 % [w/v])	100 $\mu$ l
TEMED	20 $\mu$ l	TEMED	10 $\mu$ l

#### *Procedure*

Samples were thawed on ice and denatured for 5 min at 95 °C. A prestained protein marker (Fermentas, St. Leon-Rot, Germany) was used to estimate the molecular masses. Equal sample amounts and a suitable marker volume were loaded onto the gel and separated in electrophoresis buffer (24.8 mM Tris, 1.92 mM glycine, 0.1 % [w/v] SDS) for 130 min at 80 V, followed by 2 h at 120 V. Gel preparation and electrophoresis were carried out using the Mini PROTEAN system (Bio-Rad, Richmond, CA, USA).

### 5.10.3 Blotting

The Mini-Transblot cell (Bio-Rad, Richmond, CA, USA) system was employed to transfer separated protein samples onto a polyvinylidene fluoride (PVDF) membrane (Immobilon-FL, Millipore, Billerica, MA, USA). Prior to blotting, the membrane was incubated for 30 s in methanol. Sponges, blotting papers, the gel and the membrane were equilibrated in transfer buffer, followed by gel sandwich preparation. Blotting was carried out at 80 mA over night. Afterwards, the membrane was incubated in Rockland Blocking Buffer for near-infrared Western Blotting (RBB, obtained from Rockland, Gilbertsville, PA, USA) for 1 h for 30 min in order to block unspecific binding sites.

### 5.10.4 Immunodetection

Antibodies were either diluted in PBST (0.1 % [v/v] tween 20 in PBS) containing 5 % [m/v] dried milk, gelatine buffer (0.75 % [w/v] gelatine A, 0.1 % [v/v] tween 20, 20 mM Tris, 137 mM NaCl, pH 7.5) or RBB according to table 4.

**Table 4: Antibody dilutions used for immunodetection.**

<b>Antibody</b>	<b>dilution</b>
anti-human/mouse GILZ, goat IgG	1:200 in gelatine buffer
anti-human MyD88, rabbit IgG	1:500 in PBST + 5 % [m/v] dried milk
anti-human TTP, rabbit IgG	1:2,000 in PBST + 5 % [m/v] dried milk
anti-human tubulin, mouse IgG	1:1,000 in PBST + 5 % [m/v] dried milk
IRDye <sup>®</sup> 800CW conjugated goat anti-mouse IgG	1:10,000 in RBB
IRDye <sup>®</sup> 680 conjugated mouse anti-rabbit IgG	1:5,000 in RBB
IRDye <sup>®</sup> 800 conjugated donkey anti-goat IgG	1:10,000 in RBB

Membranes were incubated with primary antibodies for 3 h at room temperature (MyD88, tubulin) or 37 °C (GILZ) or overnight at 4 °C (TTP). Subsequently, they were washed either in PBST + 5 % [m/v] dried milk or gelatine buffer for GILZ blots (2 x 5 min), followed by additional washing steps in PBST (2 x 5 min). Afterwards, membranes were incubated with the secondary antibody for 1.5 h at room temperature. After washing twice in PBST and PBS for 5 min, blots were scanned with an Odyssey Infrared Imaging System (LI-COR Biosciences, Lincoln, NE, USA) and relative signal intensities were determined using the Odyssey software.

## 5.11 Transfection of THP-1 cells

### 5.11.1 Plasmid transfection

Plasmids were introduced into THP-1 cells using Lipofectamine LTX transfection reagent according to the manufacturer's guidelines for transfection of THP-1 cells. Briefly,  $2 \times 10^5$  cells were plated in 1 ml growth medium per well in 12 well plates. For each well, 1  $\mu\text{g}$  plasmid DNA was diluted in a total volume of 200  $\mu\text{l}$  Opti-MEM, mixed with 1  $\mu\text{l}$  of PLUS reagent and incubated for 15 min at room temperature. Subsequently, 6.25  $\mu\text{l}$  Lipofectamine LTX were added and the transfection mix was incubated for another 25 min at room temperature prior to its addition to THP-1 cells. For TTP overexpression assays, cells were harvested 24 h after they were transfected with pZeo-hTTP-sense or the antisense control construct. Knockdown of TTP was performed by transfecting THP-1 cells with shTTP1 or shTTP2 plasmids. The psiRNA-LucGL3 plasmid (Invivogen) was transfected as control vector.

### 5.11.2 siRNA transfection

For knockdown of GILZ or MyD88 by siRNA, cells were transfected with siGILZ or siMyD88 and respective control siRNA using Lipofectamine 2000 transfection reagent as recommended by the supplier. In short, THP-1 cells were seeded in 12 well plates at a density of  $2 \times 10^5$  cell per well. For each well, 2  $\mu\text{l}$  of Lipofectamine 2000 were mixed with 100  $\mu\text{l}$  of Opti-MEM and incubated at room temperature for 5 min. 40 pmol siRNA were diluted in 100  $\mu\text{l}$  Opti-MEM and added to the Lipofectamine 2000 solution. After incubation at room temperature for an additional 20 min, the Lipofectamine 2000 / siRNA / Opti-MEM mixture was added to the cells. Experiments were performed either 24 h (siGILZ) or 72 h (siMyD88) after transfection.

## 5.12 Determination of mRNA stability

To analyze the effects of LPS treatment on GILZ mRNA stability, the transcription inhibitor actinomycin D (10  $\mu\text{g}/\text{ml}$ , Sigma-Aldrich, St. Louis, MO, USA), either alone or in combination with LPS (100 ng/ml), was added to AM. 0.5 to 4 h thereafter, cells were

harvested and RNA was isolated. The relative amount of GILZ mRNA was determined by real-time RT-PCR.

## 5.13 Flow cytometry

### 5.13.1 Antibodies

Antibodies and respective isotype controls (table 5) were used in an antibody / cell number ratio as recommended by the supplier.

**Table 5: Antibodies used for flow cytometry.**

<b>Antibody</b>	<b>Isotype control</b>
FITC-labelled mouse anti-human CD14, clone 61/D3	FITC-IgG1 $\kappa$ , mouse
FITC-labelled mouse anti-human CD1a, clone NA1/34	FITC-IgG2a $\kappa$ , mouse
FITC-labelled mouse anti-human CD68, clone KP1	FITC-IgG1 $\kappa$ , mouse
PE-labelled mouse anti-human HLA-DR, clone AB3	PE-IgG2a $\kappa$ , mouse
PE-labelled mouse anti-human CD83, clone HB15e	PE-IgG1 $\kappa$ , mouse
PE-labelled mouse anti-human CD90, clone 5E10	PE-IgG1 $\kappa$ , mouse

### 5.13.2 Cell staining and analysis

Adherent cells were detached from the plates in TEN buffer (40 mM Tris, 1 mM EDTA, 150 mM NaCl) before staining. For extracellular staining of CD83, CD90 and CD1a, cells were washed with PBS, resuspended in FACS buffer I and then divided into aliquots, each containing up to  $1 \times 10^6$  cells. Each aliquot was incubated with a specific or isotype control antibody for 30 min on ice. The cells were washed in FACSwash and resuspended in 1% (w/v) cold paraformaldehyde in PBS, pH 7.6. HLA-DR and CD14 staining were performed similarly, except that FACS buffer II (PBS containing 0.05% (w/v)  $\text{NaN}_3$  and 0.5% (w/v) BSA for HLA-DR) or III (PBS with 1% (w/v)  $\text{NaN}_3$  and 0.5% (w/v) BSA for CD14) were used instead of FACS buffer I. Intracellular staining of CD68 was done using the IntraStain Reagents (Dako, Carpinteria, CA, USA) according to the manufacturer's instructions. The stained cells were examined on a FACSCalibur, and results were analysed using the CellQuest software (BD Biosciences, San Jose, CA, USA). Results are reported as relative

mean fluorescence intensity (MFI; mean fluorescence intensity of specifically stained cells related to mean fluorescence intensity of isotype control).

## **5.14 Phagocytosis Assay**

### **5.14.1 Sample preparation**

To visualize the uptake of microspheres by macrophages, cells were incubated with 1.75  $\mu\text{m}$  latex beads (Fluoresbrite Carboxylated YG microspheres; Polysciences, Warrington, PA, USA) at a 100:1 bead / cell ratio for 4 h in medium containing 5 % [v/v] FCS. To block fluoreosphere uptake, cytochalasin D (10  $\mu\text{g}/\text{ml}$ ) was added 1 h prior to addition of latex beads. Alternatively, macrophages were pretreated by incubation for 1 h at 4 °C and further incubated with fluoreospheres at the same temperature as the pretreatment. After the incubation with latex beads, cells were washed 4-5 times with ice cold PBS to remove remaining fluorospheres, and detached from plates using trypsin/EDTA buffer (PAA, Pasching, Austria). Afterwards, cells were assessed for fluorosphere uptake by flow cytometry or confocal laser scanning microscopy.

### **5.14.2 Flow cytometry assessment of fluorosphere uptake**

After washing, cells were resuspended in ice-cold PBS, examined on a FACSCalibur and results were analysed using the CellQuest software (BD Biosciences, San Jose, CA, USA).

### **5.14.3 Confocal laser scanning microscopy**

Staining was performed in a wet chamber. AM and IM were washed with PBS and fixed on coverslips for 10 min in PBS supplemented with paraformaldehyde 3.7 % [w/v]. Cells were washed three times with PBS before permeabilization with 0.25 % [v/v] Triton X-100 for 10 min. After washing with PBS, blocking was performed for 30 minutes with BSA 1% [w/v] in PBS. F-actin was stained for 30 min with rhodamin-phalloidine (3.8  $\mu\text{M}$ , Sigma-Aldrich, St. Louis, MO, USA), and the coverslips were washed twice with PBST and once with PBS. Nuclei were stained for 5 min with TOTO-3 iodide (1:500, Invitrogen, Carlsbad, CA, USA) followed by three washing steps with PBS. A glass slide was covered with 3  $\mu\text{l}$  Fluorsave (Calbiochem, Nottingham, UK) and put upside down onto the coverslips. Preparations were dried for 24 h at 4 °C. Images were captured using a LSM 510 Meta run by LSM 510

software (Carl Zeiss, Oberkochen, Germany). Confocal laser scanning microscopy was done by Robert Zarbock (Saarland University, Pharmaceutical Biology).

### **5.15 Pappenheim staining**

Air-dried macrophage preparations were stained using May-Grünwald solution (Roth, Karlsruhe, Germany) for 5 min, followed by addition of the same volume of distilled water and incubation for another 5 min, after which the staining solution was removed. Subsequently, preparations were incubated with Giemsa solution (1:20; Roth, Karlsruhe, Germany) for 15 min, washed with distilled water and visualized using light microscopy.

### **5.16 Cytokine measurement**

AM and IM were seeded at a density of  $1 \times 10^5$  cells per well in 96 well plates. On day 4 post seeding, cells were incubated in a total volume of 100  $\mu$ l medium in the presence or absence of LPS (100 ng/ml), Pam<sub>3</sub>SCK<sub>4</sub> (100 ng/ml) or Poly(I:C) (10  $\mu$ g/ml) for 6 h. The supernatants were collected and stored at -80 °C until use in the multiplex cytokine assay. For cytokine measurement, a Milliplex MAP Human Cytokine Kit (Millipore, Billerica, MA, USA) was used, containing the following cytokines: IL1 $\beta$ , IL1ra, IL6, IL10, IL12p40, IL-12p70, G-CSF, TNF- $\alpha$ , IP10, and IFN $\gamma$ . The immunoassay procedure was performed using a serial dilution of the 10,000 pg/ml human cytokine standard according to the manufacturer's instructions. The plate was read on the Luminex 200 System (Luminex, Austin, TX, USA). Total cellular protein concentrations were determined by Pierce BCA protein assay (Fisher Scientific, Nidderau, Germany) using a Sunrise absorbance reader (Tecan, Grödig, Austria) according to the manufacturer's instructions. Cytokine measurement was supported by Dominik Monz (Department of Neonatology, Saarland University Hospital).

## 5.17 Atomic Force microscopy

ISS1018 or BCG DNA (6 mg/ml) diluted in PBS without  $\text{Ca}^{2+}$  and  $\text{Mg}^{2+}$  (Applichem, Darmstadt, Germany) were deposited on pretreated mica (25 mm  $\text{MgCl}_2$  spin coating for 1 min), incubated for 5 min, washed with purified water, and dried under vacuum as described earlier (Kerkmann et al., 2005). All images were performed using a Dimension 3100 Scanning Probe Microscope (Veeco, Melville, NY, USA) operating in dynamic mode at ambient conditions using etched silicon cantilevers (Ultrasharp NSC/11, MikroMasch, Portland, Oregon, USA) with a spring constant 3 N/m and a resonance frequency of  $\sim 45$  kHz. The nominal tip radius was  $< 10.0$  nm. Atomic force microscopy was performed by Ralf Jungmann (Saarland University, Department of Physics).

## 5.18 Statistics

Data analysis and statistics were performed using Origin software (OriginPro 7.5G; OriginLabs, Northampton, MA, USA). All data are displayed as mean values  $\pm$  SEM. Statistical differences were estimated by independent two-sample t-test. Differences were considered statistically significant when P values were less than 0.05.

## 6. Summary



## 6. Summary

Pulmonary macrophages play a key role in host defence against inhaled particles and pathogens. In this work pulmonary macrophage action upon TLR activation was examined.

The role of TLR activation by mycobacterial DNA during tuberculosis infection has only recently been a matter of interest, and non-methylated CpG-rich bacterial DNA is now recognized as the natural ligand for TLR9. Since TLR9 expression and responsiveness in macrophages is controversially discussed, we aimed to investigate TLR9 activation in human macrophages. We demonstrated that macrophages are markedly activated by DNA isolated from attenuated mycobacterial strains, whereas synthetic CpG oligonucleotides have a much lower stimulatory potency. AM activation upon treatment with DNA isolated from virulent bacteria was lower compared to attenuated mycobacteria. These differences between the stimulatory activities of DNA from virulent *versus* attenuated mycobacteria might indicate a mechanism how virulent strains evade the host immune response.

Interestingly, we found that the response to TLR9 activation largely differs in AM and IM, which represent the two major macrophage populations in human lungs. Investigations on pulmonary macrophages mostly focus on AM as a well-defined cell population, whereas characteristics of IM are rather ill-defined. We therefore extended our investigations on the phenotypic differences in AM and IM. We showed that IM are smaller and morphologically more heterogeneous than AM, whereas phagocytic activity was similar in both cell types. HLA-DR expression was markedly higher in IM compared to AM. Although analysis of TLR expression profiles revealed no differences between the two cell populations, AM and IM clearly varied in cell reaction upon activation. Both macrophage populations were responsive towards MyD88-dependent and -independent TLR activation. Whereas AM expressed higher amounts of inflammatory cytokines upon activation, IM were more efficient in producing immunoregulatory cytokines, such as IL10, IL1ra, and IL6. Thus, AM appear to be more effective as a first line of defence against inhaled pathogens, whereas IM show a more pronounced regulatory function.

Induction of glucocorticoid-induced leucine zipper (GILZ) by glucocorticoids is critical for their anti-inflammatory action, whereas GILZ expression is reduced under inflammatory

conditions. The mechanisms regulating GILZ expression during inflammation, however, have as yet been unknown. Within the project investigating the reaction of AM upon treatment with mycobacterial DNA as a TLR9 ligand, we aimed to determine whether TLR9 ligands affect GILZ expression. We herein show that GILZ mRNA and protein amounts were significantly diminished upon TLR9 activation. Moreover, lungs of LPS-exposed mice as well as LPS-treated human AM and THP-1 cells displayed decreased GILZ expression. We also demonstrated that LPS treatment reduces GILZ mRNA stability. This effect was strictly dependent on the adapter molecule MyD88, as shown by using specific ligands or a knockdown strategy. Overexpression and knockdown of the mRNA binding protein TTP modulated GILZ mRNA expression, suggesting an involvement of TTP in GILZ mRNA destabilization. Remarkably, activation of TLR3, i.e. signalling *via* the TRIF-dependent pathway, resulted in diminished GILZ protein-, but not mRNA-levels. This finding indicates that GILZ downregulation utilizes distinct pathways. Moreover, we show that the proteasome is critically involved in TLR-mediated GILZ downregulation on mRNA and protein level. Suppression of GILZ results in inflammatory cell activation, which might represent a regulatory mechanism in TLR activation. Interestingly, this mechanism seems to be absent in endotoxin tolerance.

Taken together, this work provides insight into the differential expression of pro- and anti-inflammatory mediators upon TLR activation in pulmonary macrophages and may contribute to a better understanding of processes involved in pulmonary immune homeostasis.

This work was supported by the Landesgraduiertenkolleg des Saarlandes and by grant #KI702/10-1 (Deutsche Forschungsgemeinschaft).

## 7. References



## 7. References

Aggarwal A, Baker CS, Evans TW, Haslam PL. G-CSF and IL-8 but not GM-CSF correlate with severity of pulmonary neutrophilia in acute respiratory distress syndrome. *Eur Respir J* 2000; 15: 895-901.

Albiger B, Sandgren A, Katsuragi H, Meyer-Hoffert U, Beiter K, Wartha F, Hornef M, Normark S, Normark BH. Myeloid differentiation factor 88-dependent signalling controls bacterial growth during colonization and systemic pneumococcal disease in mice. *Cell Microbiol* 2005; 7: 1603–1615.

Alexopoulou L, Holt AC, Medzhitov R, Flavell RA. Recognition of double-stranded RNA and activation of NF-kappaB by Toll-like receptor 3. *Nature* 2001; 413: 732–738.

Anant S, Houchen CW. HuR and TTP: two RNA binding proteins that deliver message from the 3' end. *Gastroenterology* 2009; 136: 1495-1498.

Arend WP, Palmer G, Gabay C. IL-1, IL-18, and IL-33 families of cytokines. *Immunol Rev* 2008; 223: 20-38.

Ayroldi E, Migliorati G, Bruscoli S, Marchetti C, Zollo O, Cannarile L, D'Adamio F, Riccardi C. Modulation of T-cell activation by the glucocorticoid-induced leucine zipper factor via inhibition of nuclear factor kappaB. *Blood* 2001; 98: 743-753.

Ayroldi E, Riccardi C. Glucocorticoid-induced leucine zipper (GILZ): a new important mediator of glucocorticoid action. *FASEB J* 2009; 23: 3649-3658.

Ayroldi E, Zollo O, Bastianelli A, Marchetti C, Agostini M, Di Virgilio R, Riccardi C. GILZ mediates the antiproliferative activity of glucocorticoids by negative regulation of Ras signaling. *J Clin Invest* 2007; 117: 1605-1615.

Ayroldi E, Zollo O, Macchiarulo A, Di Marco B, Marchetti C, Riccardi C. Glucocorticoid-induced leucine zipper inhibits the Raf-extracellular signal-regulated kinase pathway by binding to Raf-1. *Mol Cell Biol* 2002; 22: 7929-7941.

Baess I, Mansa B. Determination of genome size and base ratio on deoxyribonucleic acid from mycobacteria. *Acta Pathol Microbiol Scand* 1978; 86B: 309-312.

Bafica A, Scanga CA, Feng CG, Sher A, Leifer C, Cheever A. Tlr9 regulates th1 responses and cooperates with tlr2 in mediating optimal resistance to mycobacterium tuberculosis. *J Exp Med* 2005; 202:1715-1724.

Bakheet T, Frevel M, Williams BR, Greer W, Khabar KS. ARED: human AU-rich element-containing mRNA database reveals an unexpectedly diverse functional repertoire of encoded proteins. *Nucleic Acids Res* 2001; 29: 246-254.

Bals R, Hiemstra PS. Innate immunity in the lung: how epithelial cells fight against respiratory pathogens. *Eur Respir J* 2004; 23: 327–333.

Baltimore, D Boldin MP, O'Connell RM, Rao DS, Taganov KD. MicroRNAs: new regulators of immune cell development and function. *Nat Immunol* 2008; 9:839–845.

Barnes PJ, Ito K, Adcock IM. A mechanism of corticosteroid resistance in COPD: inactivation of histone deacetylase. *Lancet* 2004; 363: 731-733.

Barnes PJ, Shapiro SD, Pauwels RA. Chronic obstructive pulmonary disease: molecular and cellular mechanisms. *Eur Respir J* 2003; 22: 672-688

Barnes PJ. Immunology of asthma and chronic obstructive pulmonary disease. *Nat Rev Immunol* 2008; 8: 183–192.

Barnes PJ: Alveolar Macrophages in Chronic Obstructive Pulmonary Disease (COPD). *Cell Mol Biol* 2004; 50 Online Pub: OL627-637.

Barral PM, Sarkar D, Su ZZ, Barber GN, DeSalle R, Racaniello VR, Fisher PB. Functions of the cytoplasmic RNA sensors RIG-I and MDA-5: key regulators of innate immunity. *Pharmacol Ther* 2009; 124: 219-234.

Baseggio L, Charlot C, Bienvenu J, Felman P, Salles G, 2002. Tumor necrosis factor- $\alpha$  mRNA stability in human peripheral blood cells after lipopolysaccharide stimulation. *Eur Cytokine Netw* 2002; 13: 92-98.

Bedoret D, Wallemacq H, Marichal T, Desmet C, Quesada Calvo F, Henry E, Closset R, Dewals B, Thielen C, Gustin P, de Leval L, Van Rooijen N, Le Moine A, Vanderplasschen A, Cataldo D, Drion PV, Moser M, Lekeux P, Bureau F: Lung interstitial macrophages alter dendritic cell functions to prevent airway allergy in mice. *J Clin Invest* 2009; 119: 3723-3738.

Berrebi D, Bruscoli S, Cohen N, Foussat A, Migliorati G, Bouchet-Delbos L, Maillot MC, Portier A, Couderc J, Galanaud P, Peuchmaur M, Riccardi C, Emilie D. Synthesis of glucocorticoid-induced leucine zipper (GILZ) by macrophages: an anti-inflammatory and immunosuppressive mechanism shared by glucocorticoids and IL-10. *Blood* 2003; 101: 729-738.

Beutler B. Inferences, Questions and Possibilities in Toll-Like Receptor Signalling. *Nature* 2004; 430: 257-263.

Biswas SK, Lopez-Collazo E. Endotoxin tolerance: new mechanisms, molecules and clinical significance. *Trends Immunol* 2009; 30: 475-487.

Blasius AL, Beutler B. Intracellular toll-like receptors. *Immunity* 2010; 32:305-315.

Bousquet J, Burney P. Evidence for an increase in atopic disease and possible causes. *Clin Exp Allergy* 1993; 6: 484-492.

Brant KA, Fabisiak JP. Nickel alterations of TLR2-dependent chemokine profiles in lung fibroblasts are mediated by COX-2. *Am J Respir Cell Mol Biol* 2008; 38: 591–599.

Brennan PJ, Nikaido H. The envelope of mycobacteria. *Annu Rev Biochem* 1995; 64: 29–63.

Brooks SA, Connolly JE, Rigby WF. The role of mRNA turnover in the regulation of tristetraprolin expression: evidence for an extracellular signal-regulated kinase-specific, AU-rich element-dependent, autoregulatory pathway. *J Immunol* 2004; 172: 7263-7271.

Bruscoli S, Donato V, Velardi E, Di Sante M, Migliorati G, Donato R, Riccardi C. Glucocorticoid-induced leucine zipper (GILZ) and long GILZ inhibit myogenic differentiation and mediate anti-myogenic effects of glucocorticoids. *J Biol Chem* 2010; 285: 10385-10396.

Burr ML, Butland BK, King S, Vaughan-Williams E. Changes in asthma prevalence: two surveys 15 years apart. *Arch Dis Child* 1989; 64: 1452-1456.

Buryanov Y, Shevchuk T. The use of prokaryotic DNA methyltransferases as experimental and analytical tools in modern biology. *Anal Biochem* 2005; 338: 1-11.

Cai S, Batra S, Shen L, Wakamatsu N, Jeyaseelan S. Both TRIF- and MyD88-dependent signaling contribute to host defense against pulmonary klebsiella infection. *J Immunol* 2009; 183: 6629–6638.

Cannarile L, Zollo O, D'Adamio F, Ayroldi E, Marchetti C, Tabilio, A, Bruscoli S, Riccardi C. Cloning, chromosomal assignment and tissue distribution of human GILZ, a glucocorticoid hormone-induced gene. *Cell Death Differ* 2001; 8: 201-203.

Caramori G, Adcock I. Pharmacology of airway inflammation in asthma and COPD. *Pulm Pharmacol Ther* 2003; 16: 247-277.

Carballo E, Lai WS, Blackshear PJ. Feedback inhibition of macrophage tumor necrosis factor-alpha production by tristetraprolin. *Science* 28: 1001-1005.

Carrick DM, Blackshear PJ. Comparative expression of tristetraprolin (TTP) family member transcripts in normal human tissues and cancer cell lines. *Arch Biochem Biophys* 2007; 462: 278-285.

Cavassani KA, Ishii M, Wen H, Schaller MA, Lincoln PM, Lukacs NW, Hogaboam CM, Kunkel SL. TLR3 is an endogenous sensor of tissue necrosis during acute inflammatory events. *J Exp Med* 2008;205: 2609–2621.

Chen CY, Shyu AB. 1995. AU-rich elements: characterization and importance in mRNA degradation. *Trends Biochem Sci* 1995; 20: 465-470.

Chomarat P, Banchereau J, Davoust J, Palucka AK: IL-6 switches the differentiation of monocytes from dendritic cells to macrophages. *Nat Immunol* 2000; 6:510-4.

Cochand L, Isler P, Songeon F, Nicod LP: Human lung dendritic cells have an immature phenotype with efficient mannose receptors. *Am J Respir Cell Mol Biol* 1999; 21: 547-54.

Cohen N, Mouly E, Hamdi H, Maillot MC, Pallardy M, Godot V, Capel F, Balian A, Naveau S, Galanaud P, Lemoine FM, Emilie D. GILZ expression in human dendritic cells redirects their maturation and prevents antigen-specific T lymphocyte response. *Blood* 2006; 107: 2037-2044.

Cookson WO, Moffatt MF. Asthma: an epidemic in the absence of infection? *Science* 1997; 275: 41–42.

Cotten M, Baker A, Saltik M, Wagner E, Buschle M: Lipopolysaccharide is a frequent contaminant of plasmid DNA preparations and can be toxic to primary human cells in the presence of adenovirus. *Gene Ther* 1994; 1: 239-246.

Crozat K, Beutler B. TLR7: A new sensor of viral infection. *Proc Natl Acad Sci USA* 2004; 101: 6835-6836.

D'Adamio F, Zollo O, Moraca R, Ayroldi E, Bruscoli S, Bartoli A, Cannarile L, Migliorati G, Riccardi C. A new dexamethasone-induced gene of the leucine zipper family protects T lymphocytes from TCR/CD3-activated cell death. *Immunity* 1997; 7: 803-812.

D'Amato G, Cecchi L, D'Amato M, Liccardi G. Urban air pollution and climate change as environmental risk factors of respiratory allergy: an update. *J Investig Allergol Clin Immunol* 2010; 20: 95-102.

de Boer WI, Alagappan VK, Sharma HS. Molecular mechanisms in chronic obstructive pulmonary disease: potential targets for therapy. *Cell Biochem Biophys* 2007; 47: 131-148.

Deleault KM, Skinner SJ, Brooks SA. Tristetraprolin regulates TNF- $\alpha$  mRNA stability via a proteasome dependent mechanism involving the combined action of the ERK and p38 pathways. *Mol Immunol* 2008; 45:13-24.

Delfino DV, Spinicelli S, Pozzesi N, Pierangeli S, Velardi E, Bruscoli S, Martelli MP, Pettirossi V, Falchi L, Kang TB, Riccardi C. Glucocorticoid-induced activation of caspase-8 protects the glucocorticoid-induced protein Gilz from proteasomal degradation and induces its binding to SUMO-1 in murine thymocytes. *Cell Death Differ* 2010. [Epub ahead of print]

Demedts IK, Brusselle GG, Vermaelen KY, Pauwels RA: Identification and characterization of human pulmonary dendritic cells. *Am J Respir Cell Mol Biol* 2005; 32: 177–184.

Di Marco B, Massetti M, Bruscoli S, Macchiarulo A, Di VR, Velardi E, Donato V, Migliorati G, Riccardi C. Glucocorticoid-induced leucine zipper (GILZ)/NF- $\kappa$ B interaction: role of GILZ homo-dimerization and C-terminal domain. *Nucleic Acids Res* 2007; 35: 517-528.

Di Stefano, A, Caramori, G, Capelli, A, et al Increased expression of NF- $\kappa$ B in bronchial biopsies from smokers and patients with COPD. *Eur Respir J* 2002; 20: 556-563.

Doffinger R, Patel SY, Kumararatne DS: Host Genetic Factors and Mycobacterial Infections: Lessons From Single Gene Disorders Affecting Innate and Adaptive Immunity. *Microbes Infect* 2006; 8: 1141-1150.

Dostert C, Petrilli V, van Bruggen R, Steele C, Mossman BT, Tschopp J. Innate immune activation through Nalp3 inflammasome sensing of asbestos and silica. *Science* 2008; 320: 674–677.

Doyle SE, O'Connell RM, Miranda GA, Vaidya SA, Chow EK, Liu PT, Suzuki S, Suzuki N, Modlin RL, Yeh WC, Lane TF, Cheng G: Toll-like Receptors Induce a Phagocytic Gene Program through p38. *J Exp Med* 2004; 199: 81-90.

Doz E, Noulin N, Boichot E, Guenon I, Fick L, Le Bert M, Lagente V, Ryffel B, Schnyder B, Quesniaux VF, et al. Cigarette smoke-induced pulmonary inflammation is TLR4/MyD88 and IL-1R1/MyD88 signaling dependent. *J Immunol* 2008; 180: 1169–1178.

Droemann D, Goldmann T, Tiedje T, Zabel P, Dalhoff K, Schaaf B. Toll-like receptor 2 expression is decreased on alveolar macrophages in cigarette smokers and COPD patients. *Respir Res* 2005; 6: 68.

D'Souza NB, Nelson S, Summer WR, Deaciuc IV. Alcohol modulates alveolar macrophage tumor necrosis factor-alpha, superoxide anion, and nitric oxide secretion in the rat. *Alcohol Clin Exp Res* 1996; 20: 156-163.

Eberhardt, W., Doller, A., Akool, E., Pfeilschifter, J. Modulation of mRNA stability as a novel therapeutic approach. *Pharmacol. Ther* 2007; 114: 56-73.

Eddleston J, Herschbach J, Wagelie-Steffen AL, Christiansen SC, Zuraw BL. The anti-inflammatory effect of glucocorticoids is mediated by glucocorticoid-induced leucine zipper in epithelial cells. *J Allergy Clin Immunol* 2007; 119: 115-122.

Eisenbarth SC, Piggott DA, Huleatt JW, Visintin I, Herrick CA, Bottomly K. Lipopolysaccharide-enhanced, toll-like receptor 4-dependent T helper cell type 2 responses to inhaled antigen. *J Exp Med* 2002; 196(12): 1645-1651.

Elbert KJ, Schaefer UF, Schaefer HJ, Kim KJ, Lee VHL, Lehr CM: Monolayers of Human Alveolar Epithelial Cells in Primary Culture for Pulmonary Absorption and Transport Studies. *Pharm Res* 1999; 16: 601-608.

Endoh Y, Chung YM, Clark IA, Geczy CL, Hsu K. IL-10-dependent S100A8 gene induction in monocytes/macrophages by double-stranded RNA. *J Immunol* 2009; 182: 2258-2268.

Erwig LP, Henson PM. Immunological consequences of apoptotic cell phagocytosis. *Am J Pathol* 2007; 171: 2–8.

Fairhurst AM, Connolly JE, Hintz KA, Goulding NJ, Rassias AJ, Yeager MP, Rigby W, Wallace PK. Regulation and localization of endogenous human tristetraprolin. *Arthritis Res Ther* 2003; 5: R214-R225.

Falcone V, Bassey EB, Toniolo A, Conaldi PG, Collins FM. Differential release of tumor necrosis factor- $\alpha$  from murine peritoneal macrophages stimulated with virulent and avirulent species of mycobacteria. *FEMS Immunol Med Microbiol* 1994; 8: 225-232.

Fan H, Cook JA. Molecular mechanisms of endotoxin tolerance. *J Endotoxin Res.* 2004; 10: 71-84.

Fan J, Frey RS, Malik AB. TLR4 signaling induces TLR2 expression in endothelial cells via neutrophil NADPH oxidase. *J Clin Invest* 2003;112: 1234–1243.

Fathi M, Johansson A, Lundborg M, Orre L, Skold CM, Camner P: Functional and Morphological Differences Between Human Alveolar and Interstitial Macrophages. *Exp Mol Pathol* 2001; 70: 77-82.

Fechir M, Linker K, Pautz A, Hubrich T, Förstermann U, Rodriguez-Pascual F, Kleinert H. Tristetraprolin regulates the expression of the human Inducible nitric-oxide synthase gene. *Mol Pharmacol* 2005; 67: 2148-2161.

Fenhalls G, Squires GR, Stevens-Muller L, Bezuidenhout J, Amphlett G, Duncan K, Lukey PT: Associations between toll-like receptors and interleukin-4 in the lungs of patients with tuberculosis. *Am J Respir Cell Mol Biol* 2003; 29: 28-38.

Fernandez S, Jose P, Avdiushko MG, Kaplan AM, Cohen DA: Inhibition of IL-10 receptor function in alveolar macrophages by Toll-like receptor agonists. *J Immunol* 2004; 172: 2613-2620.

Ferrari-Lacraz S, Nicod LP, Chicheportiche R, Welgus HG, Dayer JM: Human lung tissue macrophages, but not alveolar macrophages, express matrix metalloproteinases after direct contact with activated T lymphocytes. *Am J Respir Cell Mol Biol* 2001; 24: 442-451.

Franke-Ullmann G, Pfortner C, Walter P, Steinmuller C, Lohmann-Matthes ML, Kobzik L: Characterization of murine lung interstitial macrophages in comparison with alveolar macrophages in vitro. *J Immunol* 1996; 157: 3097-3104.

Fremont CM, Yeremeev V, Nicolle DM, Jacobs M, Quesniaux VF, Ryffel B. Fatal Mycobacterium tuberculosis infection despite adaptive immune response in the absence of MyD88. *J Clin Invest* 2004; 114:1790-1799.

Fujiwara N, Kobayashi K. Macrophages in inflammation. *Curr Drug Targets Inflamm Allergy* 2005; 4: 281-286.

Garnier T, Eiglmeier K, Camus JC, Medina N, Mansoor H, Pryor M, Duthoy S, Grondin S, Lacroix C, Monsempe C, Simon S, Harris B, Atkin R, Doggett J, Mayes R, Keating L, Wheeler PR, Parkhill J, Barrell BG, Cole ST, Gordon SV, Hewinson RG. The complete genome sequence of mycobacterium bovis. *Proc Natl Acad Sci USA* 2003; 100: 7877-7882.

Gaschler GJ, Zavitz CC, Bauer CM, Skrtic M, Lindahl M, Robbins CS, Chen B, Stampfli MR. Cigarette smoke exposure attenuates cytokine production by mouse alveolar macrophages. *Am J Respir Cell Mol Biol* 2008; 38: 218–226.

George AD, Tenenbaum SA. MicroRNA modulation of RNA-binding protein regulatory elements. *RNA Biol* 2006; 3: 57-59.

Gerke AK, Hunninghake G. The immunology of sarcoidosis. *Clin Chest Med* 2008; 3: 379-390.

Godot V, Garcia G, Capel F, Arock M, Durand-Gasselien I, Asselin-Labat ML, Emilie D, Humbert M. Dexamethasone and IL-10 stimulate glucocorticoid-induced leucine zipper synthesis by human mast cells. *Allergy* 2006; 61: 886-890.

Gomez M, Raju SV, Viswanathan A, Painter RG, Bonvillain R, Byrne P, Nguyen DH, Bagby GJ, Kolls JK, Nelson S, Wang G. Ethanol upregulates glucocorticoid-induced leucine zipper expression and modulates cellular inflammatory responses in lung epithelial cells. *J Immunol* 2010; 184: 5715-5722.

Gordon S, Taylor PR. Monocyte and macrophage heterogeneity. *Nat Rev Immunol* 2005; 5: 953-964.

Gordon S, Taylor PR. Monocyte and macrophage heterogeneity. *Nature Rev Immunol* 2005; 5: 953–964.

Gordon S. The macrophage: Past, present and future. *Eur J Immunol* 2007; 37 Suppl 1:9-17.

Greene CM, McElvaney NG. Toll-like receptor expression and function in airway epithelial cells. *Arch Immunol Ther Exp (Warsz)* 2005; 53: 418–427.

Grugan KD, Ma C, Singhal S, Krett NL, Rosen ST. Dual regulation of glucocorticoid-induced leucine zipper (GILZ) by the glucocorticoid receptor and the PI3-kinase/AKT pathways in multiple myeloma. *J Steroid Biochem Mol Biol* 2008; 110: 244-254.

Gupta V, Awasthi N, Wagner BJ. Specific activation of the glucocorticoid receptor and modulation of signal transduction pathways in human lens epithelial cells. *Invest Ophthalmol Vis Sci* 2007; 48: 1724-1734.

Halapi E, Bjornsdottir US. Overview on the current status of asthma genetics. *Clin Respir J* 2009; 3: 2-7.

Hamdi H, Bigorgne A, Naveau S, Balian A, Bouchet-Delbos L, Cassard-Doulcier AM, Maillot MC, Durand-Gasselien I, Prévot S, Delaveaucoupet J, Emilie D, Perlemuter G. Glucocorticoid-induced leucine zipper: A key protein in the sensitization of monocytes to lipopolysaccharide in alcoholic hepatitis. *Hepatology* 2007; 46: 1986-1992.

Harris JK, De Groote MA, Sagel SD, Zemanick ET, Kapsner R, Penvari C, Kaess H, Deterding RR, Accurso FJ, Pace NR. Molecular identification of bacteria in bronchoalveolar lavage fluid from children with cystic fibrosis. *Proc Natl Acad Sci USA* 2007; 104: 20529–20533.

Hartmann G, Krieg AM. CpG DNA and LPS induce distinct patterns of activation in human monocytes. *Gene Ther* 1999; 6: 893-903.

Haugen TS, Nakstad B, Skjønberg OH, Lyberg T: CD14 Expression and Binding of Lipopolysaccharide to Alveolar Macrophages and Monocytes. *Inflammation* 1998; 22: 521-532.

Havenith CE, Breedijk AJ, van Miert PP, Blijleven N, Calame W, Beelen RH, Hoefsmit EC: Separation of alveolar macrophages and dendritic cells via autofluorescence: phenotypical and functional characterization. *J Leukoc Biol* 1993; 53: 504–510.

Hawn TR, Smith KD, Aderem A, Skerrett SJ. Myeloid differentiation primary response gene (88)- and toll-like receptor 2-deficient mice are susceptible to infection with aerosolized *Legionella pneumophila*. *J Infect Dis* 2006; 193: 1693–1702.

He Z, Zhu Y, Jiang H. Toll-like receptor 4 mediates lipopolysaccharide-induced collagen secretion by phosphoinositide3-kinase-Akt pathway in fibroblasts during acute lung injury. *J Recept Signal Transduct Res* 2009; 29: 119–125.

Hemavathy KC, Nagaraja V: DNA methylation in mycobacteria: absence of methylation at GATC (Dam) and CCA/TGG (Dcm) sequences. *FEMS Immunol Med Microbiol* 1995; 11: 291-296.

Hemmi H, Takeuchi O, Kawai T, Kaisho T, Sato S, Sanjo H, Matsumoto M, Hoshino K, Wagner H, Takeda K, Akira S. A toll-like receptor recognizes bacterial DNA. *Nature* 2000; 408: 740-745.

Herrmann J and Lagrange P. Dendritic cells and Mycobacterium tuberculosis: which is the Trojan horse? *Pathol Biol (Paris)* 2005; 53: 35–40.

Hirschfelder K, Diesel B, Huwer H, Kiemer AK. Glucocorticoid-induced leucine zipper (GILZ) as a suppressor of endothelial TLR2 expression. *In preparation*.

Hochstrasser M. Origin and function of ubiquitin-like proteins. *Nature* 2009; 458: 422-9.

Hoene V, Peiser M, Wanner R. Human monocyte-derived dendritic cells express TLR9 and react directly to the cpg-a oligonucleotide d19. *J Leukoc Biol* 2006; 80: 1328-1336.

Hogg JC, Chu F, Utokaparch S, Woods R, Elliott WM, Buzatu L, Cherniack RM, Rogers RM, Sciurba FC, Coxson HO, Paré PD. The nature of small-airway obstruction in chronic obstructive pulmonary disease. *N Engl J Med* 2004; 350: 2645-2653.

Hollams EM, Giles KM, Thomson AM, Leedman PJ. mRNA stability and the control of gene expression: implications for human disease. *Neurochem Res* 2002; 27: 957-980.

Holness CL, Simmons DL. Molecular cloning of CD68, a human macrophage marker related to lysosomal glycoproteins. *Blood* 1993; 81: 1607-13.

Holt PG, Strickland DH, Wikstrom ME, Jahnsen FL. Regulation of immunological homeostasis in the respiratory tract. *Nat Rev Immunol* 2008; 8: 142–152.

Hoogerwerf JJ, de Vos AF, Bresser P, van der Zee JS, Pater JM, de Boer A, Tanck M, Lundell DL, Her-Jenh C, Draing C, von Aulock S, van der Poll T. Lung inflammation

induced by lipoteichoic acid or lipopolysaccharide in humans. *Am J Respir Crit Care Med* 2008; 178: 34-41.

Horner AA. Toll-like receptor ligands and atopy: A coin with at least two sides. *J Allergy Clin Immunol* 2006; 117: 1133-1140.

Hornung V, Guenther-Biller M, Bourquin C, Ablasser A, Schlee M, Uematsu S, Noronha A, Manoharan M, Akira S, de Fougerolles A, Endres S, Hartmann G. Sequence-specific potent induction of ifn-alpha by short interfering rna in plasmacytoid dendritic cells through TLR7. *Nat Med* 2005; 11: 263-270.

Hornung V, Rothenfusser S, Britsch S, Krug A, Jahrsdorfer B, Giese T, Endres S, Hartmann G. Quantitative expression of toll-like receptor 1-10 mrna in cellular subsets of human peripheral blood mononuclear cells and sensitivity to CpG oligodeoxynucleotides. *J Immunol* 2002; 168: 4531-4537.

Houben E, Nguyen L, Pieters J. Interaction of pathogenic mycobacteria with the host immune system. *Curr Opin Microbiol* 2006; 9: 76-85.

Hume DA, Ross IL, Himes SR, Sasmono RT, Wells CA, Ravasi T. The mononuclear phagocyte system revisited. *J Leukoc Biol* 2002; 72: 621-627.

Hume DA. Macrophages as APC and the dendritic cell myth. *J Immunol* 2008; 181: 5829-5835.

Hume DA. The mononuclear phagocyte system. *Curr Opin Immunol* 2006; 18: 49-53.

Hunter M, Wang Y, Eubank T, Baran C, Nana-Sinkam P, Marsh C. Survival of monocytes and macrophages and their role in health and disease. *Front Biosci* 2009; 14: 4079-4102.

Ichinose M. Differences of inflammatory mechanisms in asthma and COPD. *Allergol Int* 2009; 58: 307-313.

Imai Y, Kuba K, Neely GG, Yaghubian-Malhami R, Perkmann T, van Loo G, Ermolaeva M, Veldhuizen R, Leung YH, Wang H, et al. Identification of oxidative stress and Toll-like receptor 4 signaling as a key pathway of acute lung injury. *Cell* 2008; 133: 235–249.

Ito K, Lim S, Caramori G, Chung KF, Barnes PJ, Adcock IM: Cigarette smoking reduces histone deacetylase 2 expression, enhances cytokine expression, and inhibits glucocorticoid actions in alveolar macrophages. *FASEB J* 2001; 15: 1110-1112.

Ito T, Schaller M, Raymond T, Joshi AD, Coelho AL, Frantz FG, Carson WF 4th, Hogaboam CM, Lukacs NW, Standiford TJ, Phan SH, Chensue SW, Kunkel SL. Toll-like receptor 9 activation is a key mechanism for the maintenance of chronic lung inflammation. *Am J Respir Crit Care Med* 2009; 180: 1227-1238.

Jenkins KA, Mansell A. TIR-containing adaptors in Toll-like receptor signalling. *Cytokine* 2010; 49: 237-44.

Jiang D, Liang J, Fan J, Yu S, Chen S, Luo Y, Prestwich GD, Mascarenhas MM, Garg HG, Quinn DA, et al. Regulation of lung injury and repair by Toll-like receptors and hyaluronan. *Nat Med* 2005; 11: 1173–1179.

Jing Q, Huang S, Guth S, Zarubin T, Motoyama A, Chen J, Di Padova F, Lin SC, Gram H, Han J. Involvement of microRNA in AU-rich element-mediated mRNA instability. *Cell* 2005; 120: 623-34.

Juarez E, Nuñez C, Sada E, Ellner JJ, Schwander SK, Torres M: Differential expression of Toll-like receptors on human alveolar macrophages and autologous peripheral monocytes. *Respir Res* 2010; 11: 2.

Kariko K, Ni H, Capodici J, Lamphier M, Weissman D. mRNA is an endogenous ligand for Toll-like receptor 3. *J Biol Chem* 2004; 279: 12542–12550.

Karimi K, Sarir H, Mortaz E, Smit JJ, Hosseini H, De Kimpe SJ, Nijkamp FP, Folkerts G. Toll-like receptor-4 mediates cigarette smoke-induced cytokine production by human macrophages. *Respir Res* 2006; 7:66.

Kawai T, Akira S. TLR signaling. *Cell Death Differ* 2006; 13: 816-825.

Kedersha N, Stoecklin G, Ayodele M, Yacono P, Lykke-Andersen J, Fritzler MJ, Scheuner D, Kaufman RJ, Golan DE, Anderson P. Stress granules and processing bodies are dynamically linked sites of mRNP remodeling. *J Cell Biol* 2005; 169:871-884.

Keene JD, Tenenbaum SA. Eukaryotic mRNPs may represent posttranscriptional operons. *Mol Cell* 2002; 9: 1161-1167.

Kerkmann M, Costa LT, Richter C, Rothenfusser S, Battiany J, Hornung V, Johnson J, Englert S, Ketterer T, Heckl W, Thalhammer S, Endres S, Hartmann G. Spontaneous Formation of Nucleic Acid-Based Nanoparticles Is Responsible for High Interferon-Alpha Induction by CpG-A in Plasmacytoid Dendritic Cells. *J Biol Chem* 2005; 280: 8086-8093.

Kiemer AK, Baron A, Gerbes AL, Bilzer M, Vollmar AM: The atrial natriuretic peptide as a regulator of Kupffer cell functions. *Shock* 2002; 17: 365-371.

Kiemer AK, Hartung T, Vollmar AM. cGMP-mediated inhibition of TNF-alpha production by the atrial natriuretic peptide in murine macrophages. *J Immunol* 2000; 165:175-181.

Kiemer AK, Senaratne RH, Hoppstädter J, Diesel B, Riley LW, Tabeta K, Bauer S, Beutler B, Zuraw BL. Attenuated Activation of Macrophage TLR9 by DNA From Virulent Mycobacteria. *J Innate Immun* 2009; 1: 29-45

Kiemer AK, Vollmar AM. Autocrine regulation of inducible nitric-oxide synthase in macrophages by atrial natriuretic peptide. *J Biol Chem* 1998; 273: 13444-13451.

Kiemer AK, Weber NC, Vollmar AM. Induction of I $\kappa$ B: atrial natriuretic peptide as a regulator of the NF- $\kappa$ B pathway. *Biochem Biophys Res Commun* 2002; 295: 1068-1076.

Kobzik L, Godleski J, Barry BE, Brain JD: Isolation and antigenic identification of hamster lung interstitial macrophages. *Am Rev Respir Dis* 1988; 138: 908-914.

Kôhalmi F, Strausz J, Egerváry M, Szekeres G, Tímár J: Differential Expression of Markers in Extensive and Restricted Langerhans Cell Histiocytosis (LCH). *Pathol Oncol Res* 1996; 2: 184-187.

Kono H, Rock KL. How dying cells alert the immune system to danger. *Nature Rev Immunol* 2008; 8: 279–289.

Krug A, Towarowski A, Britsch S, Rothenfusser S, Hornung V, Bals R, Giese T, Engelmann H, Endres S, Krieg AM, Hartmann G. Toll-like receptor expression reveals cpG DNA as a unique microbial stimulus for plasmacytoid dendritic cells which synergizes with cd40 ligand to induce high amounts of il-12. *Eur J Immunol* 2001; 31: 3026-3037.

Kunisch E, Fuhrmann R, Roth A, Winter R, Lungershausen W, Kinne RW: Macrophage specificity of three anti-CD68 monoclonal antibodies (KP1, EBM11, and PGM1) widely used for immunohistochemistry and flow cytometry. *Ann Rheum Dis* 2004; 7: 774-784.

Kuo CC, Kuo CW, Liang CM, Liang SM. A transcriptomic and proteomic analysis of the effect of CpG-ODN on human THP-1 monocytic leukemia cells. *Proteomics* 2005; 5: 894-906.

Lai WS, Carballo E, Strum JR, Kennington EA, Phillips RS, Blackshear PJ. Evidence that tristetraprolin binds to AU-rich elements and promotes the deadenylation and destabilization of tumor necrosis factor alpha mRNA. *Mol Cell Biol* 1999; 19: 4311-4323.

Lang R, Patel D, Morris JJ, Rutschman RL, Murray PJ: Shaping gene expression in activated and resting primary macrophages by IL-10. *J Immunol* 2002; 169: 2253-2263.

Lasa M, Mahtani KR, Finch A, Brewer G, Saklatvala J, Clark AR, 2000. Regulation of cyclooxygenase 2 mRNA stability by the mitogen-activated protein kinase p38 signaling cascade. *Mol Cell Biol* 2000. 20: 4265-4274.

Laskin DL, Weinberger B, Laskin JD: Functional heterogeneity in liver and lung macrophages. *J Leukoc Biol* 2001; 70: 163-70.

Latz E, Schoenemeyer A, Visintin A, Fitzgerald KA, Monks BG, Knetter CF, Lien E, Nilsen NJ, Espevik T, Golenbock DT. Tlr9 signals after translocating from the er to cpg DNA in the lysosome. *Nat Immunol* 2004; 5: 190-198.

Lavnikova N, Prokhorova S, Helyar L, Laskin DL: Isolation and partial characterization of subpopulations of alveolar macrophages, granulocytes, and highly enriched interstitial macrophages from rat lung. *Am J Respir Cell Mol Biol* 1993; 8: 384–392.

Lee KW, Jung J, Lee Y, Kim TY, Choi SY, Park J, Kim DS, Kwon HJ. Immunostimulatory oligodeoxynucleotide isolated from genome wide screening of mycobacterium bovis chromosomal DNA. *Mol Immunol* 2006;43: 2107-2118.

Lee RU, Eddleston J, Herschbach J, Zuraw BL. Cigarette Smoke Impaired Antiviral Responses of Airway Epithelial Cells to dsRNA are Associated with Upregulation of Glucocorticoid Induced Leucine Zipper (GILZ). *J Allergy Clin Immunol* 2009; 123: S171.

Leifer CA, Kennedy MN, Mazzoni A, Lee C, Kruhlak MJ, Segal DM. Tlr9 is localized in the endoplasmic reticulum prior to stimulation. *J Immunol* 2004; 173: 1179-1183.

Lensmar C, Prieto J, Dahlen B, Eklund A, Grunewald J, Roquet A: Airway inflammation and altered alveolar macrophage phenotype pattern after repeated low-dose allergen exposure of atopic asthmatic subjects. *Clin Exp Allergy* 1999; 29: 1632-1640.

Li J, Ma Z, Tang ZL, Stevens T, Pitt B, Li S. CpG DNA-mediated immune response in pulmonary endothelial cells. *Am J Physiol Lung Cell Mol Physiol* 2004; 287: L552–L558.

Li YQ, Zhang ZX, Xu YJ, Ni W, Chen SX, Yang Z, Ma D.N-Acetyl-L-cysteine and pyrrolidine dithiocarbamate inhibited nuclear factor-kappaB activation in alveolar macrophages by different mechanisms. *Acta Pharmacol Sin* 2006; 27: 339-346.

Li Z, Potts EN, Garantziotis S, Foster WM, Hollingsworth JW. Hyaluronan Fragments Released By Ozone Exposure Contribute To Airway Hyperresponsiveness Via TLR4-MyD88-TIRAP. *Am J Respir Crit Care Med* 2010; 181: A1166

Libert C, Takahashi N, Cauwels A, Brouckaert P, Bluethmann H, Fiers W: Response of interleukin-6-deficient mice to tumor necrosis factor-induced metabolic changes and lethality. *Eur J Immunol* 1994; 24: 2237–2242.

Lohmann-Matthes ML, Steinmuller C, Franke-Ullmann G. Pulmonary Macrophages. *Eur Respir J* 1994; 7: 1678-1689.

Lundberg AM, Drexler SK, Monaco C, Williams LM, Sacre SM, Feldmann M, Foxwell BM. Key differences in TLR3/poly I:C signaling and cytokine induction by human primary cells: a phenomenon absent from murine cell systems. *Blood* 2007; 110: 3245-3252.

Lundberg AM, Hansson GK. Innate immune signals in atherosclerosis. *Clin Immunol* 2010; 134: 5-24.

Lykke-Andersen J, Wagner E. Recruitment and activation of mRNA decay enzymes by two ARE-mediated decay activation domains in the proteins TTP and BRF-1. *Genes Dev* 2005; 19: 351-361.

Mao TK, Lian ZX, Selmi C, Ichiki Y, Ashwood P, Ansari AA, Coppel RL, Shimoda S, Ishibashi H, Gershwin ME. Altered monocyte responses to defined TLR ligands in patients with primary biliary cirrhosis. *Hepatology* 2005; 42:802-808.

Maris NA, Dessing MC, de Vos AF, Bresser P, van der Zee JS, Jansen HM, Spek C A, van der Poll T: Toll-Like Receptor mRNA Levels in Alveolar Macrophages After Inhalation of Endotoxin. *Eur Respir J* 2006; 28: 622-626.

Matute-Bello G, Liles WC, Radella F, Steinberg KP, Ruzinski JT, Hudson LD, Martin TR. Modulation of neutrophil apoptosis by granulocyte colony-stimulating factor and granulocyte/macrophage colony-stimulating factor during the course of acute respiratory distress syndrome. *Crit Care Med* 2000; 28:1-7.

Mayer AK, Muehmer M, Mages J, Gueinzus K, Hess C, Heeg K, Bals R, Lang R, Dalpke AH. Differential recognition of TLR-dependent microbial ligands in human bronchial epithelial cells. *J Immunol* 2007; 178: 3134–3142.

Medvedev AE, Kopydlowski KM, Vogel SN. Inhibition of lipopolysaccharide-induced signal transduction in endotoxin-tolerized mouse macrophages: dysregulation of cytokine, chemokine, and toll-like receptor 2 and 4 gene expression. *J Immunol* 2000; 164: 5564-74.

Meneghin A, Choi ES, Evanoff HL, Kunkel SL, Martinez FJ, Flaherty KR, Toews GB, Hogaboam CM. TLR9 is expressed in idiopathic interstitial pneumonia and its activation promotes in vitro myofibroblast differentiation. *Histochem Cell Biol* 2008; 130: 979–992.

Meng ZH, Dyer K, Billiar TR, Tweardy DJ. Distinct effects of systemic infusion of G-CSF vs. IL-6 on lung and liver inflammation and injury in hemorrhagic shock. *Shock* 2000; 14: 41-48.

Miettinen M, Sareneva T, Julkunen I and Matikainen S: IFNs activate toll-like receptor gene expression in viral infections. *Genes Immun* 2001; 2: 349-355.

Mittelstadt PR, Ashwell JD. Inhibition of AP-1 by the glucocorticoid-inducible protein GILZ. *J Biol Chem* 2001; 276, 29603-29610.

Mizgerd JP. Acute lower respiratory tract infection. *N Engl J Med* 2008; 358:716-727.

Moore KW, de Waal Malefyt R, Coffman RL, O'Garra A: Interleukin-10 and the interleukin-10 receptor. *Annu Rev Immunol* 2001; 19: 683–765.

Mosser DM, Edwards JP: Exploring the full spectrum of macrophage activation. *Nat Rev Immunol* 2008; 8: 958-969.

Mukherjee D, Gao M, O'Connor JP, Raijmakers R, Pruijn G, Lutz CS, Wilusz J. The mammalian exosome mediates the efficient degradation of mRNAs that contain AU-rich elements. *EMBO J* 2002; 21: 165-174.

Munder M, Eichmann K, Modolell M. Alternative metabolic states in murine macrophages reflected by the nitric oxide synthase/arginase balance: competitive regulation by CD4+ T cells correlates with Th1/Th2 phenotype. *J Immunol* 1998; 160: 5347-5354.

Naiki Y, Michelsen KS, Zhang W, Chen S, Doherty TM, Arditi M. Transforming growth factor-beta differentially inhibits MyD88-dependent, but not TRAM- and TRIF-dependent, lipopolysaccharide-induced TLR4 signaling. *J Biol Chem* 2005; 280: 5491-5495.

Nathan C, Ding A. Nonresolving inflammation. *Cell* 2010; 140: 871-882.

Nelson S, Kolls JK. Alcohol, host defence and society. *Nat Rev Immunol* 2002; 2: 205-209.

Noble PW, McKee CM, Cowman M, Shin HS. Hyaluronan fragments activate an NF-kappa B/I-kappa B alpha autoregulatory loop in murine macrophages. *J Exp Med* 1996; 183: 2373-2378.

O'Brien R. Drug-resistant tuberculosis: etiology, management and prevention. *Semin Respir Infect* 1994; 9: 104-112.

O'Donnell R, Breen D, Wilson S, Djukanovic R. Inflammatory cells in the airways in COPD. *Thorax* 2006; 61: 448-454.

Onyebujoh P, Rook GA. Tuberculosis. *Nat Rev Microbiol* 2004; 12: 930-942.

Opal SM, DePalo VA: Anti-inflammatory cytokines. *Chest* 2000; 117: 1162-72.

Opitz B, van Laak V, Eitel J, Suttorp N. Innate immune recognition in infectious and noninfectious diseases of the lung. *Am J Respir Crit Care Med* 2010; 181: 1294-309.

Oshikawa K, Yamasawa H, Sugiyama Y. Human lung fibroblasts inhibit macrophage inflammatory protein-1alpha production by lipopolysaccharide-stimulated macrophages. *Biochem Biophys Res Commun*. 2003; 312: 650-655.

Park JS, Gamboni-Robertson F, He Q, Svetkauskaite D, Kim JY, Strassheim D, Sohn JW, Yamada S, Maruyama I, Banerjee A, et al. High mobility group box 1 protein interacts with multiple Toll-like receptors. *Am J Physiol Cell Physiol* 2006; 290: C917-C924.

Peden D, Reed CE. Environmental and occupational allergies. *J Allergy Clin Immunol* 2010; 125(2 Suppl 2): S150-S160.

Pilling D, Fan T, Huang D, Kaul B, Gomer RH: Identification of markers that distinguish monocyte-derived fibrocytes from monocytes, macrophages, and fibroblasts. *PLoS One*. 2009; 4: e7475.

Qualls JE, Neale G, Smith AM, Koo MS, DeFreitas AA, Zhang H, Kaplan G, Watowich SS, Murray PJ. Arginine usage in mycobacteria-infected macrophages depends on autocrine-paracrine cytokine signaling. *Sci Signal* 2010; 3: ra62.

Rabe KF, Hurd S, Anzueto A, Barnes PJ, Buist SA, Calverley P, Fukuchi Y, Jenkins C, Rodriguez-Roisin R, van Weel C, Zielinski J. Global Strategy for the Diagnosis, Management, and Prevention of Chronic Obstructive Pulmonary Disease: GOLD Executive Summary. *Am J Respir Crit Care Med* 2007; 176: 532-555.

Remer KA, Brcic M, Sauter KS, Jungi TW. Human monocytoïd cells as a model to study toll-like receptor-mediated activation. *J Immunol Met* 2006; 313: 1-10.

Riccardi C, Cifone MG, Migliorati G. Glucocorticoid hormone-induced modulation of gene expression and regulation of T-cell death: role of GITR and GILZ, two dexamethasone-induced genes. *Cell Death Differ* 1999; 6: 1182-1189.

Roberts TL, Dunn JA, Terry TD, Jennings MP, Hume DA, Sweet MJ, Stacey K J: Differences in Macrophage Activation by Bacterial DNA and CpG-Containing Oligonucleotides. *J Immunol* 2005a; 175: 3569-3576.

Roberts TL, Sweet MJ, Hume DA, Stacey KJ: Cutting edge: Species-specific TLR9-mediated recognition of CpG and non-CpG phosphorothioate-modified oligonucleotides. *J Immunol* 2005b; 174: 605-608.

Rohde G, Klein W, Arinir U, Hagedorn M, Duerig N, Bauer T, Gillissen A, Schultze-Werninghaus G, Epplen T: Association of the ASP299GLY TLR4 Polymorphism With COPD. *Respir Med* 2006; 100: 892-896.

Rook GA, Stanford JL. Give us this day our daily germs. *Immunol Today* 1998; 19: 113–116.

Rutz M, Metzger J, Gellert T, Lupp P, Lipford GB, Wagner H, Bauer S. Toll-like receptor 9 binds single-stranded CpG-DNA in a sequence- and pH-dependent manner. *Eur J Immunol* 2004; 34: 2541-2550.

Sabroe I, Parker LC, Dower SK, Whyte MK. Practical and conceptual models of chronic obstructive pulmonary disease. *Proc Am Thorac Soc* 2007; 4: 606–610.

Sanjuan MA, Rao N, Lai KTA, Gu Y, Sun S, Fuchs A, Fung-Leung WP, Colonna M, Karlsson L. CpG-induced tyrosine phosphorylation occurs via a tlr9-independent mechanism and is required for cytokine secretion. *J Cell Biol* 2006; 172: 1057-1068.

Santos AR, de Miranda AB, Lima LM, Suffys N, Degraeve WM. Method for high yield preparation in large and small scale of nucleic acids from mycobacteria. *J Microbiol Methods* 1992; 15: 83-94.

Sasai M, Matsumoto M, Seya T. The kinase complex responsible for IRF-3-mediated IFN- $\beta$  production in myeloid dendritic cells (mDC). *J Biol Chem* 2006; 139: 171-175.

Sawamura D, Abe R, Goto M, Akiyama M, Hemmi H, Akira S, Shimizu H. Direct injection of plasmid DNA into the skin induces dermatitis by activation of monocytes through toll-like receptor 9. *J Gene Med* 2005; 7: 664-671.

Scanga CA, Bafica A, Feng CG, Cheever AW, Hieny S, Sher A. MyD88-Deficient Mice Display a Profound Loss in Resistance to Mycobacterium tuberculosis Associated with Partially Impaired Th1 Cytokine and Nitric Oxide Synthase 2 Expression. *Infect Immun* 2004; 72: 2400-2404.

Schröder NW. The role of innate immunity in the pathogenesis of asthma. *Curr Opin Allergy Clin Immunol* 2009; 9: 38-43.

Schütz A, Scheller N, Breinig T, Meyerhans A: The Autographa californica nuclear polyhedrosis virus AcNPV induces functional maturation of human monocyte-derived dendritic cells. *Vaccine* 2006; 24: 49-50.

Sethi S and Murphy TF. Infection in the pathogenesis and course of chronic obstructive pulmonary disease. *N Engl J Med* 2008; 359: 2355-2365.

Shimada S, Yano O, Inoue H, Kuramoto E, Fukuda T, Yamamoto H, Kataoka T, Tokunaga T. Antitumor activity of the DNA fraction from mycobacterium bovis BCG. Effects on various syngeneic mouse tumors. *J Natl Cancer Inst* 1985; 74: 681-688.

Soundararajan R, Wang J, Melters D, Pearce D. Differential activities of glucocorticoid-induced leucine zipper protein isoforms. *J Biol Chem* 2007; 282: 36303-36313.

Srivastava R, Gopinathan KP, Ramakrishnan T: Deoxyribonucleic acid methylation in mycobacteria. *J Bacteriol* 1981; 148: 716-719.

Staples KJ, Smallie T, Williams LM, Foey A, Burke B, Foxwell BM, Ziegler-Heitbrock L: IL-10 induces IL-10 in primary human monocyte-derived macrophages via the transcription factor Stat3. *J Immunol* 2007; 178: 4779-4785.

Stempin CC, Dulgerian LR, Garrido VV, Cerban FM. Arginase in parasitic infections: macrophage activation, immunosuppression, and intracellular signals. *J Biomed Biotechnol* 2010; 2010: 683485.

Stoecklin G, Stubbs T, Kedersha N, Wax S, Rigby WF, Blackwell TK, Anderson P. MK2-induced tristetraprolin:14-3-3 complexes prevent stress granule association and ARE-mRNA decay. *EMBO J* 2004; 23: 1313-1324.

Stoecklin G, Tenenbaum SA, Mayo T, Chittur SV, George AD, Baroni TE, Blackshear PJ, Anderson P. Genome-wide analysis identifies interleukin-10 mRNA as target of tristetraprolin. *J Biol Chem* 2008; 283: 1689-1699.

Sugiura H, Ichikawa T, Koarai A, Yanagisawa S, Minakata Y, Matsunaga K, Hirano T, Akamatsu K, Ichinose M. Activation of Toll-like receptor 3 augments myofibroblast differentiation. *Am J Respir Cell Mol Biol* 2009; 40: 654-662.

Sukkar MB, Xie SP, Khorasani NM, Kon OM, Stanbridge R, Issa R, Chung KF. Toll-like receptor 2, 3, and 4 expression and function in human airway smooth muscle. *J Allergy Clin Immunol* 2006; 118: 641-648.

Suswam E, Li Y, Zhang X, Gillespie GY, Li X, Shacka JJ, Lu L, Zheng L, King PH. Tristetraprolin down-regulates interleukin-8 and vascular endothelial growth factor in malignant glioma cells. *Cancer Res* 2008; 68: 674-682.

Suzuki K, Suda T, Naito T, Ide K, Chida K, Nakamura H. Impaired Toll-like receptor 9 expression in alveolar macrophages with no sensitivity to CpG DNA. *Am J Respir Crit Care Med* 2005;171: 707-713.

Tabeta K, Georgel P, Janssen E, Du X, Hoebe K, Crozat K, Mudd S, Shamel L, Sovath S, Goode J, Alexopoulou L, Flavell RA, Beutler B. Toll-like receptors 9 and 3 as essential components of innate immune defense against mouse cytomegalovirus infection. *Proc Natl Acad Sci USA* 2004; 101: 3516-3521.

Takeshita F, Suzuki K, Sasaki S, Ishii N, Klinman DM, Ishii KJ. Transcriptional regulation of the human tlr9 gene. *J Immunol* 2004; 173: 2552-2561.

Taylor GA, Carballo E, Lee DM, Lai WS, Thompson MJ, Patel DD, Schenkman DI, Gilkeson GS, Broxmeyer HE, Haynes BF, Blackshear PJ. A pathogenetic role for TNF alpha in the syndrome of cachexia, arthritis, and autoimmunity resulting from tristetraprolin (TTP) deficiency. *Immunity* 1996; 4: 445-454.

Tlaskalová-Hogenová H, Stepánková R, Hudcovic T, Tucková L, Cukrowska B, Lodinová-Zádníková R, Kozáková H, Rossmann P, Bártová J, Sokol D, Funda DP, Borovská D, Reháková Z, Sinkora J, Hofman J, Drastich P, Kokesová A. Commensal bacteria (normal microflora), mucosal immunity and chronic inflammatory and autoimmune diseases. *Immunol Lett* 2004; 93: 97-108.

Tokunaga T, Yamamoto H, Shimada S, Abe H, Fukuda T, Fujisawa Y, Furutani Y, Yano O, Kataoka T, Sudo T. Antitumor activity of deoxyribonucleic acid fraction from mycobacterium bovis bcg. I. Isolation, physicochemical characterization, and antitumor activity. *J Natl Cancer Inst* 1984; 72: 955-962.

Tudor C, Marchese FP, Hitti E, Aubareda A, Rawlinson L, Gaestel M, Blackshear PJ, Clark AR, Saklatvala J, Dean JL. The p38 MAPK pathway inhibits tristetraproline-directed decay of interleukin-10 and pro-inflammatory mediator mRNAs in murine macrophages. *FEBS Lett* 2009; 583:1933-1938.

Van Haarst JM, Hoogsteden HC, de Wit HJ, Verhoeven GT, Havenith CE, Drexhage HA: Dendritic cells and their precursors isolated from human bronchoalveolar lavage: immunocytologic and functional properties. *Am J Respir Cell Mol Biol* 1994; 11: 344-350.

Vermaelen K, Pauwels R: Accurate and simple discrimination of mouse pulmonary dendritic cell and macrophage populations by flow cytometry: methodology and new insights. *Cytometry A* 2004; 61: 170.

Vissers JL, van Esch BC, Jeurink PV, Hofman GA, van Oosterhout AJ: Stimulation of Allergen-Loaded Macrophages by TLR9-Ligand Potentiates IL-10-Mediated Suppression of Allergic Airway Inflammation in Mice. *Respir Res* 2004; 5: 21.

von Mutius E, Fritsch C, Weiland SK, Roll G, Magnussen H. Prevalence of asthma and allergic disorders among children in united Germany: a descriptive comparison. *Br Med J* 1992; 305: 395-1399.

Wang JP, Hayashi T, Datta SK, Kornbluth RS, Raz E, Guiney DG: Cpg oligonucleotides partially inhibit growth of mycobacterium tuberculosis, but not salmonella or listeria, in human monocyte-derived macrophages. *FEMS Immunol Med Microbiol* 2005; 45: 303-310.

Watz H, Bitter-Suermann S, Kannies F, Magnussen H. Pharmacological treatment of COPD and future of anti-inflammatory therapy. *Med.Klin.(Munich)* 2006; 101: 283-292.

WHO, 2010a. The global burden of disease: 2004 update. Geneva, 2004. Available from: [http://www.who.int/healthinfo/global\\_burden\\_disease/GBD\\_report\\_2004update\\_full.pdf](http://www.who.int/healthinfo/global_burden_disease/GBD_report_2004update_full.pdf)

WHO, 2010b. Tuberculosis. Fact sheet No. 104. Available from: <http://who.int/mediacentre/factsheets/fs104/en/>

WHO, 2010c. Chronic obstructive pulmonary disease. Fact sheet No. 315. Available from: <http://www.who.int/mediacentre/factsheets/fs315/en/>

Wieland CW, Florquin S, Maris NA, Hoebe K, Beutler B, Takeda K, Akira S, van der Poll T. The MyD88-dependent, but not the MyD88-independent, pathway of TLR4 signaling is important in clearing nontypeable *Haemophilus influenzae* from the mouse lung. *J Immunol* 2005; 175: 6042–6049.

Wilusz CJ, Wormington M, Peltz SW. The cap-to-tail guide to mRNA turnover. *Nat Rev Mol Cell Biol* 2001; 2: 237-246.

Wilusz, C.J., Wilusz, J. Bringing the role of mRNA decay in the control of gene expression into focus. *Trends Genet* 2004; 20: 491-497.

Wissinger E, Goulding J, Hussell T. Immune homeostasis in the respiratory tract and its impact on heterologous infection. *Semin Immunol* 2009; 21:147-55.

Wu CC, Lee J, Raz E, Corr M, Carson DA. Necessity of oligonucleotide aggregation for Toll-like receptor 9 activation. *J Biol Chem* 2004; 279: 33071-33078.

Xing Z, Gauldie J, Cox G, Baumann H, Jordana M, Lei XF, Achong MK: IL-6 is an anti-inflammatory cytokine required for controlling local or systemic acute inflammatory responses. *J Clin Invest* 1998; 101: 311-320

Yawn BP. Factors accounting for asthma variability: achieving optimal symptom control for individual patients. *Prim Care Resp J* 2008; 17: 138-147.

Zetterberg G, Johansson A, Lundahl J, Lundborg M, Skold CM, Tornling G, Camner P, Eklund A: Differences between rat alveolar and interstitial macrophages 5 wk after quartz exposure. *Am J Physiol* 1998; 274: 226-234.

Zhang X, Mosser DM. Macrophage activation by endogenous danger signals. *J Pathol* 2008; 214: 161-178.

Zhang XH, Lu X, Long XB, You XJ, Gao QX, Cui YH, Liu Z. Chronic rhinosinusitis with and without nasal polyps is associated with decreased expression of glucocorticoid-induced leucine zipper. *Clin Exp Allergy* 2009; 39: 647-654.



## Publications

### Original Publications

Kierner AK, Senaratne RH, **Hoppstädter J**, Diesel B, Riley LW, Tabeta K, Bauer S, Beutler B, Zuraw BL: Attenuated Activation of Macrophage TLR9 by DNA From Virulent Mycobacteria. *J Innate Immun* 2009; 1: 29-45.

**Hoppstädter J**, Diesel B, Zarbock R, Breinig T, Monz D, Koch M, Meyerhans A, Gortner L, Lehr CM, Huwer H, Kierner AK. Differential cell reaction upon Toll-like receptor 4 and 9 activation in human alveolar and lung interstitial macrophages. *Respir Res* 2010a; 11: 124.

**Hoppstädter J**, Diesel B, Eifler LK, Schmid T, Brüne B, Kierner AK. Downregulation of Glucocorticoid-Induced Leucine Zipper in alveolar macrophages upon Toll-like receptor activation occurs MyD88-dependently. 2010b; *submitted*.

### Abstracts to short talks / poster presentations

**Hoppstädter J**, Diesel B, Kierner AK. Downregulation of the Glucocorticoid-Induced Leucine Zipper upon Toll-like receptor activation in human alveolar macrophages. Short talk at the 50<sup>th</sup> annual meeting of the Deutsche Gesellschaft für Experimentelle und Klinische Pharmakologie und Toxikologie, Mainz, Germany. *Naunyn-Schmiedeberg's Archives of Pharmacology* 2009; 379: S1.

**Hoppstädter J**, Zang EM, Tutdibi E, Gortner L, Kierner AK. Differential cytokine and chemokine expression profile in human cord blood mononuclear cells determined by the Toll-like receptor adapter molecule MyD88. Abstract presented at the 500<sup>th</sup> ECMO, Mannheim, Germany. *Conference proceedings*, 2009.

**Hoppstädter J**, Diesel B, Eifler LK, Schmid T, Brüne B, Kierner AK. Downregulation of the Glucocorticoid-Induced Leucine Zipper upon Toll-like receptor activation in human alveolar

macrophages. Poster presentation at the Keystone meeting “The Macrophage: Intersection of Pathogenic and Protective Inflammation (J8)”, Banff, Alberta, Canada. *Conference proceedings*, 2010. Supported by the National Institute of Allergy and Infectious Diseases, Grant #1R13AI085791-01.

## **Acknowledgements / Danksagungen**

Prof. Dr. Alexandra K. Kiemer möchte ich für die Möglichkeit, in ihrer Arbeitsgruppe promovieren zu dürfen, ganz herzlich danken. Ihre ausgezeichnete Betreuung, Geduld, Anteilnahme und ermutigenden Worte haben diese Arbeit entscheidend vorangebracht.

Prof. Dr. Ludwig Gortner danke ich für die Übernahme des Koreferats und die gute Zusammenarbeit.

PD Dr. Hanno Huwer und seinen Mitarbeitern in der SHG Klinik Völklingen möchte ich für die Überlassung des Lungengewebes danken.

Außerdem möchte ich mich bei Prof. Dr. Bernhard Brüne und Tobias Schmid für die gute Kooperation und ihr Interesse an meiner Arbeit bedanken.

Aus der Arbeitsgruppe von Prof. Dr. Claus-Michael Lehr möchte ich insbesondere Leon Muijs für die Hilfe bei der Isolierung der Makrophagen danken.

Des Weiteren danke ich Dr. Dominik Monz für die Hilfe bei der Zytokin-Bestimmung, Ralf Jungmann für die Anfertigung der AFM-Aufnahmen und Prof. Dr. Hartmut Kleinert für die Überlassung der TTP-Plasmide.

Dr. Britta Diesel danke ich sehr herzlich für die Hilfestellung bei Problemen aller Art und das stets offene Ohr.

Allen wissenschaftlichen und technischen Mitarbeitern des Arbeitskreises danke ich für die fachliche Unterstützung. Besonders herzlich möchte ich mich bei Sonja Keßler und Kerstin Hirschfelder für die freundschaftliche Unterstützung und zahlreiche interessante Diskussionen bedanken, aus denen so manche Erkenntnis erwuchs. Sonja M. Keßler danke ich darüber hinaus für die Behandlung der Mäuse und das Präparieren des Mausegewebes. Außerdem möchte ich mich bei Nadège Ripoche bedanken, die mich an ihrer Erfahrung in Sachen Real-Time PCR teilhaben ließ. Robert Zarbock danke ich für die Anfertigung der CLSM-Aufnahmen. Ferner bedanke ich mich bei meinen ehemaligen

Diplomandinnen Lisa Eifler und Sabine Meiser sowie bei Jenni Schmidt, Rebecca Risch und Astrid Decker für die gute Zusammenarbeit und viele erinnernswerte Momente.

Mein Dank gilt nicht zuletzt meinen Eltern, meiner Familie und meinen Freunden, die mich während meiner gesamten Ausbildung unterstützten und mir zu jeder Zeit mit Rat und Tat zur Seite standen.